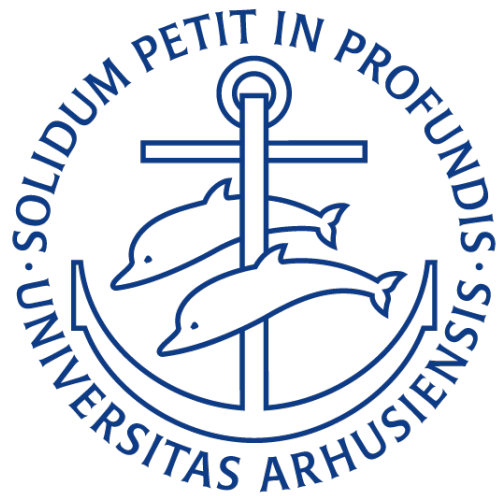


Deep Options Hedging in Uncertain Trading Environments
A Study of Greeks-Free Hedging under Real Life Model Uncertainty

Jacob Kruse Jensen
201707097

Supervisor: Pierluigi Vallarino
PhD Student, Aarhus University

AARHUS UNIVERSITY, DEPARTMENT OF ECONOMICS AND BUSINESS ECONOMICS
IMSQE MASTER'S THESIS



Hand-in date: Aug. 21st 2022
The thesis may be published
146841 Characters (61 Pages)

Abstract

This thesis studies the robustness of a Greeks-free options hedging method known as deep hedging towards real-life model risk. The method is designed to minimize global hedging risk in incomplete markets. I leverage an extensive options dataset spanning the past decade to test its empirical vanilla SPX options hedging performance against different versions of daily recalibrated Practitioner's Black-Scholes and Heston hedging models in a realistic trading environment. I disregard trading costs to leave the Greeks-based models a fair chance, but still find that deep hedging composes a competitive alternative compared to Greeks-based models despite the real-world model risk. However, the empirical analysis stresses the fact that deep hedging performance is highly dependent on the assumed underlying market dynamics during training. Average losses are substantially higher, but the tail risk lower, when the model is trained on paths generated by the Heston model with variance dynamics inferred from the pricing measure. Leveraging realized measures based on intra-daily price data aids in reducing deep hedging losses when volatility spikes. The empirical findings are backed up by controlled experiments in both constant and stochastic volatility models. I find that hedging with the wrong constant volatility in a Black-Scholes model can turn out more costly for deep hedging than conventional delta-hedging and that practitioners should be particularly concerned about correct estimation of the elasticity of variance when training the deep hedging model in a Heston environment.

Contents

1	Introduction	1
2	Hedging in Complete and Incomplete Markets	4
2.1	Setting the Stage: Martingale-Based Pricing and Hedging of Derivatives	4
2.2	Quantifying Options Hedging Risk in Incomplete Markets	8
2.3	Optimal Global Hedging in a Realistic Setup	10
3	Towards a Solvable Statistical Learning Problem and Deep Hedging	13
3.1	Neural Networks as Policy Function Approximators	15
3.2	Optimization of Parameterized Hedge Policy Functions	18
4	Market Scenario Generation with Time-Varying Volatility Models	20
5	Continuous-Time Markov Models for Option Pricing and Hedging	23
5.1	Hedging with Black-Scholes	23
5.2	Hedging and Simulating with the Heston Model	25
6	Assessing the Impact of Model Risk on Deep Hedging	31
6.1	Hedging a call option in a Known Black-Scholes environment	31
6.2	Deep Hedging with the Wrong Black Volatility	34
6.3	The Poor Quant's Attempt at Deep Hedging with the Heston Model under \mathbb{Q}	36
7	Data and Volatility Descriptives	39
7.1	Options data	39
7.2	High-Frequency Data and Realized Measures	40
7.3	Volatility Descriptives and Calibration Results for Heston and PBS Models	40
8	Empirical Evaluation	44
8.1	Replicating Vanilla Options Hedging Experiment	45

8.2	Deep Hedging ATM Call Options	47
8.3	Deep Hedging Performance under \mathbb{P} -Estimated Dynamics	53
8.4	Volatility Information and Hedging Performance	55
8.5	The Empirical Significance of Training Risk Aversion	57
9	Conclusion	59
	Appendices	65
A	Figures	66
B	Tables	70
B	Equivalent Measure Changes in the Heston Model	71
C	Extracting Implied Dividend Yield and Bond Yields from Option Prices	72
D	Heston Characteristic Function and Greeks	73
E	Delta Hedging and Options Pricing in the Black & Scholes Model	74

1 Introduction

This thesis aims to study whether the real-life performance of a recent data-driven approach to hedging of non-linear trading books exceeds that of traditional hedging strategies based on the Heston model and variants of the Black-Scholes delta hedging strategy. In extension to this, the thesis furthermore addresses the natural question of how information from the stock and option markets can be optimally leveraged to optimize the real-life performance of the deep hedger by training the model in environments as close to reality as possible. To address this question, the thesis compares different time-varying volatility models from the classic econometrics literature to the Heston stochastic volatility model, calibrated to options data, as market generators. To cope with the natural limitations of an empirical study, the thesis also presents novel simulation studies in Heston, Black-Scholes, and GARCH environments that aim to shed light on the efficiency of this type of Greeks-free and data-driven hedging approach under model and estimation uncertainty. Focus is on hedging plain vanilla call options in all applications, although the deep hedging methodology applies to general trading books.

Hedging activities are a central part of any larger financial institution and serve to protect the current value of trading books. Traditionally, financial institutions have employed what one might refer to as classic continuous-time models or *Greeks* models from the traditional quantitative finance literature for pricing and hedging trading books that contain products with non-linear payoff structures.

The literature on pricing and hedging of options and other non-linear derivatives is highly well-developed, and substantial literature has suggested different dynamic continuous time models for the underlying assets. In formulating these models, one typically postulates that the values of relevant market variables and risk factors evolve as continuous time diffusion processes. In these models, the value of a derivative portfolio and its constituents can be computed as the expected terminal payout under an appropriate probability measure. The associated hedging strategies typically involve immunizing the portfolio value locally against changes in risk factors by taking offsetting positions in other assets, calculated as the derivatives of the portfolio value w.r.t. those risk factors - the so-called *Greeks*. When the value of a portfolio is only protected against changes in the underlying assets, this is also popularly referred to as delta-hedging - a concept central to the derivation of the Black & Scholes option pricing formula in the seminal paper by [Black \(1976\)](#).

In particular, when these continuous-time models are *complete*, essentially meaning that there are limited sources of stochasticity driving the market variables, perfect replication of any derivative is possible and its price uniquely determined. However, this result relies on assumptions such as the absence of transaction costs, continuous portfolio rebalancing, and lack of model risk. In practice, such assumptions are never

satisfied, thus rendering delta and other Greeks-based hedges imperfect.

In recognition that real markets are incomplete, substantial literature has been occupied with constructing risk-minimizing hedging strategies in incomplete markets. [Föllmer et al. \(1990\)](#) suggested constructing locally risk-optimal portfolios, minimizing the risk of the portfolio over small time steps. Other authors such as [Schweizer \(1995\)](#) and [Godin \(2016\)](#) have suggested a *global* criterion, penalizing instead terminal portfolio losses. The former article focuses on optimal discrete-time hedging with a quadratic loss criterion, which has the unfortunate consequence of penalizing losses and gains equally. The latter article prescribes optimal hedging in the presence of transaction costs under a Conditional Value at Risk (CVaR) criterion. However, their approach allows for derivatives of the vanilla type only.

On the contrary, the so-call *deep hedging* approach studied in this thesis and first introduced in [Buehler et al. \(2019\)](#) seeks to minimize the global risk of completely general derivative portfolios using classic statistical learning methods. Quite remarkably, this approach to hedging applies to arbitrary dynamics for the prices of hedge instruments. Additionally, the method allows for trading constraints, frictions and very general specifications of the objective function defined over terminal portfolio losses. This stands in contrast to all of the previous literature.

The original authors of deep hedging presented a theoretical justification for using deep neural networks for approximating risk-optimal hedging strategies and exhibited its superior performance under different simulated model settings and in an empirical application to the S&P500 vanilla options market. However, the competing models in the empirical analysis did not leverage information from the options market, which has been shown to be empirically important and is popular among practitioners. Since then, several authors have continued working along the lines of the original paper, providing results on the theoretical deep hedging performance in various simulated model settings. For instance, [Horvath et al. \(2021\)](#) investigate the robustness of the deep hedging algorithm in a non-Markovian model setting where volatility is assumed rough, and [Carboneau \(2021\)](#) shows that deep hedging improves upon locally risk-minimizing strategies in the Black-Scholes and Merton Jump-Diffusion models when hedging long-term vanilla options.

Deep hedging as a discipline opens the door to incorporating information based on the historical measure to a much greater extent than traditional Greeks-based approaches. While the existing literature seems to agree that deep hedging can improve hedging performance in most cases for a given discretized continuous-time model e.g., Black-Scholes or Heston, relatively little work has been done on the empirical side where model risk is naturally present given that the data-generating process for relevant market variables is unknown and must be estimated using traditional methods that incorporate information from the stock and options markets. An important objective of this thesis is to provide some first empirical insights on how the real-life

deep hedging performance depends on the assumed market dynamics.

Especially given the fact that variations of deep hedging, and data-driven hedging methods in general, are currently being implemented in leading large financial institutions and very well might become industry standard within the coming years, there seems to be ample space in the current literature for a thorough quantification of the empirical performance of deep hedging, benchmarked against a serious line-up of alternative model candidates.

While this thesis operates precisely in this space and seeks to provide new perspectives on empirical deep hedging, significant work has already been done. In addition to the original work by [Buehler et al. \(2019\)](#), [Lütkebohmert et al. \(2021\)](#) demonstrate that a so-called *robust* version of the deep hedging algorithm, which is exactly supposed to take into account the fact that model parameters are subject to statistical uncertainty, outperforms the standard version of deep hedging where the stock price paths are simulated with fixed model parameters. However, no reference is made to traditional hedging models widely employed in the industry, such as the Practitioner's Black-Scholes (PBS) and Heston models. [Giurca and Borovkova \(2021\)](#) and [Mikkilä and Kanniainen \(2021\)](#) both show that a version of deep hedging based on Q-learning and the dynamic programming formulation of the optimization problem outperforms variants of the Practitioner's Black-Scholes hedging strategy in terms of a mean-variance criterion when hedging short to medium term vanilla call options on the S&P500. The latter paper further shows that a hedging agent trained purely on empirical data outperforms an equivalent agent trained on data simulated under Heston model dynamics calibrated to option prices. However, the evaluation period is just one year in both papers. Furthermore, neither of the two evaluate the performance of the version of deep hedging originally presented in [Buehler et al. \(2019\)](#), which is based on a direct policy search.

The remainder of the thesis proceeds as follows. Section 2 presents the theory of options pricing and hedging in complete and incomplete markets. Section 3 explains the concept of Deep Hedging, in particular how deep neural networks can be used to approximate global risk-optimal hedging strategies. Section 4 presents several candidate models for the stock price dynamics used for training the deep hedging agent. Section 5 outlines the Black-Scholes and Heston benchmark models and how they may be calibrated to market data. Section 6 analyses deep hedging performance in several controlled experiments. Section 7 presents the data used in the empirical study and details the data cleaning process. Finally, 8 presents the empirical results. Section 9 concludes.

2 Hedging in Complete and Incomplete Markets

The goal of this section is to introduce fundamental concepts that are central to pricing and hedging of derivatives. The first part takes the perspective of the complete-market paradigm and describes the options pricing and hedging problem and its solution in an idealized and general continuous-time setting. These results are fairly standard, and the majority of the theory covered is based on Bjork (2009) Ch. 11, 12 & 14. Although a thorough theoretical treatment of martingale-based pricing and hedging of derivatives is not within the focus of the thesis, a brief review of this vast theory is still essential for building a fundamental theoretical understanding of the nature of the options hedging problem and the class of models encompassing the Black-Scholes and Heston benchmark models and also to help understanding where the assumptions underlying these models break down in practice.

The last part of the section introduces global risk-optimal hedging in incomplete markets under convex risk measures, which is the fundamental concept studied throughout the thesis.

2.1 Setting the Stage: Martingale-Based Pricing and Hedging of Derivatives

In this section, we shall assume the existence of a finite-horizon financial market living in continuous time on a probability space $(\Omega, \mathcal{F}, \mathbb{P})$ equipped with the filtration $\mathbb{F} := (\mathcal{F}_t)_{0 \leq t \leq T}$. In this section, a multivariate market will be considered to demonstrate the general applicability of martingale pricing and hedging. However, in the empirical section, the focus is on markets with a single underlying asset. Assume hence that the market consists of n tradable risky and non dividend-paying¹ assets $\mathbf{S}_t = (S_t^1, \dots, S_t^n)^\top$ and the bank account B_t , which earns the locally risk-free and \mathcal{F}_t -adapted rate of return r_t . The market variables are assumed to have dynamics described by

$$\begin{aligned} d\mathbf{S}_t &= D(\mathbf{S}_t) \boldsymbol{\mu}_t dt + D(\mathbf{S}_t) \boldsymbol{\sigma}_t d\mathbf{W}_t, \quad \mathbf{S}_0 = \mathbf{s}_0 \in \mathbb{R}^+ \\ dB_t &= r_t B_t dt, \quad B_0 := 1 \end{aligned} \tag{2.1}$$

where \mathbf{W}_t is a standard, i.e. uncorrelated, d -dimensional \mathbb{P} -Brownian Motion and $D(\cdot)$ is the diagonal operator. The two \mathcal{F}_t -adapted and regular processes $\boldsymbol{\mu}_t \in \mathbb{R}^{n \times 1}$ and $\boldsymbol{\sigma}_t \in \mathbb{R}_+^{n \times d}$ represent, respectively, the deterministic drift vector and diffusion, or volatility, matrix of the n risky assets. The purely diffusive specification for the risky assets of course rules out more general Lévy processes with jumps. Still, it is selected for ease of exposition since this class of models nests all models used in the empirical section.

¹I abstract from dividends in this section to convey only the essentials of the theory, which can be easily adapted to the positive dividend case by working with normalized gains processes as opposed to normalized price processes.

Furthermore, the martingale pricing theory presented here easily generalizes to more general dynamics, including Poisson-driven jump processes or purely jump-driven ones.

The First Fundamental Theorem, in its general form attributable to Delbaen and Schachermayer (1994), stipulates that the market model 2.1 is free of arbitrage, essentially, if and only if there exists an equivalent martingale measure (EMM). That is, absence of arbitrage requires the existence of a measure \mathbb{Q} corresponding to a numeraire asset A_t such that $\mathbb{Q} \sim \mathbb{P}$ ² and such that $\mathbf{Z}_t := \mathbf{S}_t A_t^{-1}$ is an \mathcal{F}_t -martingale³. The process \mathbf{Z}_t is considered an \mathcal{F}_t -martingale if it is \mathcal{F}_t -adapted and if it satisfies the martingale condition $\mathbb{E}^{\mathbb{Q}} [\mathbf{Z}_{t'} | \mathcal{F}_t] = \mathbf{Z}_t$, $t' > t$. In many cases, it is convenient to take the EMM as the risk-neutral measure, which is obtained by letting $A_t := B_t$ for $0 \leq t \leq T$. In the remainder of the thesis, the EMM referred to is the risk-neutral measure. Under the assumption that \mathbb{F} hosts only the Wiener process \mathbf{W} , all changes of measure from \mathbb{P} to another equivalent measure $\tilde{\mathbb{P}}$ can be obtained by the following class of stochastic exponential processes

$$\frac{d\tilde{\mathbb{P}}}{d\mathbb{P}} \Big|_{\mathcal{F}_t} = L_t := \exp \left(\int_0^t \boldsymbol{\varphi}_s d\mathbf{W}_s - \frac{1}{2} \int_0^t \boldsymbol{\varphi}_s^\top \boldsymbol{\varphi}_s ds \right), \quad t \in [0, T] \quad (2.2)$$

where the \mathcal{F}_t -adapted process $\boldsymbol{\varphi}_t = (\varphi_t^1, \dots, \varphi_t^d)^\top$ in the sequel will be referred to simply as the Girsanov kernel. Under the assumption that $\boldsymbol{\varphi}_t$ square integrable and such that L_t is a true \mathbb{P} -martingale, the Girsanov Theorem then stipulates that the $\tilde{\mathbb{P}}$ -dynamics of the risky assets are

$$d\mathbf{S}_t = D(\mathbf{S}_t)(\boldsymbol{\mu}_t + \boldsymbol{\sigma}_t \boldsymbol{\varphi}_t) dt + D(\mathbf{S}_t) \boldsymbol{\sigma}_t d\mathbf{W}_t^{\tilde{\mathbb{P}}} \quad (2.3)$$

where $\mathbf{W}_t^{\tilde{\mathbb{P}}}$ is a standard $\tilde{\mathbb{P}}$ -Brownian Motion. An application of Ito's Lemma to the process \mathbf{Z}_t then implies the no-arbitrage condition $\boldsymbol{\mu}_t + \boldsymbol{\sigma}_t \boldsymbol{\varphi}_t = \mathbf{r}_t$,⁴ which has a solution only if $\text{rank}(\boldsymbol{\sigma}_t) \geq n$, requiring that $d \geq n$. If there exists an equivalent measure $\tilde{\mathbb{P}}$ with kernel $\boldsymbol{\varphi}_t$ satisfying this no-arbitrage condition, then it is an EMM for the bank account B_t , i.e. $\tilde{\mathbb{P}} = \mathbb{Q}$. If such a measure exists, the risk-neutral dynamics read

$$d\mathbf{S}_t = D(\mathbf{S}_t) \mathbf{r}_t dt + D(\mathbf{S}_t) \boldsymbol{\sigma}_t d\mathbf{W}_t^{\mathbb{Q}}. \quad (2.4)$$

Define now a derivative, or contingent claim, χ , which is an asset whose payoff is an \mathcal{F}_T -measurable r.v. that is determined by one or more of the n tradable assets \mathbf{S} and whose terminal payoff, that is $\chi = \Phi((\mathbf{S}_u)_{0 \leq u \leq T})$ for a function Φ mapping from the path of the underlying assets to a real number. Since χ is also a traded asset, absence of arbitrage requires its price process to be a martingale under the risk-neutral measure \mathbb{Q} , so

²Two measures are equivalent if the null sets of the two measures coincide and we write \sim to denote the equivalence.

³Strictly speaking, \mathbf{Z}_t has to be only a local martingale. I abstract away from the difference here.

⁴ $\mathbf{r}_t := (r_t, \dots, r_t) \in \mathbb{R}^{n \times 1}$.

by applying the martingale condition to the process \mathbf{Z}_t , one obtains the fundamental pricing equation for a general derivative whose time t price will be denoted by

$$p_t^\chi = \mathbb{E}^{\mathbb{Q}} \left[e^{-\int_t^T r_s ds} \chi \mid \mathcal{F}_t \right]. \quad (2.5)$$

In short, this means that under the fairly general model in 2.1 for the risky assets, an arbitrage-free price of a general derivative can be computed as the expectation of the discounted terminal payoff, where the expectation should be taken under the risk-neutral measure under which the risky asset dynamics are given by 2.4.⁵ Accordingly, this is exactly how option prices should be computed for any fully-fledged parametric pricing model, such as the Heston or Black-Scholes models.

From a hedging perspective, the interesting question for a particular model of the type in 2.1 is now whether the arbitrage-free price in 2.5 is unique since, intuitively, that must be closely linked to the replicability of the claim, or the existence of a so-called replicating portfolio. To this end, define the value process of a hedge portfolio as

$$V_t = \boldsymbol{\delta}_t \mathbf{S}_t + \alpha_t B_t, \quad \alpha_t \in \mathbb{R}, \quad t \in [0, T] \quad (2.6)$$

which represents the time t value of a portfolio with positions $\boldsymbol{\delta}_t \in \mathbb{R}^{1 \times n}$ in the risky assets and a position α_t in the bank account. Throughout the thesis, only self-financing versions of such portfolios are considered for hedging purposes. The self-financing property implies exactly what its name suggests, namely that changes to the portfolio value only come from changes in the value of the assets in the portfolio and not from exogenous infusions of money. That is,

$$dV_t = \boldsymbol{\delta}_t d\mathbf{S}_t + \alpha_t dB_t. \quad (2.7)$$

By multivariate Ito's Lemma, the corresponding self-financing dynamics for the discounted value process is

$$d(V_t B_t^{-1}) = \boldsymbol{\delta}_t d\mathbf{Z}_t. \quad (2.8)$$

For a self-financing portfolio with initial value $V_0 \equiv v_0$, the terminal discounted value thus has the following stochastic integral representation

$$V_T B_T^{-1} = v_0 + \int_0^T \boldsymbol{\delta}_s d\mathbf{Z}_s. \quad (2.9)$$

At this point it is useful to note the rather important result⁶ that for any fixed risky asset holdings $\boldsymbol{\delta}$ and initial portfolio value v_0 , there exist *unique* positions in the bank account $(\alpha_s)_{0 \leq s \leq T}$ such that the value

⁵In fact, the result holds also for much more general models belonging to the class of semi-martingale models.

⁶Please refer to Bjork (2009) Ch. 11. for a proof.

process V_t is self-financing. This explains why the remainder of the thesis is essentially void of any mentions of the bank account in relation to optimal global hedging strategies - the number of bonds to be held in the hedge portfolio at any point in time is implicitly given by the risky asset positions and the requirement that the portfolio is self-financing. For a given initial value \bar{p} , I will denote the set of discounted terminal portfolio values that can be obtained with a self-financing and admissible strategy as

$$V_T^\delta := \left\{ \bar{p} + \int_0^T \delta_s d\mathbf{Z}_s \mid \delta \in \mathcal{D} \right\} \quad (2.10)$$

where \mathcal{D} is the set of admissible trading strategies. The discounted terminal hedging error associated with selling a claim χ with initial value \bar{p} and following an admissible and self-financing trading strategy is thus given by

$$\varepsilon_T^\delta := V_T^\delta - \chi B_T^{-1} \quad (2.11)$$

and a given contingent claim χ is said to be replicable, or hedgeable, if there exists a portfolio such that $\mathbb{P}(\varepsilon_T^\delta = 0) = 1$. The intuition is that by investing an initial cash amount \bar{p} and following the trading strategy δ , the claim χ can be replicated without any risk. Note that ε_T^δ represents the discounted profit-and-loss (PnL) to the *seller* of a given claim χ . The remainder of the thesis takes the perspective of a financial institution that has *sold* an asset χ , which hence represents a liability.

The market is said to be complete if all claims are replicable, i.e. if $\mathbb{P}(\varepsilon_T^\delta = 0) = 1$ holds for any conceivable claim χ . Arbitrage-free and complete markets hence must be characterized by $p_t^\chi = B_t V_t^\delta$ for $t \in [0, T]$ and for all claims χ when δ represents a replicating portfolio, i.e. the price of the claim must be uniquely determined. In particular, it must be given by 2.5, which is also the value of the replicating portfolio.

In the diffusion model considered here, uniqueness of the derivative price is equivalent to uniqueness of the Girsanov kernel φ_t , requiring σ_t to be invertible and $d = n$. Since the EMM, under the assumption that it exists, is uniquely determined by the choice of the Girsanov kernel φ , the result that the market is complete if and only if the EMM is unique hence comes as no surprise. This is also referred to as the Second Fundamental Theorem. I refrain from boring the reader with any proofs, which rely on abstract existence results and can be found in standard textbooks, e.g., Bjork (2009) Ch. 11.

In short, the results stated here imply that in models where the number of risk factors is equal to the number of traded assets, $d = n$, the hedging problem has a unique solution in the sense that risk preferences play no role in the solution to the problem. That is because there exists a unique self-financing portfolio such that the terminal hedging error is zero with probability one. However, this result also hinges on the blatantly unrealistic assumptions of continuous portfolio rebalancing and the absence of both trading costs

and model uncertainty. The following section covers the hedging decision problem in the incomplete market case.

2.2 Quantifying Options Hedging Risk in Incomplete Markets

While the previous part covered options pricing and hedging in the complete market case, real markets are always incomplete due to the reasons previously listed. In the real world, the terminal hedging error is hence generally an \mathcal{F}_T -measurable random variable whose law depends on the self-financing hedging strategy δ . Consequently, before setting up the hedging problem, one must introduce a risk-measure, which generates a preference ordering over different discounted terminal loss distributions associated with hedging a contingent claim under a given self-financing strategy. In other words, we must introduce a function mapping from the space of random variables to a real number. I denote this space by $L^\infty(\mathbb{P})$. The choice to work with preferences defined over discounted gains is in line with the previous theoretical section and other literature such as [Carbonneau \(2021\)](#).

I follow much of the recent related literature on optimal global hedging (e.g. [Godin \(2016\)](#), [Ilhan et al. \(2009\)](#)) and focus on the class of convex risk measures that can be generated by Optimized Certainty Equivalents (OCEs), which are described in detail in [Ben-Tal and Teboulle \(2007\)](#) and has a number of desirable properties. Define a non-decreasing and concave utility function $u : \mathbb{R} \mapsto \mathbb{R}$, describing the trader's preferences over certain outcomes. The OCE associated to the discounted terminal hedge PnL ε_T^δ is then defined as the map $OCE : L^\infty(\mathbb{P}) \mapsto \mathbb{R}$

$$OCE(\varepsilon_T^\delta) := \sup_{\eta \in \mathbb{R}} \left\{ \eta + \mathbb{E} [u(\varepsilon_T^\delta - \eta)] \right\}, \quad (2.12)$$

which induces a preference ordering over different random variables, similar in spirit to the certainty equivalent central to the well-known Expected Utility theory of von-Neumann and Morgenstern. Intuitively, the OCE is the sure present monetary value of the unknown future outcome ε_T^δ when optimally splitting the value of ε_T^δ between now and the future, here corresponding to the expiry date of the claim χ , i.e., T . The corresponding convex risk measure $\rho : L^\infty \mapsto \mathbb{R}$ then may be generated by taking

$$\rho(\varepsilon_T^\delta) := -OCE(\varepsilon_T^\delta), \quad (2.13)$$

The class of convex risk measures has the following intuitively appealing properties

1. If $\mathbb{P}(\varepsilon_T^{\delta_1} \geq \varepsilon_T^{\delta_2}) = 1$ then $\rho(\varepsilon_T^{\delta_1}) \leq \rho(\varepsilon_T^{\delta_2})$ (monotonicity)

$$2. \rho(\lambda\varepsilon_T^{\delta_1} + (1-\lambda)\varepsilon_T^{\delta_2}) \leq \lambda\rho(\varepsilon_T^{\delta_1}) + (1-\lambda)\rho(\varepsilon_T^{\delta_2}), \quad \forall\lambda \in [0,1] \text{ (convexity)}$$

$$3. \rho(\varepsilon_T^{\delta_1} + m) = \rho(\varepsilon_T^{\delta_1}) - m, \quad m \in \mathbb{R} \text{ (translational/cash invariance)}$$

Convex risk measures are based on the fundamental idea that the risk of a given financial portfolio should be measured by the initial cash amount that must be added to the portfolio to make it acceptable. For a normalized risk measure with $\rho(0) = 0$, we can also write the risk of the hedging strategy δ_1 as

$$\rho(\varepsilon_T^{\delta_1}) = \inf \left\{ a \in \mathbb{R} : \varepsilon_T^{\delta_1} + a \in \left\{ \varepsilon_T^\delta : \rho(\varepsilon_T^\delta) \leq 0 \right\} \right\}, \quad (2.14)$$

which exactly states that the risk of the δ_1 hedging strategy is the least amount of cash a that must be added to the hedging portfolio such that the augmented portfolio $\varepsilon_T^{\delta_1} + a$ belongs to the acceptance set of portfolios with non-positive risk.

Several popular and frequently employed risk measures belong to this class of convex risk measures generated by OCEs. Among these is the Conditional Value at Risk (CVaR). For a given confidence level $\alpha \in (0,1)$, the CVaR is obtained by setting $u(x) = -\alpha^{-1} \min(0, x)$ ⁷ in 2.12 and using the definition 2.13

$$\text{CVaR}_\alpha(\varepsilon_T^\delta) := \mathbb{E} \left[L_T \mid L_T \geq F_{L_T}^{-1}(\alpha) \right] = \inf_\eta \left\{ \eta - \alpha^{-1} \mathbb{E} \left[[-\eta - \varepsilon_T^\delta]^+ \right] \right\}, \quad \alpha \in (0,1). \quad (2.15)$$

where $F_{L_T}^{-1} : (0,1) \mapsto S$ is the quantile function of the loss random variable $L_T := -\varepsilon_T^\delta$. The parameter α governs the risk aversion of the trader and essentially truncates the part of the terminal profit-loss distribution taken under consideration when governing its desirability. For $\alpha \rightarrow 0$, the CVaR reduces to the unconditional mean of the loss, while for the highest level of risk aversion, $\alpha \rightarrow 1$, the CVaR reduces to the worst-case loss.

Another important example is the entropic risk measure, which can be obtained by assuming an exponential utility function $u(x) = \frac{1}{\lambda} (1 - e^{-\lambda x})$, and reads

$$\text{Entropic}_\lambda(\varepsilon_T^\delta) := \lambda^{-1} \log \mathbb{E} \left[e^{-\lambda \varepsilon_T^\delta} \right], \quad \lambda \in \mathbb{R}^+. \quad (2.16)$$

Intuitively, the entropic risk measure is another way to compute a risk-adjusted expected return that respects all required properties of a convex risk measure. However, contrary to the CVaR in 2.15, the entropic risk measure considers the entire loss distribution. The parameter λ governs the degree of risk aversion.

Sometimes, to evaluate the hedging models, I will also consider the Mean Squared Error (MSE) and SemiMSE. Neither of the two are convex risk measures, and they also do not focus on tail risk as is the

⁷The reference here is again Ben-Tal and Teboulle (2007) in which a more elaborate description is available.

case for e.g. CVaR. The inspiration to use the SemiMSE risk measure comes from the work in [Carboneau and Godin \(2021b\)](#) where it is used to measure risk in the objective function when optimizing deep hedging neural networks. The SemiMSE has an intuitive appeal as it penalizes only losses and not gains. The two non-convex risk measures are defined, respectively, as

$$\text{MSE}(\varepsilon_T^\delta) := \mathbb{E} \left[(\varepsilon_T^\delta)^2 \right], \quad \text{SemiMSE}(\varepsilon_T^\delta) := \mathbb{E} \left[(\varepsilon_T^\delta)^2 \mathbb{1}_{\varepsilon_T^\delta < 0} \right]. \quad (2.17)$$

Finding optimal hedging strategies under convex risk measures has the advantage that the learned strategy is not specific to the assumed (or exogenously provided) initial price of the hedged asset(s). An approach to learning optimal hedging under non-convex risk measures for large number of initial portfolio values is available in [Carboneau and Godin \(2021b\)](#). I always use a convex risk measure in the objective function, with one exception in Section 8.3. The next part describes the hedging optimization problem under the assumption that the risk objective is of the convex type.

2.3 Optimal Global Hedging in a Realistic Setup

With the definition of relevant risk measures, I am now ready to pose the main optimization problem. As in several other papers, e.g. [Godin \(2016\)](#), [Ilhan et al. \(2009\)](#) and [Schweizer \(1995\)](#), I focus on optimal global hedging strategies as opposed to local ones as is considered for instance in [Poulsen et al. \(2009\)](#) in an application to the Heston model. While the former type considered here is guaranteed to be self-financing by construction and measures the efficiency of the hedge only by the risk at the maturity date, the latter measures the risk on a somewhat more myopic period-by-period basis and unfortunately does not guarantee the strategy to be self-financing. Please refer to [Schweizer \(1999\)](#) for an excellent account and mathematical treatment of the differences between the two approaches.

Starting from the setup and notation from the idealized setting from Section 2.1, I now lift the majority of the quite uncomfortably imposed assumptions there and describe the financial market setting and hedging problem corresponding to the real-world hedging problem considered in the empirical part in Section 8. First, the assumption that the traded risky assets evolve in continuous time with the diffusive dynamics in 2.1 is discarded. The dynamics of S can be completely general in the present framework. Second, rather than assuming continuous portfolio rebalancing times, I construct a set of discrete points in time $\mathcal{T} := \{0 = t_0 < t_1 \dots < t_N = T\}$ at which the hedging portfolio may be adjusted. To calculate the discrete-time equivalent of the self-financing hedging gains and losses in 2.9, I discretize the stochastic integral by using the fact that a stochastic integral is constructed with respect to forward increments of the Wiener

process, thus yielding the discrete-time discounted gains process

$$G_s^\delta = \sum_{i=0}^{s-1} \boldsymbol{\delta}_{t_i}^\top (\mathbf{Z}_{t_{i+1}} - \mathbf{Z}_{t_i}), \quad s \in \{1, \dots, N\} \quad (2.18)$$

where, in contrast to the expression in 2.9, the initial value is now normalized to be $G_0^\delta := 0$. This is done to separate the value of the hedging gains process from the initial cash infusion from selling the claim, for which I reserve the notation \bar{p} . Given the discretization of time, the market filtration is now naturally given by $\{\mathcal{F}_t\}_{t \in \mathcal{T}}$. As in Buehler et al. (2019), I will assume the filtration to be generated by the stochastic information process $\{\mathcal{I}_i\}$ with values in $\subseteq \mathbb{R}^D$. The idea is that \mathcal{I}_i includes all relevant new information at time t_i such as the current values of traded assets, past trading decisions, news, or other trading signals. It is thus the case that $(\mathcal{I}_0, \dots, \mathcal{I}_i) \in \mathcal{F}_{t_i}$.

Additionally, trading costs are introduced with the introduction of the following discrete-time process, which tracks the accumulated discounted trading costs of the portfolio⁸

$$C_s^\delta = \sum_{i=0}^s B_{t_i}^{-1} \left(\mathbf{c}_{t_i}^0 \mathbf{1}_{\{\Delta \boldsymbol{\delta}_{t_i} > 0\}} + \mathbf{c}_{t_i}^1 \mathbf{S}_{t_i} |\Delta \boldsymbol{\delta}_{t_i}| \right), \quad \Delta \boldsymbol{\delta}_{t_i} := \boldsymbol{\delta}_{t_i} - \boldsymbol{\delta}_{t_{i-1}}, \quad s \in \{0, \dots, N\}. \quad (2.19)$$

Although the per-period trading costs can be selected arbitrarily for deep hedging purposes, the specification in 2.19 imposes a fixed cost $\mathbf{c}_t^0 \in \mathbb{R}_+^n$ for trading and another cost $\mathbf{c}_t^1 \in \mathbb{R}_+^n$ that is proportional to the amount traded and the current value of the hedged asset. Under these modified and much more realistic assumptions, the discounted terminal hedging error from 2.11 now reads

$$\varepsilon_T^\delta = \bar{p} + G_N^\delta - C_N^\delta - \chi B_T^{-1} \quad (2.20)$$

when the initial value of the claim is \bar{p} , which I will take to be exogenously given throughout the thesis - mostly in the form of a quoted market price. The global risk-optimal hedging strategy is the sequence of permissible hedge asset positions $\boldsymbol{\delta}^* := (\boldsymbol{\delta}_{t_0}^*, \dots, \boldsymbol{\delta}_{t_{N-1}}^*) \in \mathbb{R}^{n \times N}$ that minimize the terminal hedge risk, i.e.

$$\boldsymbol{\delta}^* = \arg \min_{\boldsymbol{\delta} \in \mathcal{D}} \rho(\varepsilon_T^\delta). \quad (2.21)$$

Accordingly, our task is to find a sequence of policy functions that map from the at-the-time available information set to a vector representing the positions in the hedge assets. With some abuse of notation, we

⁸Formally, define $\boldsymbol{\delta}_{t_{-1}} := 0$.

are thus looking for an optimal strategy of the form

$$\delta_{t_i}^* = f_{t_i}(\mathcal{F}_{t_i}), \quad f_i : \mathbb{R}^D \mapsto \mathbb{R}^n, \quad i \in \{0, \dots, N-1\}, \quad (2.22)$$

which highlights the fact that the optimal hedging problem in 2.21 is a complex infinite-dimensional dynamic programming problem. Even if one is sufficiently bold to postulate having access to the relevant information set \mathcal{F}_t for each t , we are optimizing in function space. The problem can be simplified slightly if the hedged derivative is of the simple (vanilla) type $\chi = \Phi(\mathbf{S}_T)$ and if we are willing to assume a Markovian market. In that case, the optimal strategies are of the seemingly identical but quite significantly different form

$$\delta_{t_i}^* = f_{t_i}(\mathcal{I}_i), \quad f_i : \mathbb{R}^D \mapsto \mathbb{R}^n, \quad i \in \{0, \dots, N-1\}, \quad (2.23)$$

In any case, there is no doubt that the optimal strategy in 2.21, as well as the relevant information set for the hedging strategy, must depend on the dynamics, which govern the evolution of the prices of hedge instruments. In the remainder of the thesis, I represent the information that is actually used in practice, the so-called feature set, by \mathcal{I}_t .

The following section features an increasingly practical discussion of a direct policy search approach to solving the global hedging problem in the remarkably general setting presented here.

3 Towards a Solvable Statistical Learning Problem and Deep Hedging

The optimization problem presented in the previous Section 2.3 can essentially be regarded as a classic statistical learning, or regression, problem as covered in e.g. [Sain \(1996\)](#). In a classic supervised statistical learning problem, the aim is, for two generic vector-valued random variables $\mathbf{X} \in \mathbb{R}^N$ and $\mathbf{Y} \in \mathbb{R}^N$ with joint distribution $p(\mathbf{X}, \mathbf{Y})$, to approximate a prediction function $f : \mathbb{R}^N \times \mathbb{R}^N \mapsto \mathbb{R}$ in the feasible function space \mathcal{H} by solving a minimization problem of the following kind

$$f^* := \arg \min_{f \in \mathcal{H}} \int_{\mathbb{R} \times \mathbb{R}} L(f(\mathbf{x}, \mathbf{y}), \mathbf{y}) dp(\mathbf{x}, \mathbf{y}) \quad (3.1)$$

for a loss function L . Given that the expectation appearing in the objective in 3.1 rarely can be computed analytically, and since optimizing in function space is infeasible, one normally proceeds by solving the problem with the following two steps

1. Draw an iid sample $\{\mathbf{x}_i, \mathbf{y}_i\}_{1 \leq i \leq \tilde{N}}$ of the random variables \mathbf{X} and \mathbf{Y} . Under the assumption that the sample is drawn in such a way that it is representative for the distribution of interest, $p(\mathbf{X}, \mathbf{Y})$, rely on the Law of Large Numbers (LLN), stating that the empirical expectation converges to the true one as $\tilde{N} \rightarrow \infty$.
2. Approximate f by a parametric family of functions, thus reducing the search space to the domain of a finite-element parameter vector $\boldsymbol{\theta}$.

Classic deep hedging, as first presented in [Buehler et al. \(2019\)](#), proceeds to solve the hedging problem in 2.21 essentially in the same way. The difference to the generic statistical learning problem presented above is that we have no labels \mathbf{Y} entering the problem. Rather, the loss depends only on the state of the market, here corresponding to \mathbf{x} , and the associated hedging decisions made in each of those states, $f(\mathbf{Y})$. In the notation above, the hedging problem thus may be written as

$$f^* := \arg \min_{f \in \mathcal{H}} \int_{\mathbb{R}} L(f(\mathbf{x})) dp(\mathbf{x}) \quad (3.2)$$

where one should think about the loss function L as representing a risk measure of the kind introduced above. Abstracting from this difference, deep hedging is really about approximating the theoretical optimization problem in 2.21 using steps 1) and 2) above to obtain a problem that can be solved in practice. However, rather than sampling empirically observed data in step 1), the idea is to simulate data, or market scenarios, which hopefully represent the true distribution of the future market state well. Proceeding in this way is

particularly useful when the amount of available data is sparse relative to the complexity of the function being approximated in step 2), which is often the case in practice.

First, denote by \mathbb{G} a generic *market generator*. One should think of this as an object that allows for simulation of the future state of relevant market variables under a given probability distribution. In the sequel, I will let \mathbb{G} represent the generator pertaining to the true data-generating process and $\hat{\mathbb{G}}$ a market generator that simulates market scenarios based on an *estimated* model. In an empirical setting, one, unfortunately, must employ $\hat{\mathbb{G}}$. At this point, it might appear strange to introduce this peculiar and somewhat abstract object. However, as will be clear, the empirical performance of deep hedging-based hedging strategies depends significantly on the selection of this object. How, and by how much, is precisely one of the research questions of this thesis, so formalizing its existence and where it shows up in the deep hedging problem seems reasonable.

As in step 1) above, and relying on the LLN, the risk measure appearing in 2.21 is then approximated by simulating $\tilde{B} \in \mathbb{N}$ independent market scenarios with one such market generator $\hat{\mathbb{G}}$. Denote by $\varepsilon_T^{\delta, \hat{\mathbb{G}}} \in \mathbb{R}^D$ the corresponding vector of terminal hedge errors pertaining to the hedging strategy δ when computed according to 2.20. After such an approximation, the optimal hedge strategy reads

$$\delta^* \simeq \arg \min_{\delta \in \mathcal{D}} \hat{\rho}(\varepsilon_T^{\delta, \hat{\mathbb{G}}}). \quad (3.3)$$

where the relation holds with equality in the limit $B \rightarrow \infty$. $\hat{\rho} : \mathbb{R}^{\tilde{B}} \mapsto \mathbb{R}$ is the empirical counterpart to the class of risk measures in 2.13.

However, this problem is still formulated as an optimization with respect to the optimal hedging policy in *function space* \mathcal{H} , i.e. an infinite dimensional problem. One possible solution to overcoming this problem is to proceed exactly as in point 2) above and parameterize the unknown functions $\{f_i(\mathcal{I}_i)\}_{0 \leq i < N}$ in 2.22 as $\{g_i^{\theta_i}(\mathcal{I}_i)\}_{0 \leq i < N}$ where $g_i : \mathbb{R}^D \mapsto \mathbb{R}^n$ for $i = 0, \dots, N - 1$.⁹ With this additional approximation in the dimension concerning the learning capacity of the regression functions g_t , the optimal sequence of optimal hedging decisions in 3.3 can be written as

$$\delta(\theta^*) \simeq \arg \min_{\theta \in \Theta} \hat{\rho}(\varepsilon_T^{\delta(\theta), \hat{\mathbb{G}}}), \quad \theta := (\theta_0, \dots, \theta_{N-1}) \quad (3.4)$$

Heuristically, we hence have the result that the optimal hedging policy in 2.21 may be approximated arbitrarily well by replacing the true risk measure 2.13 with its empirical counterpart obtained by computing

⁹Here, the setting with a Markovian market and a simple claim is assumed in the interest of brevity and for ease of exposition. The description readily carries over to the non-Markovian case in 2.22.

the loss across a set of simulated training hedge errors and training a number of parameterized regression functions to minimize this empirically estimated loss. Intuitively, the deep hedging approximation algorithm is hence asymptotically valid in the number of simulated samples B and the approximation, or learning, capacity of the regression functions $\left\{g_i^{\theta_i}(\mathcal{I}_i)\right\}_{0 \leq i < N}$.

Until now, we have remained agnostic concerning the choice of parametric family for the regression functions g , and the kind of data-driven hedging methodology described above places absolutely no restrictions on the choice of parametric function. Motivated by the Universal Approximation Property (UAP), this thesis proceeds as in [Buehler et al. \(2019\)](#) and essentially the remainder of the related literature by focusing on the class of deep neural networks as functional approximators. The following section describes why neural networks are sensible candidate regression functions in this setting and explains the deep hedging parameter estimation, also known as training, problem in detail.

3.1 Neural Networks as Policy Function Approximators

When a statistical learning problem is solved by parameterizing the unknown regression functions by deep neural networks, one often refers to the learning problem as *deep learning*. Although this fancy name does not change the nature of the problem, this thesis shall refer to this version of the statistical learning problem in the same way. There are different versions of the neural network. This section covers two of them, both used in the empirical section of the thesis, namely the Feed-Forward Neural Network (FFNN) and the Long Short-Term Memory Network (LSTM). However, to avoid boring the reader excessively with theory, which can be found in any standard textbook on the topic, the theory will be presented in the specific context of the deep hedging problem.

FFNN

Employing a FFNN for the hedging problem amounts to setting $g_i^{\theta_i}(\mathcal{I}_i) = \mathcal{NN}_{\theta_i}(\mathcal{I}_i)$ for $i = 0,..,N - 1$ where $\mathcal{NN}_{\theta_i} : \mathbb{R}^D \mapsto \mathbb{R}^n$ is a neural network that applies, in an alternating fashion, the following series of affine and non-affine functional transformations to the input vector $\mathbf{z}_0^i := \mathcal{I}_i$

$$\begin{aligned} \mathbf{z}_j^i &= a_j (\mathbf{W}_j^i \mathbf{z}_{j-1}^i + \mathbf{b}_j^i), \quad j \in \{1,..,L\} \\ \mathcal{NN}_{\theta_i}(\mathcal{I}_i) &:= \mathbf{z}_L^i. \end{aligned} \tag{3.5}$$

In the data science literature, $a_j^i : \mathbb{R} \mapsto \mathbb{R}$, $j = 1,..,L$ are typically referred to as activation functions that may be linear or non-linear. It is implicitly understood that these functions are applied elementwise

when given a non-scalar input. In this thesis, I always employ the ReLu activation function for the layers a_1, \dots, a_{L-1} , which is equivalent to setting $a_j(x) = (x)^+$ for $j = 1, \dots, L - 1$. To output the actual hedge, one may use the identity function as activation in the output layer, i.e., $a_L(x) = x$. However, I find that there is no need to challenge the model excessively and choose to instead truncate the hedge by means of a modified logistic mapping of the form $a_L(x) = \underline{\delta} + \frac{\bar{\delta} - \underline{\delta}}{1 + \exp(-x)}$, where $\bar{\delta}$ and $\underline{\delta}$ are natural upper, respectively, lower bounds for the hedge. For instance, for a short call option, I set $\bar{\delta} = 1$ and $\underline{\delta} = 0$. More generally, this type of transformation may be used to ensure that the learned strategy of the network belongs to a given admissible set \mathcal{D} . $\mathbf{W}_j^i \in \mathbb{R}^{d_j \times d_{j-1}}$ and $\mathbf{b}_j^i \in \mathbb{R}^{d_j}$, $j = 1, \dots, L$, are referred to as the weight matrices and bias vectors, respectively.

To maintain consistency, we must have that $d_0 := D$ is the dimensionality of the input vector and $d_L := n$ is the number of hedge assets. Although case-dependent, one may think of the input vector as containing for instance the logarithm of the stock price, i.e. $\mathcal{I}_i = (\log S_{t_i})$. By stacking the parameters appearing in each layer as $\psi_j^i := \text{vec}(\mathbf{W}_j^i) \oplus \mathbf{b}_j^i$, the complete set of parameters appearing in the optimization problem 3.4 reads

$$\boldsymbol{\theta}_i := \left(\psi_1^\top, \dots, \psi_L^\top \right)^\top \in \mathbb{R}^{\sum_{k=1}^L d_k(1+d_{k-1})}, \quad i \in \{0, \dots, N-1\} \quad (3.6)$$

Notice that, in this formulation, a separate neural network is used to approximate the optimal hedge policy function at each point in time. In this case, the time to expiry of the hedged portfolio assets is usually omitted for obvious reasons. However, since even just a single FFNN often consists of several hundred thousand parameters, this method becomes infeasible as the hedge frequency increases, corresponding to $N \rightarrow \infty$. An alternative is to include time to maturity in the input vector \mathcal{I}_i and use the same network for all time stamps by fixing $g_i^{\boldsymbol{\theta}_i} = g^{\boldsymbol{\theta}}$ as in e.g. [Carboneau and Godin \(2021a\)](#).

One notable drawback of the FFNN is that it carries no sense of memory. For instance, in the specification above, the FFNN at time step t_i has no clue about the state of the market or the holding in the hedge asset at time t_{i-1} . This is perfectly fine for Markovian markets and simple non-path-dependent derivatives where the current state leaves any other information redundant. However, for instance in the presence of a positive transaction cost process as defined in 2.19, $\delta_{t_{i-1}}$ contains relevant useful information when picking the hedge position at time t_i . The case of a non-Markovian market is also covered in [Horvath et al. \(2021\)](#) who propose an interesting and simple modification to the vanilla FFNN that facilitates carrying information over time with little additional model complexity. For a given fixed initial information set \mathcal{I}_i for $i = 0, \dots, N-1$ as above, the modified network, which I dub the Semi-Recurrent Feed-Forward Neural Network (SR-FFNN),

consists of the equations¹⁰

$$\begin{aligned}\mathbf{z}_j^i &= a_j (\mathbf{W}_j^i \mathbf{z}_{j-1}^i + \mathbf{b}_j^i), \quad j \in \{1, \dots, L\} \\ \boldsymbol{\delta}_{t_i} &= \mathcal{NN}_{\boldsymbol{\theta}_i}(\mathcal{I}_i) := \mathbf{z}_L^i [1 : n] \\ \tilde{\mathcal{I}}_i &:= \mathbf{z}_L^i [n+1 : n+p]\end{aligned}\tag{3.7}$$

where the initial input vector in each network is dynamically updated by appending the output from the previous network, i.e. $\mathbf{z}_0^i := \mathcal{I}_i \otimes \tilde{\mathcal{I}}_{i-1}$ for $i = 0, \dots, N-1$ with $\tilde{\mathcal{I}}_{-1} := \emptyset$. The dimension of the process $\tilde{\mathcal{I}}$, which can be considered a latent state process without a specific financial interpretation, is $p \in \mathbb{N}$. Under this specification, the output dimension of the last layer must be increased to $d_L = n+p$. The idea is that the network must learn during the optimization phase which information to carry from one time step to the next. This also avoids the need to manually engineer new features for different types of path-dependent derivatives and non-Markovian models, which is important for any serious large-scale implementation of the method.

LSTM

Another viable approach to adding memory to the neural network is to use generic *recurrent neural networks*, which are essentially networks whose architecture is designed to carry information across time. The LSTM network due to Hochreiter and Schmidhuber (1997) covered here is a specific type of recurrent network that avoids the so-called vanishing gradient problem, which is known to hinder learning long-term dependencies. The network consists of a sequence of *cells* lstm_i^θ for $i = 0, \dots, N-1$. Each cell outputs both the hedge and a latent state to be used as input for the cell at the next time step. In that sense, the network is conceptually similar to the SR-FFNN, particularly if one enforces that the SR-FFNN weights be fixed for all time steps. Formally, we set $g_i^{\theta_i}(\mathcal{I}_i) = a_L(\text{lstm}_i^\theta(\mathcal{I}_i)) \in \mathbb{R}^n$ for $i = 0, \dots, N-1$ where $\text{lstm}_i^\theta : \mathbb{R}^D \mapsto \mathbb{R}^n$ is an *LSTM cell*. The specific structure of each cell is

$$\begin{aligned}\boldsymbol{\delta}_{t_i} &= \text{lstm}_i^\theta(\mathcal{I}_i) = \mathbf{o}_{t_i} \circ \tanh(\mathbf{c}_{t_i}) \\ \mathbf{c}_{t_i} &= \mathbf{f}_{t_i} \circ \mathbf{c}_{t_{i-1}} + \tilde{\mathbf{i}}_{t_i} \circ \tanh(\mathbf{W}_c \mathbf{x}_{t_i} + \mathbf{U}_c \mathbf{h}_{t_{i-1}} + \mathbf{b}_c) \\ \mathbf{o}_{t_i} &= \sigma_g(\mathbf{W}_o \mathbf{x}_{t_i} + \mathbf{U}_o \mathbf{h}_{t_{i-1}} + \mathbf{b}_o) \\ \tilde{\mathbf{i}}_t &= \sigma_g(\mathbf{W}_{\tilde{i}} \mathbf{x}_{t_i} + \mathbf{U}_{\tilde{i}} \mathbf{h}_{t_{i-1}} + \mathbf{b}_{\tilde{i}}) \\ \mathbf{f}_{t_i} &= \sigma_g(\mathbf{W}_f \mathbf{x}_{t_i} + \mathbf{U}_f \mathbf{h}_{t_{i-1}} + \mathbf{b}_f),\end{aligned}\tag{3.8}$$

¹⁰Square brackets indicate array indexation

where σ_g is the sigmoid function. It is important to note that the parameters, here defined as $\boldsymbol{\theta} := (\mathbf{W}_c, \mathbf{U}_c, \mathbf{b}_c, \dots, \mathbf{W}_f, \mathbf{U}_f, \mathbf{b}_f)$, are the same for all cells, which makes the network truly recurrent. In principle, several LSTM networks may be stacked to construct even deeper model architectures.

3.2 Optimization of Parameterized Hedge Policy Functions

Especially for the class of parametric models described above, the optimization problem in 4.1 is non-trivial due to the extensive dimensionality of the parameter vector. The idea of this section, hence, is to describe in detail the training procedure, which proceeds in the same way regardless of the specific parametric model used to approximate the hedge policy function.

In short, optimization of the model parameters $\boldsymbol{\theta}$ is performed numerically by a stochastic gradient descent (SGD) algorithm, which initializes the model parameters at $\boldsymbol{\theta}_0$ and iteratively updates them by gradient descent. Even for high-dimensional models, the model gradient may be effectively computed using back-propagation. That is essentially an algorithm that applies the chain rule in a backward fashion to compute the model gradient efficiently and has facilitated the successful use of deep neural networks with as many as millions of parameters in several applications in recent years.

In this thesis, I specifically optimize the parameters by use of a TensorFlow implementation of the Adaptive Moment Estimation (Adam) optimizer developed by Da (2014), which is a slight modification of the standard SGD algorithm. In practice, the model training specifically proceeds in the following steps¹¹

1. Simulate B paths of the prices of relevant hedge instruments using a model $\hat{\mathbb{G}}$, that is $\mathbf{S}_t^{(1)}, \dots, \mathbf{S}_t^{(B)}$ and features $\mathcal{I}_t^{(1)}, \dots, \mathcal{I}_t^{(B)}$ for $t \in \{t_0, \dots, t_N\}$. Note that $\mathbf{S}_{t_0}^{(b)}$, and $\mathcal{I}_{t_0}^{(b)}$ contains, respectively, the initial prices of hedge instruments and market information and is common to all batches b .
2. Split the simulated paths into $M := B/\tilde{B}$ batches defined as $\mathbb{B}_j = \left\{ \left\{ \mathbf{S}_{t_s}^{(k)}, \mathcal{I}_{t_s}^{(k)} \right\}_{s=0}^N \right\}_{k=(j-1)\tilde{B}}^{j\tilde{B}}$ for $j = 1, \dots, M$. \tilde{B} is also referred to as the *batch size* and M the number of batches.
3. Let the current batch number $j = 1$, the number of full sample iterations epoch = 0, the number of gradient descent updates $l = 0$ and initialize the parameters at $\boldsymbol{\theta}_0$. All biases in neural networks are initialized at zero, and weights are initialized using the Glorot uniform initializer.
4. Take the batch \mathbb{B}_j and use the strategy implied by the current parameters $\boldsymbol{\delta}(\boldsymbol{\theta}_l)$ to calculate an empirical estimate of the hedge error in 2.20 for $k = (j-1)\tilde{B}, \dots, j\tilde{B}$. Assuming a zero interest rate

¹¹Here, the training procedure is described for standard SGD for ease of exposition.

$r = 0$, each hedge error can be computed as

$$\varepsilon_k = \bar{p} + \sum_{i=0}^{N-1} \boldsymbol{\delta}_{t_i}^{(k)} (\boldsymbol{\theta}_l)^\top \left(\mathbf{S}_{t_{i+1}}^{(k)} - \mathbf{S}_{t_i}^{(j)} \right) - \sum_{i=0}^N \left(\mathbf{c}_{t_i}^0 \mathbf{1}_{\{\Delta \boldsymbol{\delta}_{t_i}^{(k)}(\boldsymbol{\theta}_l) > 0\}} + \mathbf{c}_{t_i}^1 \mathbf{S}_{t_i}^{(k)} |\Delta \boldsymbol{\delta}_{t_i}^{(k)}(\boldsymbol{\theta}_l)| \right) - \chi. \quad (3.9)$$

5. Collect all ε_k 's in $\boldsymbol{\varepsilon}_j \in \mathbb{R}^{\tilde{B}}$ and calculate the empirically estimated risk of the loss distribution on the batch \mathbb{B}_j , e.g. for the entropic risk measure in 2.16

$$\hat{\rho}_j (\boldsymbol{\varepsilon}_j) = \lambda^{-1} \log \sum_{k=(j-1)\tilde{B}}^{j\tilde{B}} \tilde{B}^{-1} \exp(-\varepsilon_k). \quad (3.10)$$

6. Compute the model gradient $\nabla_{\boldsymbol{\theta}} \hat{\rho}_j (\boldsymbol{\varepsilon}_j)$ using backpropagation and update the parameters with gradient descent

$$\boldsymbol{\theta}_{l+1} \leftarrow \boldsymbol{\theta}_l - \eta_l \nabla_{\boldsymbol{\theta}} \hat{\rho}_j (\boldsymbol{\varepsilon}_j), \quad \eta_l \in \mathbb{R}^+. \quad (3.11)$$

7. If $j < M$ increment $j \leftarrow j + 1$. Otherwise, if the full sample has been iterated over, set $j = 1$ and increment epoch \leftarrow epoch + 1. Set $l \leftarrow l + 1$.

8. Iterate on 4) - 7) until a stopping criterion has been reached. Then set $\boldsymbol{\theta}^* = \boldsymbol{\theta}_l$.

Unless otherwise explicitly stated, this thesis applies the convention that the training sample size is $B = 2^{18}$, the batch size $\tilde{B} = 2^{14}$.¹² The learning rate η is initialized at a relatively high value $\eta = 0.01$ and an algorithm, which iteratively decreases the learning rate to $1 \cdot 10^{-8}$ as the speed of loss improvements declines, is applied. Training stops either if the average loss across all B training paths has not improved for 15 epochs, if epoch > 300 or if the learning rate has decreased below $1 \cdot 10^{-8}$.

¹²Note that it would be of particular importance to choose a sufficiently large batch size when evaluating risk in terms of an extreme tail risk measure.

4 Market Scenario Generation with Time-Varying Volatility Models

As is clear from Section 3, the empirical performance of the deep hedging algorithm naturally will depend greatly on the environment in which it is trained - in the notation introduced previously represented by the market generator \mathbb{G} . It would make sense to formally define the hedge optimization problem that one is facing in practice when deep hedging, which is to simultaneously optimize across optimal hedge policies for a given \mathbb{G} and across different market generators as in

$$\delta(\theta^*), \hat{\mathbb{G}} \simeq \arg \min_{\theta \in \Theta, \mathbb{G} \in \mathcal{G}} \hat{\rho} \left(\varepsilon_T^{\delta(\theta), \hat{\mathbb{G}}} \right) \quad (4.1)$$

where \mathcal{G} is the space of market generators under consideration. Posing this problem only makes sense from an empirical perspective since in any theoretical or simulated case, the market model \mathbb{G} is fixed. This section discusses different kinds of such market generators and how they can be estimated given observed data from the risk neutral (\mathbb{Q}) or statistical (\mathbb{P}) measures. Since the empirical section focuses on hedging derivatives written on a single stock, I focus here on models $\hat{\mathbb{G}}$ for univariate stock price dynamics. Given the intimate connection between volatility and options pricing and hedging, I focus on implementing observation-driven time-varying volatility models. For all time-varying volatility models under consideration, the time t logarithmic return is assumed to be described by the discrete-time model

$$\begin{aligned} r_t &:= \log S_t - \log S_{t-1} = z_t + \mu, \quad S_0 \in \mathbb{R}^+, \quad \mu \in \mathbb{R}, \\ z_t &:= \sqrt{h_t} \eta_t, \quad h_0 \in \mathbb{R}^+, \quad \eta_t \stackrel{iid}{\sim} \mathcal{C}(\Psi), \quad h_t \in \mathcal{F}_{t-1} \end{aligned} \quad (4.2)$$

where $\mathcal{C}(\Psi)$ is the return distribution conditional to h_t with parameters Ψ such that $\mathbb{E}[\eta_t] = 0$ and $\mathbb{E}[\eta_t^2] = 1$, implying that h_t is the variance of the time t log-return, conditional to information up to time $t-1$. The assumption that h_t is measurable w.r.t. time $t-1$ information is particularly convenient for estimation purposes as it allows for factorizing the likelihood function as a product of conditional densities. The family of GARCH models that have been introduced since the seminal work of Engle (1982) all belong to this model class. These models all postulate that h_t is measurable with respect to past returns, rather than the entire market filtration. They essentially infer the latent variance based on the squared daily returns. In the empirical section, I choose to work with the GJR-GARCH model from Glosten et al. (1993) with standardized Student's t innovations, i.e. $\eta_t \stackrel{iid}{\sim} t(\nu)$ with $\nu \geq 2$, as is also done in Buehler et al. (2019). This model accommodates the leverage effect by allowing for an asymmetric reaction in volatility to a large

positive respectively negative return. The GJR-GARCH recursion for the conditional return variance reads

$$h_t = \omega + \alpha z_{t-1}^2 + \gamma z_{t-1}^2 \mathbb{1}_{z_{t-1} < 0} + \beta h_{t-1}. \quad (4.3)$$

When estimating the model, I impose the standard constraints that $\omega, \alpha, \gamma, \beta \in \mathbb{R}^+$ for positivity of the conditional variance and $\alpha + 0.5\gamma + \beta \in (0, 1)$ for stationarity. In the remainder of the thesis, I sometimes refer to this model just as the GARCH model.

A major drawback for all types of classic GARCH models is that they rely on a volatility news measure, z_t^2 , that is a very noisy proxy of the true latent variance. Intuitively, this implies that volatility updates very slowly to new information from the market in these models, which is reflected in a high estimated autoregressive coefficient β in most cases.

It is not unlikely that one could benefit from employing a more sophisticated volatility model for options hedging. This is true both for deep hedging, where such a model could be used as a better scenario generator \mathbb{G} and for ad-hoc Practitioner's Black Scholes models where a filtered volatility is plugged in as volatility parameter in 5.2. Following Hansen et al. (2012), I hence try to incorporate information from high-frequency prices in the updating equation for the conditional volatility by modeling jointly the dynamics for the conditional variance h_t and a realized measure RM_t as follows

$$\begin{aligned} \log h_t &= \omega + \alpha \log RM_{t-1} + \beta \log h_{t-1}, \\ \log RM_t &= \xi + \varphi \log h_t + \tau(z_t) + u_t. \end{aligned} \quad (4.4)$$

Here, the first equation is the state equation used to filter the latent variance, and the second is referred to as a measurement equation. The important difference to the GARCH model family is the introduction of the realized measure, RM_t , which is supposed to be a consistent estimator of the quadratic variation of the price process. When there are $K \in \mathbb{N}$ intra-daily log returns $r_{t,1}, \dots, r_{t,K}$ on a given day t , the quadratic variation (QV) of the stock price process S is defined as (see e.g. Shephard et al. (2008))

$$[\log S]_t := \underset{K \rightarrow \infty}{\text{plim}} \sum_{k=1}^K r_{t,k}^2. \quad (4.5)$$

In absence of market microstructure noise, the quadratic variation may be consistently estimated by the realized variance, which is obtained essentially by truncating the above sum at finite K . However, the estimator is inconsistent in real markets where noise is present. A popular way to mitigate the adverse effects of said noise is to employ a subsampling scheme where returns are sampled at e.g. 5 min. frequency. I

choose to use instead the realized kernel estimator presented in [Shephard et al. \(2008\)](#) that is a noise-robust estimator of the quadratic variation since it is often found as a more exact estimator of the QV compared to the sub-sampled realized variance estimator. I denote the realized kernel estimator on a given day t as RK_t in the remainder of the thesis.

Intuitively, the realized measure, here RK_t , takes the role of the squared return r_t^2 in the GARCH model. As in [Hansen et al. \(2012\)](#), I prefer to work with the logarithmic specification of the model since it reduces the degree of heteroskedasticity of the error term u_t in the measurement equation by improving the functional form.¹³

Notice that if the only purpose of the model were to filter the latent variance, there would be no need to introduce the measurement equation for the realized variance. However, since one must simulate future realizations of S_t to train the deep hedging model, a full characterization of the distribution of (h_t, RK_t) is required. This also explains why a model such as the Heterogeneous Auto-Regressive (HAR) model of [Corsi \(2009\)](#) is not sufficient in itself to train a deep hedging model as it characterizes the distribution of the variance, without providing any link to the conditional variance of daily (close-to-close) returns.

The function $\tau : \mathbb{R} \mapsto \mathbb{R}$ is also referred to as the leverage function since it explicitly controls the relation between return shocks and the variance. When implementing the model empirically, I fix the function as $\tau(z) = \tau_1 z + \tau_2 (z^2 - 1)$ as in [Hansen et al. \(2012\)](#). One would normally expect to observe $\tau_1 < 0$ and $\tau_2 > 0$ to capture the typically negative relation between returns and their variance.

In terms of estimating the model, I follow [Hansen et al. \(2012\)](#) in assuming that $z_t \sim \mathcal{N}(0, 1)$ with $\sigma_u^2 \in \mathbb{R}^+$, $u_t \sim \mathcal{N}(0, \sigma_u^2)$, which allows me to estimate the model parameters $\Xi := (\omega, \alpha, \beta, \xi, \tau_1, \tau_2, \xi, \mu)$ by maximizing the quasi log-likelihood

$$\Xi^* = \arg \max_{\Xi} \sum_{t=1}^{\hat{n}} (\log h_t + z_t^2/h_t + \log \sigma_u^2 + u_t^2/\sigma_u^2), \quad (4.6)$$

where $\hat{n} \in \mathbb{N}$ is the size of the estimation sample. I impose the constraint that $\beta + \alpha\phi < 1$ during the numerical optimization procedure.

In order to simulate from either the GJR-GARCH or the Realized-GARCH models, I just use their respective definitions in [4.2](#), [4.3](#) and [4.4](#). I always initialize the simulations with the latest filtered variances available upon the start of the simulation.

¹³If one wants to work with an equivalent model from the GARCH family specified in log terms, the EGARCH model is the best bet. The GJR-GARCH model presented here does not immediately admit a log specification due to the possibility of a zero daily return. The Realized-GARCH model does not have this problem since the realized measure is always positive.

5 Continuous-Time Markov Models for Option Pricing and Hedging

This section presents the robust lineup of alternative, and more traditional, hedge models often applied in the industry due to their analytically tractable properties and, especially for the Black & Scholes model, easy interpretability for traders. These models belong to the class of continuous-time Wiener-driven models introduced in Section 2.1. In addition to serving as reasonable benchmark models, I will also exploit that the model dynamics can be easily discretized and subsequently employed as market scenario generators to train the deep hedging agent.

5.1 Hedging with Black-Scholes

The celebrated Black & Scholes (BS) option pricing model was first presented in [Black \(1976\)](#) and is still a popular choice among practitioners due to its simplicity. However, substantial empirical evidence has ruled out many of its embedded assumptions on the dynamics of stock prices, such as absence of jumps, constant volatility, and Gaussian of log-price increments. The model postulates diffusive dynamics for the stock price as in 2.1, but with constant drift rate $\mu \in \mathbb{R}$ and volatility parameter $\sigma \in \mathbb{R}^+$. Under the physical measure \mathbb{P} , the stock price is specifically assumed to evolve in continuous time as a geometric Brownian motion (GBM) according to the SDE

$$dS_t = \mu S_t dt + S_t \sigma dW_t, \quad S_0 := s_0 \in \mathbb{R}^+. \quad (5.1)$$

When the claim χ is a standard call option, and under the assumption of a constant riskless interest rate and a constant dividend yield, the conditional expectation in 2.5, famously, can be computed in closed form. The result is *the* BS formula, in the sequel denoted by the function $p_t^{BS}(s, K, \tau; \sigma)$ when evaluated for a current stock price s , volatility parameter σ and for a call option with time to maturity (TTM) τ and strike K .¹⁴ The formula is given in Appendix (E). Associated to this model is also the important notion of implied volatility (IV). For a given call price $p \in \mathbb{R}^+$ quoted at stock price s , strike K and TTM τ , the implied volatility at strike K and TTM τ , $IV(K, \tau)$, is defined as the implicit solution to the equation $p_t^{BS}(s, K, \tau; IV(K, \tau)) = p$, which can be found with simple numerical methods.¹⁵ The market-implied IV surface obtained by evaluating the IV on a grid of strikes and times to maturity for market-quoted call prices is famously known to be non-constant and exhibit a downward-sloping *smile* in the strike dimension, providing evidence against the assumptions of the model.¹⁶ On the contrary, the smile is often interpreted as providing evidence for a market-perceived presence of excess kurtosis in returns, partly due to a non-zero

¹⁴The corresponding put price can be found using put-call parity.

¹⁵I use the extremely efficient and tailor-made algorithm from [Jäckel \(2015\)](#).

¹⁶See e.g. [Kokholm and Stisen \(2015\)](#) or the illustrations in Section 7.3.

correlation between stock returns and its variance and partly due to jumps in stock prices. An extensive literature has documented the presence of both of these phenomena in observed financial time series.

Regarding hedging, it can be noted that there is a single tradable asset and one Wiener-driven source of stochasticity, implying that the model is complete, i.e. $n = d$ in the notation of Section 2.1. The unique risk neutral measure is obtained by letting $\varphi_t = (-\frac{\mu-r}{\sigma})$, and the theoretically optimal hedge that replicates a call option is the well-known Black-Scholes delta

$$\delta_t^{BS}(s, K, \tau; \sigma) := \nabla_s p_t^{BS}(s, K, \tau; \sigma). \quad (5.2)$$

The analytical expression is available in Appendix (E).

Practitioners Black-Scholes

In acknowledgment of the unfortunate assumptions made about the stock price dynamics based on which the delta is calculated, ad-hoc adjustments are often made to the model-implied delta in 5.2 when hedging with the Black & Scholes model in practice. To mitigate the unrealistic assumption of a constant volatility, one popular such adjustment is to vary the volatility parameter σ entering in the calculation of the delta in 5.2 by hedging with the IV of the option. Since empirically observed implied volatilities are non-constant in the strike and time to maturity dimensions, this is an ad-hoc way to effectively introduce time-variation in the volatility in both time and asset space. This so-called Practitioners Black-Scholes (PBS) hedging strategy may be written as

$$\delta_t^{PBS}(K, \tau) := \nabla_s p_t^{BS}(s, K, \tau; IV(K, \tau)). \quad (5.3)$$

I use the regression-smearing technique in [Yin and Moffatt \(2019\)](#), similar in spirit to the approach in [Dumas et al. \(1998\)](#), to interpolate in the implied volatility surface. The procedure for calculating the relevant PBS IV for an option with strike K and TTM τ goes as follows

1. With $N_{options}$ observed option quotes at hand, fit the following model to the corresponding observed implied volatilities with a least squares regression

$$\log IV(K_i, \tau_i) = \theta_0 + \theta_1 K_i + \theta_2 K_i^2 + \theta_3 \tau_i + \theta_4 \tau_i^2 + \theta_5 \tau_i K_i + \eta_i, \quad i = 1, \dots, N_{options}. \quad (5.4)$$

2. Denote the fitted regression function as $\widehat{\log IV}$ and compute

$$\tilde{c}(K, \tau) := N_{options}^{-1} \sum_{i=1}^{N_{options}} p_t^{BS} \left(s, K, \tau; \exp \left(\widehat{\log IV}(K, \tau) + \eta_i \right) \right). \quad (5.5)$$

3. Compute the implied volatility of $\tilde{c}(K, \tau)$ and define it as $IV(K, \tau)$ to be used in 5.3.

Alternatively, the volatility parameter to be used for calculating the delta may be based on the statistical measure. As in Buehler et al. (2019), the empirical section also includes a PBS model where the volatility plugged into the BS delta in 5.2 is the volatility filtered from a model belonging to the GARCH model class covered in Section 4. This facilitates a comparison to the empirical results obtained in the original deep hedging paper .

5.2 Hedging and Simulating with the Heston Model

Although the Black & Scholes model is popular among practitioners, substantial research has gone into developing more sophisticated models with more realistic dynamics for the underlying asset and which can fit more closely observed option prices, also referred to as "fitting the smile". Although not the most modern or fancy of its kind, the popular Heston model originally presented in Heston (1993) is one such model. Rather than assuming a constant volatility, this model assumes volatility to be time-varying and to be driven by a stochastic process of its own. The exact specification of the variance process is the mean-reverting Cox-Ingersoll-Ross (CIR) process with long-run level $\theta^{\mathbb{P}} \in \mathbb{R}^+$, speed of mean reversion $\kappa \in \mathbb{R}^+$ and the parameter $\varepsilon \in \mathbb{R}^+$.¹⁷, which controls the volatility of volatility. Under the historical measure, the model dynamics are given by the following bivariate system for the Markovian pair (S_t, v_t)

$$\begin{aligned} dS_t &= \mu S_t dt + S_t \sqrt{v_t} dW_t, \quad S_0 = s_0 \in \mathbb{R}^+ \\ dv_t &= \kappa^{\mathbb{P}} \left(\theta^{\mathbb{P}} - v_t \right) dt + \varepsilon \sqrt{v_t} d\widetilde{W}_t, \quad v_0 = \bar{v} \in \mathbb{R}^+. \end{aligned} \quad (5.6)$$

A non-zero correlation between the two Wiener drivers is allowed to accommodate the leverage effect often observed in financial time series, i.e. $\langle W_t, \widetilde{W}_t \rangle = \tilde{\rho} \in (-1, 1)$. One notable difference is that the model is incomplete due to the introduction of an additional source of uncertainty, \tilde{W} . In the notation of Section 2.1, the one element of the Girsanov kernel φ_t pertaining to the variance process, let us denote it by φ_t^v , is not

¹⁷Strictly speaking, one should impose the so-called Feller condition $\varepsilon \in (0, \sqrt{2\kappa^{\mathbb{P}}\theta^{\mathbb{P}}})$, see also Feller (1971), which ensures that the variance stays strictly positive with probability one. I do not impose the condition in this thesis. As in Kokholm and Stisen (2015), I find the restriction to be binding on almost every trading day and to restrict the parameter solution space significantly. Not imposing the condition can be seen as an ad hoc way to deal with the inherent misspecification of the model.

identified without further restrictions on the model. From an economic point of view, the market price of variance risk must be selected by the user of the model, possibly based on further economically motivated restrictions. The only formal restriction that must be placed a priori on the market price of variance risk to preserve the affine structure of the model under an equivalent change of measure is that $\varphi_t^v = \frac{\lambda}{\varepsilon} \sqrt{v_t}$ for $\lambda \in \mathbb{R}$.¹⁸ Under this assumption, the risk-neutral variance dynamics are of the CIR type as in 5.6, but with parameters κ^Q and θ^Q replacing κ^P and θ^P in the variance dynamics and r replacing μ in the stock price drift. As shown in Appendix (B), the relation between the risk-neutral and physical parameters can be written as

$$\kappa^Q = \kappa^P + \lambda, \quad \theta^Q = \frac{\kappa^P \theta^P}{\kappa^P + \lambda}. \quad (5.7)$$

Different choices of λ give rise to different changes in the variance dynamics as a result of the measure change. Typically, a negative variance risk premium ($\lambda < 0$) is observed, meaning that the market implies a slower speed of variance mean reversion and a higher stationary level of variance (e.g. Bakshi and Kapadia (2003)). Section 5.9 below describes the choice of EMM employed in the empirical evaluation of deep hedging.

Calibration of model parameters

Practitioners in the business of pricing exotic OTC options or hedging often infer the EMM from the options market, corresponding to imposing the additional informal restriction on the model that the option prices generated by the model should correspond to those quoted in the market. In this way, the risk-neutral parameters $\theta_{Heston}^Q := [\kappa^Q, \theta^Q, \bar{v}, \varepsilon]$ ¹⁹ are inferred directly from market prices.

However, even for the case of simple European calls and puts χ , the risk-neutral expectation in 2.5 unfortunately cannot be computed analytically. To calibrate the risk-neutral parameters in the model, it is customary to instead use Fourier inversion, a numerical integration technique that allows for rapid computation of option prices in models for which the characteristic function (c.f.) is available. Fortunately, the Heston model belongs to the class of affine models as defined in Duffie et al. (2000), for which the c.f. is available. For reasons of numerical stability and computational speed, the Lewis formulation of the call option pricing formula, see e.g. Schmelzle (2010), is used in the empirical section as opposed to the original formulation in Heston (1993). For a call option with strike K , TTM $\tau = T - t$, current stock price s and

¹⁸This assumption is completely standard and also imposed in the original paper Heston (1993).

¹⁹Formally, the current variance \bar{v} is not a parameter, but the current state of a latent stochastic process. Here, it is taken to be a parameter since, in practice, its value must be calibrated based on data from the statistical measure or the market-implied EMM.

risk-neutral parameters $\boldsymbol{\theta}^{\mathbb{Q}} = (\kappa^{\mathbb{Q}}, \theta^{\mathbb{Q}}, \tilde{\rho}, \varepsilon, \bar{v})$, the pricing formula reads²⁰

$$c^{Lewis}(s, K, \tau; \boldsymbol{\theta}^{\mathbb{Q}}) = se^{-q\tau} \left(1 - \frac{e^{k/2}}{\pi} \int_0^\infty \frac{du}{u^2 + 1/4} \operatorname{Re} \left[e^{-iuk} \phi_\tau(u - 0.5i; \boldsymbol{\theta}^{\mathbb{Q}}) \right] \right), \quad k := \log \frac{K}{se^{(r-q)\tau}}, \quad (5.8)$$

where $\phi_T : S_X \subseteq \mathbb{C} \mapsto \mathbb{C}$ is the characteristic function of the standardized log price defined as $\log \frac{S_T}{S_t e^{(r-q)\tau}}$, conditional to the current Markov state being $(S_t, V_t) = (s, \bar{v})$. The constant dividend yield is q and r is the relevant bond yield. S_X is the set of complex numbers, also called the strip of regularity, for which the c.f. is well defined. The expression for the relevant Heston c.f. can be found in Appendix (D).

With the ability to price liquidly quoted call options,²¹ the risk-neutral parameters may then be calibrated by minimizing a weighted sum of squared pricing errors across all options. Although there are many viable options (no pun intended), the weight is here set as the inverse of the price to penalize harder pricing errors for cheaper options

$$\boldsymbol{\theta}_{Heston}^{\mathbb{Q}} := \arg \min_{\boldsymbol{\theta}} \sum_T \sum_K \frac{(c_{market}(s, K, T) - c^{Lewis}(s, K, T; \boldsymbol{\theta}))^2}{c_{market}(s, K, T)}. \quad (5.9)$$

The incompleteness of the model implies that, even in the idealized model setting, perfect replication of contingent claims is impossible without introducing an additional traded asset. One may complete the model by adding an additional hedge asset to the market, for instance a call option or a variance swap, whose dynamics depend on \widetilde{W} , as is done in e.g. Buehler et al. (2019). That option is, however, not pursued in this thesis. To hedge only with the stock as hedge instrument, one could then, despite the incompleteness of the model, try to use the model delta as in the Black-Scholes model, which is defined as the first derivative of 5.8 w.r.t. the stock price, i.e.

$$\delta_t^{Heston}(s, K, T; \boldsymbol{\theta}_{Heston}^{\mathbb{Q}}) := \nabla_s c^{Lewis}(s, K, \tau; \boldsymbol{\theta}_{Heston}^{\mathbb{Q}}). \quad (5.10)$$

However, unlike the Black & Scholes model, the naïve Heston model delta is in general not risk-minimizing, as is also pointed out in e.g. Poulsen et al. (2009) who propose the following alternative locally risk-minimizing

²⁰The pricing formula can be modified to price call options in more general Affine Jump-Diffusion models just by modifying the c.f. The pricing formula is valid under the assumption of a constant dividend yield q and interest rate r .

²¹Put option prices are converted to call prices using put-call parity before calibration.

hedging strategy²²

$$\delta_t^{H,local} \left(s, K, T; \boldsymbol{\theta}_{Heston}^{\mathbb{Q}} \right) := \nabla_s c^{Lewis} \left(s, K, T; \boldsymbol{\theta}_{Heston}^{\mathbb{Q}} \right) + \tilde{\rho} \varepsilon \frac{\nabla_v c^{Lewis} \left(s, K, T; \boldsymbol{\theta}_{Heston}^{\mathbb{Q}} \right)}{s}. \quad (5.11)$$

Intuitively, while the raw delta in 5.10 ignores the fact that volatility and stock prices may be correlated, the hedge in 5.11 adds a skew correction term, which corrects for the leverage effect. That is, the risk-minimizing hedge is an attempt to correct for volatility risk. Doing so is more consistent with the model itself, which postulates variance to be stochastic and correlated with the stock price. Although this strategy is not designed to minimize the global hedging risk under which the strategies are evaluated, it is arguably a more serious attempt at presenting a risk-minimizing hedge in a stochastic volatility model where only trading in the underlying asset is allowed. Other authors, such as Hull and White (2017) have suggested adding a similar skew-correction, also known as a *vega* hedge, to the PBS delta hedge, despite it being inconsistent with the constant volatility assumption of the Black-Scholes model. That option is not pursued in this thesis. The raw and skew-corrected Heston delta-hedging strategies are included in the empirical comparison in Section 8. I compute the relevant Greeks for the Heston model using Fourier inversion by taking the relevant partial derivatives in 5.8. The relevant expressions are given in Appendix (D).

Leveraging the Heston Model as Deep Hedging Market Generator

Following the idea that options markets are generally considered forward-looking by nature, a hypothesis could be that utilizing information from this market in the deep hedging training procedure could improve its empirical performance when compared to relying solely on the statistical measure for scenario generation. When the market price of variance risk is low, the risk-neutral parameters $\boldsymbol{\theta}_{Heston}^{\mathbb{Q}}$ calibrated according to the procedure described above are close to the ones governing the variance dynamics in the statistical measure, $\boldsymbol{\theta}_{Heston}^{\mathbb{P}}$. In particular, the options market might contain valuable information about the volatility of volatility ε and the skewness parameter $\tilde{\rho}$, both of which, by the Girsanov theorem, are supposed to be invariant to the change of measure from \mathbb{Q} to \mathbb{P} . Both parameters are of first-degree importance for hedging purposes since they control the implied skewness and kurtosis in the return distribution.

Ideally, we want to generate scenarios for the stock price and variance under the physical dynamics. The variance process generally differs from what is implied by the options market whenever the variance risk premium is non-zero, i.e. $\lambda \neq 0$ in 5.7. Still, there is the notion that the options market is forward looking,

²²Strictly speaking, the hedge should be computed under a so-called minimal martingale measure, which is generally different from the risk-neutral measure. However, it is shown in Poulsen et al. (2009) that the penalty for hedging under the market-implied EMM is small.

in which case practitioners still might prefer to simulate the variance dynamics under the options market-implied dynamics. The idea to employ a stochastic volatility model calibrated to the options market as a market scenario generator for empirical deep hedging purposes is in fact also pursued in [Mikkilä and Kanniainen \(2021\)](#). However, there is no mention of the potential issue of a non-zero variance risk premium in their paper.²³ The estimation of λ is a research area of its own and is not pursued in this thesis. In fact, there is overwhelming evidence and economic intuition suggesting that λ is time-varying, see e.g. [Wu and Carr \(2007\)](#). Instead, Section 6.3 presents an analysis of the, in practice, highly relevant case where deep hedging is carried out under misspecified Heston model dynamics. The empirical section somewhat naively, and conveniently, enforces $\lambda = 0$ and examines deep hedging performance when market scenarios are generated under this assumption, i.e. under options market-implied variance dynamics.

To generate scenarios, I need to be able to simulate from the Heston model. Although the transition density for the CIR variance process in 5.6 is known to be non-central chi-square, simulation of the exact stock price process requires evaluation of special functions and Fourier inversion methods as described in [Broadie and Kaya \(2006\)](#). As a more straightforward alternative, I apply the following standard Euler scheme to simulate the system between a given point in time t_i and $t_{i+1} > t_i$

$$\begin{aligned}\log S_{t_{i+1}} &= \log S_{t_i} + (\mu - 0.5v_{t_i})(t_{i+1} - t_i) + \sqrt{v_{t_i}}B_i^{(1)}, \quad B_i^{(1)} \sim \mathcal{N}(0, t_{i+1} - t_i) \\ v_{t_{i+1}} &= v_{t_i} + \kappa^{\mathbb{P}}(\theta^{\mathbb{P}} - v_{t_i})(t_{i+1} - t_i) + \varepsilon\sqrt{v_{t_i}}(\tilde{\rho}B_i^{(1)} + \sqrt{1 - \tilde{\rho}^2}B_i^{(2)}), \quad B_i^{(2)} \sim B_i^{(1)}.\end{aligned}\tag{5.12}$$

As indicated, the bivariate Gaussian process may be generated using the Cholesky factorization. Other more accurate simulation schemes exist, such as the Milstein scheme, but the difference is negligible when the distance between two adjacent time points is small. Furthermore, since the variance process is not sampled from the exact CIR process, the sampled variance may turn negative. This unfortunate circumstance is mitigated by applying a reflecting assumption, meaning that I assign $v_t \leftarrow -v_t$ whenever the variance turns negative.

For deep hedging, it is generally not perfectly clear whether it is better to simulate the market dynamics under a martingale measure, that is in a drift-less world. If, historically, there has been a strong drift in the market, the deep hedging model may try to exploit the statistical arbitrage opportunities implicit in the simulations.. This can be risky since the estimation of the drift is notoriously difficult. The recently published paper [Buehler et al. \(2021\)](#) is concerned with how one may *remove* the drifts of market variables in black box market simulators, before training the deep hedging model. In the empirical section, I always

²³A footnote on p. 3 actually claims that their method "takes the volatility risk-premium into account", but this must be a typo since their only source of information for calibration purposes is options data.

estimate a physical drift and employ that estimate for simulating stock price paths. For the Heston model, I estimate the drift off the average past 5 year daily log returns.

6 Assessing the Impact of Model Risk on Deep Hedging

In this section, I test the deep hedging model in various controlled experimental settings. First, I focus on developing a fundamental understanding for how deep hedging works in a simple constant volatility environment and how the optimal strategy of a risk-averse agent differs from the classic delta hedge when time is discrete.

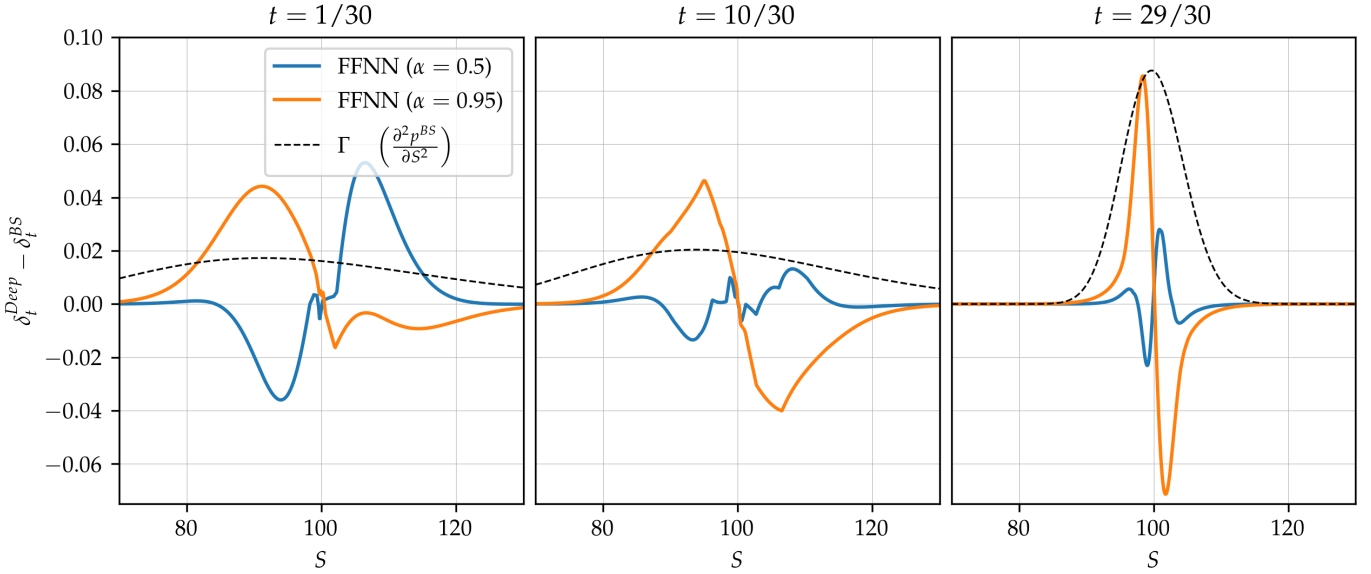
To the best of my knowledge, the entire literature on deep hedging, except the work in [Lütkebohmert et al. \(2021\)](#), assume a known stochastic market environment in simulated environments. Unfortunately, the underlying market dynamics are, however, not known in practice. I focus on analyzing the robustness of the deep hedging strategy towards model risk. Specifically, I ask the question to what extent one can expect deep hedging performance to deteriorate when the strategy is learned based on a misspecified underlying Heston or Black-Scholes model for the hedge asset. The answer to this question is already well known for popular delta (and vega) hedging strategies in Heston and Black-Scholes models and can be found in [Poulsen et al. \(2009\)](#) and [Ellersgaard et al. \(2017\)](#). Zero dividends and bond yields are assumed throughout the section.

6.1 Hedging a call option in a Known Black-Scholes environment

In the first experiment, assume a Black-Scholes environment with zero drift, $\mu = 0$, volatility $\sigma = 0.25$ and $s_0 = 100$. The hedged asset is a short position in an ATM call option with one month to expiry. Also, assume that transaction costs are absent. This is an almost-complete setting, with the only source of incompleteness coming from the discretization of time. In this environment, I train two different deep hedging models, both parameterized as neural networks with information set $\mathcal{I}_t = (\log S_t)$, $L = 2$ hidden layers and $d_1 = d_2 = 15$ neurons in each layer. The first model is trained to minimize the CVaR_{0.50} risk measure on 2^{18} paths simulated from this Black-Scholes model using the explicit solution to the SDE in [5.1](#). The second model is trained to minimize the CVaR_{0.95} risk measure. Subsequently, the hedging performance of the two deep hedging models is evaluated on 2^{19} new test paths simulated from the same model against a correctly specified BS delta hedge. A daily rebalancing frequency is assumed. Since, in this case, the only departure from the idealized and complete BS environment is the daily rebalancing frequency, the neural network strategy would be expected to resemble quite closely the delta hedging strategy in eq. [5.2](#). However, they should not be the same given that the Black-Scholes delta is not the optimal strategy for a risk-averse agent in the discrete time setting.

Figure [1](#) first compares the two learned deep hedging strategies to the Black-Scholes strategy on the 1st, 10th, and 29th rebalancing days and displays the Black-Scholes gamma.

FIGURE 1: DIFFERENCE BETWEEN DEEP HEDGING AND BLACK-SCHOLES HEDGING STRATEGIES



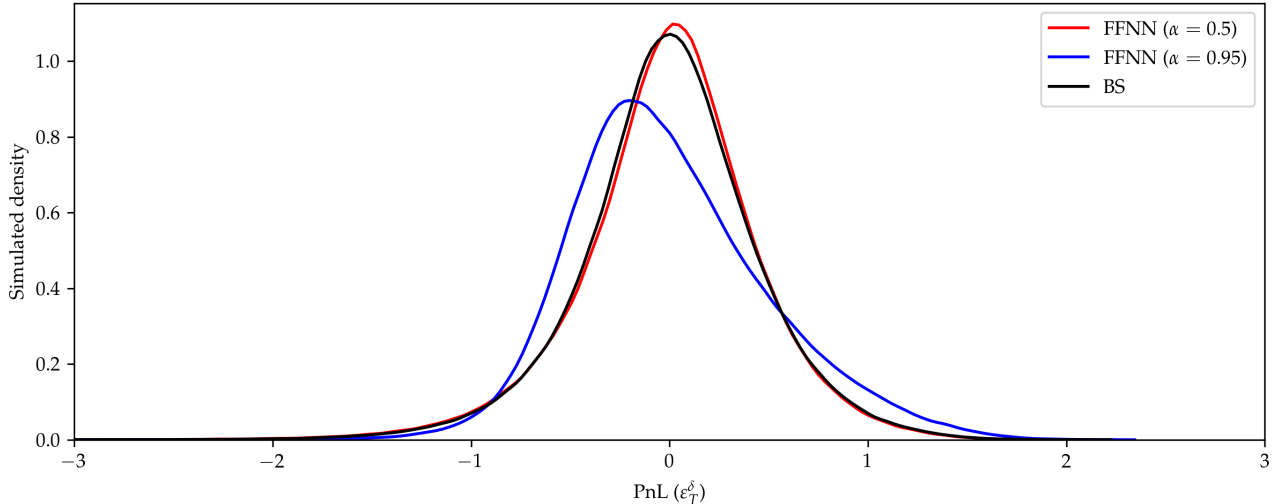
Note: Figure shows the difference in deep hedging strategies and the BS delta hedging strategy for two configurations of the deep hedging model trained to minimize, respectively, the CVaR_{0.5} and CVaR_{0.5} risk. The derivative being hedged is a short ATM call option with 1 month to expiry. The environment is Black-Scholes with zero drift, $\sigma = 25\%$ volatility for both training and evaluation purposes and a daily rebalancing frequency is assumed.

Just by observing the nature of the discretized Black-Scholes stock price paths and without being given any information about the model under which the paths are generated, the deep hedging model is able to improve slightly on the BS delta strategy as measured by the respective risk measure under which the model is trained.

When trained under a high risk-aversion, the deep hedging agent over (under) hedges OTM (ITM) options to limit tail risk. Intuitively, the discretization of the trading environment can be understood as having a similar effect as introducing sudden, unexpected jumps. During the training process, the deep hedging model observes, through experience, that this risk is present in the given market environment and seeks to navigate optimally under those conditions as measured by the choice of risk measure. When the option is ITM, the agent hence lowers her holdings of the underlying asset, compared to the continuous-time strategy, because of the fear that the stock price suddenly drops before the next rebalancing date. The same logic holds when the option is OTM and the agent's current stock holdings are low. In this case, she limits the risk of facing a high loss in the case of a large positive jump, which would trigger the counterparty to exercise the option, by increasing her holdings of the underlying stock slightly. As is clear from the figure, the differences are more pronounced when the rate of change in the continuous-time delta, i.e. the gamma, is high. This is sensible since the "jump" risk is at its highest when a frequent rebalancing is required to maintain delta neutrality.

Figure 2 compares the distributions of terminal hedge errors and the hedging strategy along a simulated

FIGURE 2: ESTIMATED KERNEL DENSITY OF HEDGE PNL



Note: Figure shows the estimated kernel density of out-of-sample simulated terminal hedging errors for two configurations of the deep hedging model, trained to minimize, respectively CVaR_{0.5} and CVaR_{0.95}. The derivative being hedged is a short ATM call option with 1 month to expiry. The environment is Black-Scholes with zero drift, 25% volatility for both training and evaluation purposes and a daily rebalancing frequency is assumed.

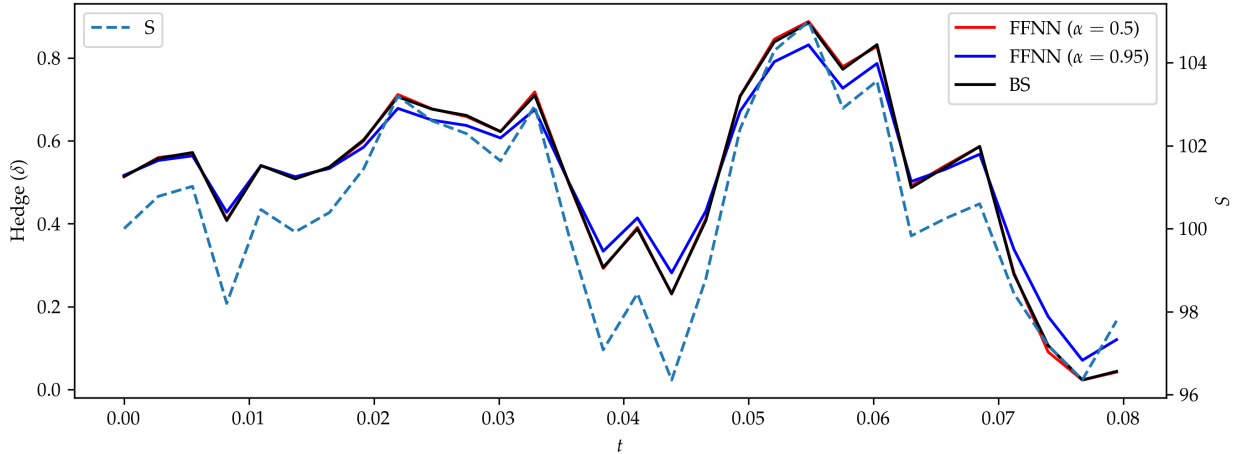
path. Table 1 makes apparent that deep hedging always improves upon the BS delta hedge when risk is measured in terms of the training objective. For the deep hedging strategies, the Table 1 displays the normalized difference

$$\Delta\rho(\mathcal{M}_1, \mathcal{M}_2) := \frac{\rho^{\mathcal{M}_1} - \rho^{\mathcal{M}_2}}{|\rho^{\mathcal{M}_2}|} \cdot 100 \quad (6.1)$$

when the alternative model \mathcal{M}_1 is the deep hedging model and the benchmark model \mathcal{M}_2 is BS model hedge.

Figure 3 compares the deep hedging and BS delta hedging strategies along a simulated path, confirming visually that the deep hedging strategy resembles closely the optimal continuous-time delta hedge. Although well known, these results are quite remarkable and illustrate the flexibility of the deep hedging approach; all one needs to optimize hedging strategies for real trading environments is a proper probabilistic representation of future possible market scenarios represented by the market generator \mathbb{G} and a corresponding featurization vector \mathcal{I}_t that carries information about the market and derivative states. As such, deep hedging really opens the door to including and optimizing the use of relevant information from the *statistical measure*. However, this naturally also implies that any practical implementation of deep hedging is subject to model risk and statistical uncertainty. The remainder of this section focuses on analyzing how deep hedging performs in different controlled experiments where the true data-generating process is unknown and deep hedging is performed under a misspecified model.

FIGURE 3: BLACK-SCHOLES HEDGE AND DEEP HEDGE ALONG A SIMULATED MODEL PATH



Note: Figure compares the hedging strategies for two configurations of the deep hedging model, trained to minimize, respectively $\text{CVaR}_{0.5}$ and $\text{CVaR}_{0.95}$. The derivative being hedged is a short ATM call option with 1 month to expiry. The environment is Black-Scholes with zero drift, 25% volatility for both training and evaluation purposes and a daily rebalancing frequency is assumed.

TABLE 1: SUMMARY OF SIMULATED HEDGE PNL DISTRIBUTION

	$\text{CVaR}_{0.0}$	MSE	SemiMSE	$\text{CVaR}_{0.99}$	$\text{CVaR}_{0.95}$	$\text{CVaR}_{0.75}$	$\text{CVaR}_{0.5}$
BS	-0.0	0.2	0.21	1.53	1.04	0.56	0.34
FFNN ($\alpha = 0.5$)	-72.67%	0.73%	6.47%	3.46%	3.07%	1.44%	-0.45%
FFNN ($\alpha = 0.95$)	36.82%	24.9%	-8.09%	-18.55%	-12.02%	4.16%	15.97%

Note: Table displays loss risk measures in a simulated Black-Scholes model when hedging a short 1-month ATM call option. The loss is centered at the continuous-time BS price for all models. For the PBS model, the loss displayed is the absolute loss. For deep hedging models, the figures displayed are the normalized risk differences as defined in 6.1 where \mathcal{M}_1 is the PBS strategy. The best performance for a given risk measure is indicated by bold typography.

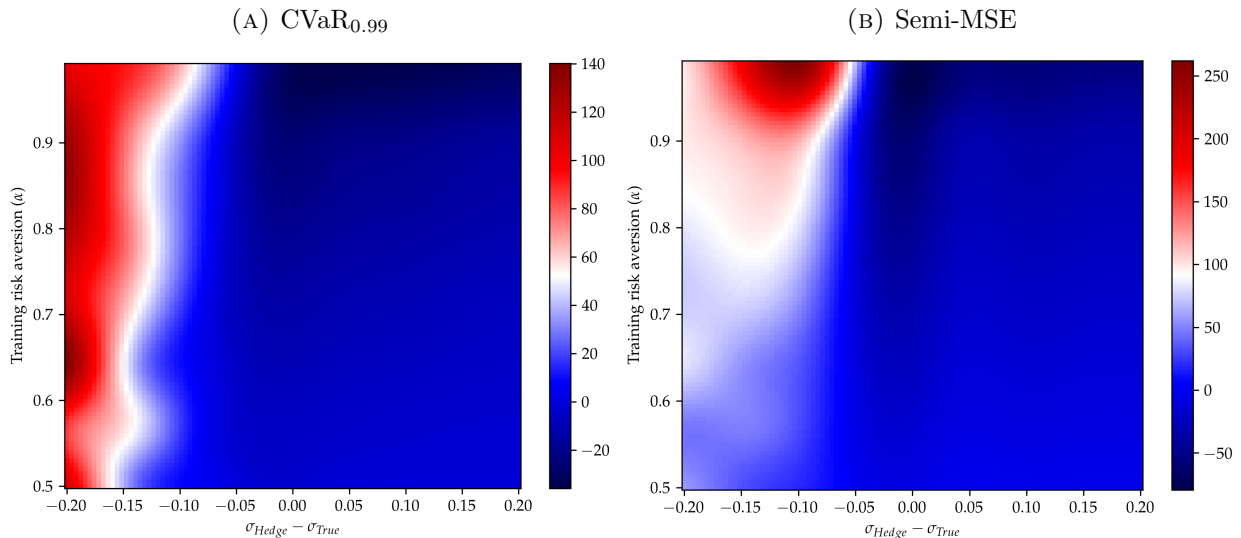
6.2 Deep Hedging with the Wrong Black Volatility

The consequences of hedging with the wrong volatility in the class of local volatility models, which includes the Black & Scholes model, are well known from previous studies such as Ahmad and Wilmott (2005) and Ellersgaard et al. (2017). In particular, suppose that one decides to sell at time $t < T$ a time T -expiring call option quoted at the implied volatility σ_{Hedge} and sets out to delta-hedge that option at volatility σ_{Hedge} in a market that is in fact driven by a geometric Brownian motion with volatility parameter σ_{True} . The so-called Fundamental Theorem of Derivatives Trading from the latter article then implies that the terminal profit-and-loss is given by

$$\varepsilon_T^\delta = \frac{1}{2} (\sigma_{\text{Hedge}}^2 - \sigma_{\text{True}}^2) \int_t^T S_u^2 \Gamma_u^{\text{Hedge}} du \quad (6.2)$$

where Γ_s^{Hedge} is the time s Black & Scholes gamma evaluated at the hedge volatility. Although stochastic and, as noted in the article, path-dependent, this is a rather comforting result in the sense that the terminal loss for a , with the BS model, delta-hedged short option position is limited to that of a scaled variance swap when the realized volatility turns out higher than the hedge volatility at which the option was sold. However, this type of result does not even carry over to models with several state variables, such as the Heston model. Quite naturally, there also do not exist any such analytical results for hedge performance under a misspecified model for deep hedging-based strategies.²⁴

FIGURE 4: THE RISK OF DEEP HEDGING WITH THE WRONG VOLATILITY



Note: Figure shows the normalized difference in risk 6.1 as measured by the $\text{CVaR}_{0.99}$ and SemiMSE risk measures as defined in 2.15 and 2.17 when the deep hedger is trained under a given CVaR_α risk measure and σ_{Hedge} BS volatility. The difference is evaluated on a uniform 8×8 grid of (σ_{Hedge}, α) 's. The risks are subsequently interpolated using a bivariate spline. Recall that lower values indicate over-performance of deep hedging since the risk is measured in terms of losses.

The following simulation experiment examines how the distribution of terminal hedging losses for a deep hedged option position compares to the corresponding distribution for a BS delta hedge when either over- or underestimating the volatility in a Black-Scholes environment. To this end, I assume hedging a short one month ATM call option and that the underlying stock price evolves as the geometric Brownian motion in 5.1 with true volatility $\sigma_{True} = 30\%$ and zero drift $\mu = 0$. In this environment, a deep hedging strategy is repeatedly trained to minimize the CVaR_α risk measure, each time assuming the correct Black & Scholes model class, but with the wrong hedge volatility $\sigma_{Hedge} \in \{\sigma_{True} - 0.2, \dots, \sigma_{True} + 0.2\}$. Each time, after training the deep hedging model with structure $d_1 = d_2 = 15$, the strategy is evaluated on 2^{19} paths simulated from the true model dynamics with volatility σ_{True} and compared to a standard BS delta hedge

²⁴This is particularly understandable given that, even for a fixed market state, the deep hedging strategy is itself stochastic, c.f. the optimization procedure described in Section 3.2.

that also assumes the erroneous hedge volatility σ_{Hedge} . The experiment is repeated for different levels of $\alpha \in \{0.5, \dots, 0.99\}$ to analyze how the model risk associated with deep hedging interacts with the degree of risk aversion assumed during the model training phase.

Only the *difference* in model risk between deep hedging and BS delta hedging based on this experiment is reported since, up to a discretization bias, the simulated hedge errors for the BS delta hedge are known to be given by 6.2. Figure 4 displays the normalized risk difference in 6.1 as implied by the simulation exercise when the alternative model \mathcal{M}_1 is the deep hedging model and the benchmark model \mathcal{M}_2 is BS model hedge. Specifically, the left panel reports the normalized risk difference for the mean squared loss SemiMSE in 2.17) and the right panel reports the corresponding difference for the tail risk measure CVaR_{0.99}. As is clear from the left panel of the figure, the risk of incurring extreme losses increases *much more* for deep hedging compared to BS if the actual volatility turns out higher than expected. This conclusion holds, irrespectively of the level of risk aversion during training, although the effect is slightly more pronounced when training is undertaken with a high degree of risk aversion. The right panel shows that the same conclusion holds when simply comparing the squared losses. However, as measured by this risk measure, the effect is smaller when training with a lower risk aversion.

6.3 The Poor Quant's Attempt at Deep Hedging with the Heston Model under \mathbb{Q}

This section analyses model risk when deep hedging with the popular Heston stochastic volatility model. Estimating the physical parameters of stochastic volatility models is notoriously difficult due to the latent nature of the variance process. There are, however, several options available for estimating such stochastic volatility models. For instance, Aït-Sahalia and Kimmel (2007) suggest estimating the parameters by maximizing an approximate joint likelihood function for both option and stock prices. Given the difficulty associated to the estimation of the physical parameters, an approach could be to calibrate the model to option prices and hope for the best (i.e. set $\lambda = 0$), as is done both in the empirical analysis in this thesis and in Mikkilä and Kanniainen (2021) and Giurca and Borovkova (2021).

Thus, a highly relevant question is, what happens if we get the price of variance risk wrong, or completely ignore it, when switching from \mathbb{Q} to \mathbb{P} and subsequently use the model to generate market scenarios for training of the deep hedging model. Inspired by Siven and Poulsen who carry out a similar analysis of the sensitivity of a static options hedging strategy towards model risk, I refer to the fallacy of ignoring the fact that the variance dynamics are likely to differ under the physical measure and the EMM as the "poor quant's approach". In addition to analyzing the consequences of deep hedging under the wrong measure, I also examine the implications of assuming a wrong vol-of-vol, ε , which controls the extent of

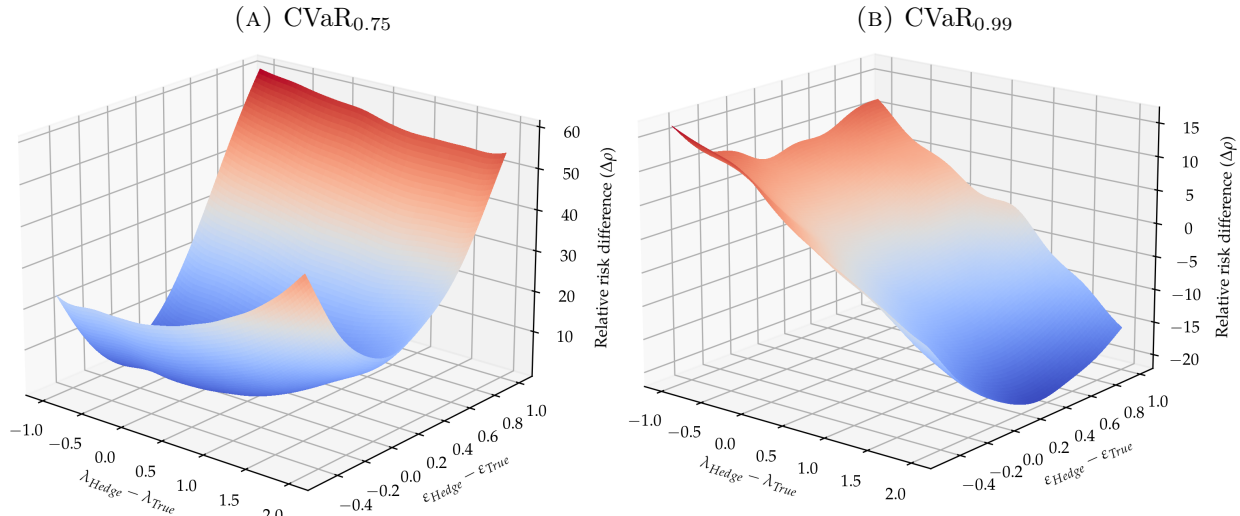
excess kurtosis in the return distribution. There is a particular reason for also analyzing the impact of this particular parameter. Based on the previously stated assumption of an affine market price of variance risk specification, ε should, theoretically, be invariant under an equivalent change of measure. However, it is inevitable that the, to the options market, calibrated estimate of ρ will be artificially inflated if said market is consistently characterized by an excessive fear of sudden extreme jumps in the stock price as compared to the statistical distribution.

To conduct a hedging experiment for a short one-month at-the-money call option as above. However, I now assume a weekly rebalancing frequency and fix the training objective to be the CVaR_{0.75} risk measure. Furthermore, the market environment where the strategies are evaluated is a Heston model with parameters

$$\kappa^{\mathbb{Q}} = 3.2, \quad \theta^{\mathbb{Q}} = 0.25^2, \quad \varepsilon = 0.6, \quad \tilde{\rho} = -0.78, \quad \mu = r = 0, \quad \lambda = -2.0. \quad (6.3)$$

By relation 5.7, this parameterization implies that $\kappa^{\mathbb{P}} = 5.2$ and $\theta^{\mathbb{P}} = 0.196^2$.

FIGURE 5: DEEP HEDGING MODEL RISK IN THE HESTON MODEL



Note: Figure shows the normalized difference in risk 6.1 as measured by the CVaR_{0.75} and CVaR_{0.99} risk measures as defined in 2.15 when one of the deep hedging agents is trained under a misspecified Heston model and the other is trained under the correctly specified one with parameters $\theta^{\mathbb{Q}} = 0.25^2$, $\kappa^{\mathbb{Q}} = 3.2$, $\tilde{\rho} = -0.78$, $\varepsilon = 0.6$, $\lambda = -2.0$, $\mu = 0$.

The difference is evaluated on a uniform 8×8 grid of $(\varepsilon_{\text{Hedge}}, \lambda_{\text{Hedge}})$'s. The risks are subsequently interpolated using a bivariate spline. Recall that lower values indicate over-performance of the misspecified model since the risk is measured in terms of losses. Both deep hedging models are trained under the CVaR_{0.75} risk measure.

In this environment, I evaluate the performance of two hedging strategies. One is the hedging policy learned by a deep hedging model that is trained with 2^{18} simulated Heston stock price paths under the correct statistical measure described. The second strategy is the poor quant's strategy, where the same deep hedging model is trained under 2^{18} simulated Heston scenarios with the parameters in 6.3, except that

she uses the variance risk premium $\lambda_{Hedge} \in \{\lambda - 1.0, \dots, \lambda + 2.0\}$ and the vol-of-vol parameter $\varepsilon_{Hedge} \in \{\varepsilon - 0.4, \dots, \varepsilon + 1.0\}$. Both strategies are parameterized with $d_1 = d_2 = 20$, are trained to minimize the $CVaR_{0.75}$ risk and I assume that the information set is $\mathcal{I}_t = (\log S_t)$.²⁵ I assume that the variance process is always initialized at its stationary level under the statistical measure $\theta^{\mathbb{P}}$, implying that the poor quant also uses a wrong initial level for the variance process. Paths are simulated using 5.12 with time-discretization $\Delta t = 2.3 \cdot 10^{-4}$. I retrain the poor quant's model 64 times, each time on a new point in a uniform 8×8 grid of $(\varepsilon_{Hedge}, \lambda_{Hedge})$'s, and evaluate the difference in risks to the correctly trained model on 2^{18} out-of-sample paths.

The normalized difference in risk in 6.1 between the two strategies are displayed in Figure 5 where the reference strategy \mathcal{M}_2 is the correctly trained Heston model. Panel (A) evaluates the cost of deep hedging assuming the wrong model in terms of the training objective, i.e. $CVaR_{0.75}$ risk. The figure shows that if one trains the deep hedging model under the correct stationary variance level and the correct mean reversion speed, but happens to severely overestimate the vol-of-vol, the resulting strategy is associated with around a 56% higher loss on average in the 25% worst cases. On the other hand, the risk penalty is *much* lower if the trader ignores the variance risk premium and sets $\lambda_{Hedge}=0$. The corresponding increase in risk is just around 17% if she happens to bang-on all other parameter estimates. The implication if this finding is that the trader should be significantly more concerned about the *elasticity* of the variance process rather than its level when deep hedging. On the other hand, Panel (B) shows that the precision of the ε estimate plays less of a role if the trader only cares about extreme tail risk, as measured by $CVaR_{0.99}$.

²⁵Theoretically, one should include the current level of the variance process since S_t is not Markovian in this model. I do not include it here for simplicity and since I find it to have a negligible impact in unreported experiments.

7 Data and Volatility Descriptives

This section describes the data used in the empirical analysis and the data cleaning process applied before said analysis. I insist that a proper, realistic benchmarking of deep hedging against existing hedging methods should allow competing methods to leverage volatility information embedded in the options market. The scope of the empirical analysis is hence limited to hedging of options written on the S&P500 index from 2010 throughout 2020. Call and put options data is used for calibrating the PBS and Heston models for benchmarking purposes and for computing realized hedging errors for vanilla options. Additionally, I collect realized measures based on high-frequency tick data, and daily adjusted closing prices for the S&P500 index to compute hedging errors. Below, I first describe the procedures for cleaning and collecting the options data and the realized measures. The last part of the section gives a brief overview of the S&P 500 volatility dynamics and the Heston and Practitioner's Black-Scholes calibration results.

7.1 Options data

Options data is collected from the IvyDB OptionMetrics database. The dataset contains daily cross sections of end-of-day S&P500 call and put option bid and ask quotes for all strikes and maturities over the years 2010-2020. Notably, the dataset also includes the relevant price of the underlying index, implying that there should be no issues due to nonsynchronous prices. The total number of option quotes over this period is just over 21.1 million. When, below, I refer to *the* market option price, then what I mean is the average of the bid and ask prices. Based on the raw dataset, I first back out, on each trading date, the implied dividend yield, and a term structure curve based on the most liquid option quotes for each maturity date and the put-call parity. A complete term-structure curve is constructed by fitting the model of [Nelson and Siegel \(1987\)](#) to the implied yields for each maturity date. I give a more detailed account of the procedure in Appendix (C) and display the time series of filtered dividend yields and one-year bond yields in Figure [A1](#). Then, I append to the raw dataset the Black & Scholes implied volatility for the bid, ask and mid-prices and apply the following cleaning procedure

1. Remove all in-the-money options for liquidity reasons and to avoid redundancy of information due to put-call parity.
2. Remove all options with time to maturity less than six days or longer than one year.
3. Remove all options whose moneyness is outside $\pm 30\%$.

4. Remove all options with undefined implied volatility for the bid or ask price. This condition removes quotes with zero bid and quotes outside standard model-independent arbitrage intervals.

After the cleaning procedure, the final dataset used for calibration of the Heston and PBS models consists of 7.7 million option quotes on put and call options, or around 2,800 per trading day.

7.2 High-Frequency Data and Realized Measures

As in much of the high-frequency econometrics literature, I collect daily observations on the realized kernel estimator for the S&P500 index directly from the Oxford-Man Realized Library rather than calculating them based on Trade and Quote data myself. The realized measures in this library are based on data from the Thomson Reuters Tick database that has been cleaned roughly according to the procedure described in [Barndorff-Nielsen et al. \(2009\)](#). For instance, all observations outside the exchange's opening hours are removed, and outliers and negative prices are discarded.

7.3 Volatility Descriptives and Calibration Results for Heston and PBS Models

This section briefly illustrates and discusses the nature of the data that is subject to analysis in the empirical section. The first Figure 6 displays the implied volatilities corresponding to observed option prices on a representative date (July 20, 2020) within the sample period under consideration. Panel (A) additionally illustrates the corresponding interpolated Practitioner's Black-Scholes implied volatilities using the methodology outlined in Section 5.1 and Panel (B) displays the corresponding best fitting (calibrated according to the criterion 5.9) surface of implied volatilities generated by the Heston model. At this point in time, the smile (or hockey-stick) effect appears particularly pronounced, indicating a significant market-perceived risk of extreme tail-events, probably amplified by the recent breakout of the Covid crisis.

It makes little sense to compare the pricing fit of the two models since the former model is merely an ad-hoc interpolation tool while the latter represents a dynamic model that is significantly more constrained in the sense that it must produce internally consistent option prices. However, both calibration methods appear to be performing as intended. The Heston model is observed to have difficulty generating a sufficiently steep skew for short-maturity options. This is entirely as expected and empirically well documented, see e.g. [Gatheral \(2011\)](#) Ch. 3. The introduction of stochastic volatility alone is rarely sufficient to generate the significant kurtosis in the (risk-neutral) return distribution implied by short maturity option prices.

The results from the daily calibrations of the Heston model are summarized in Table 2, and Figure A2 in the appendix displays the time series of relative model pricing errors, which are around 6% on average.

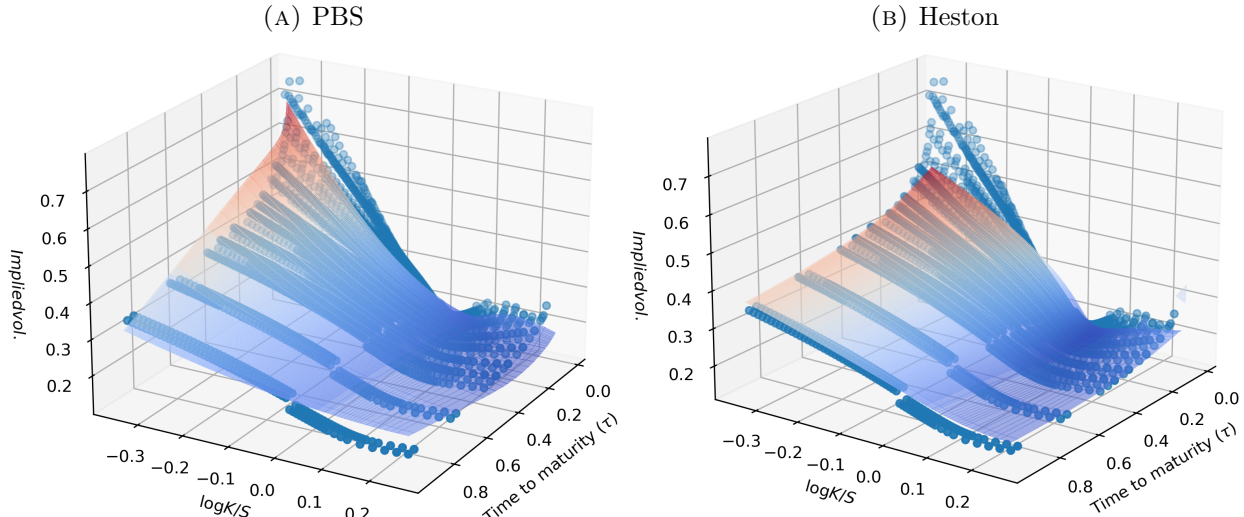
TABLE 2: DISTRIBUTION OF CALIBRATED HESTON PARAMETERS AND VOLATILITIES

	κ^Q	$\tilde{\rho}$	ε	$\sqrt{\theta^Q} \cdot 10^2$	$\sqrt{\bar{v}} \cdot 10^2$	\sqrt{RK}	IV _{ATM}	σ^{GJR}	σ^{RG}
Mean	3.95	-0.77	1.30	25.60	16.60	10.91	16.84	15.27	14.13
Median	3.21	-0.78	1.20	22.80	14.79	8.74	15.22	12.03	12.28
SD	2.64	0.05	0.47	9.20	8.10	8.18	6.08	10.36	7.63
AC(5)	-	-	-	-	-	0.58	0.91	0.86	0.79

Table summarizes the distribution of Heston parameters calibrated to OTM SPX options over the period 2010-2020. The last 4 columns display the corresponding statistics for a number of S&P500 volatility time-series over the same period. AC(5) is the autocorrelation at lag 5.

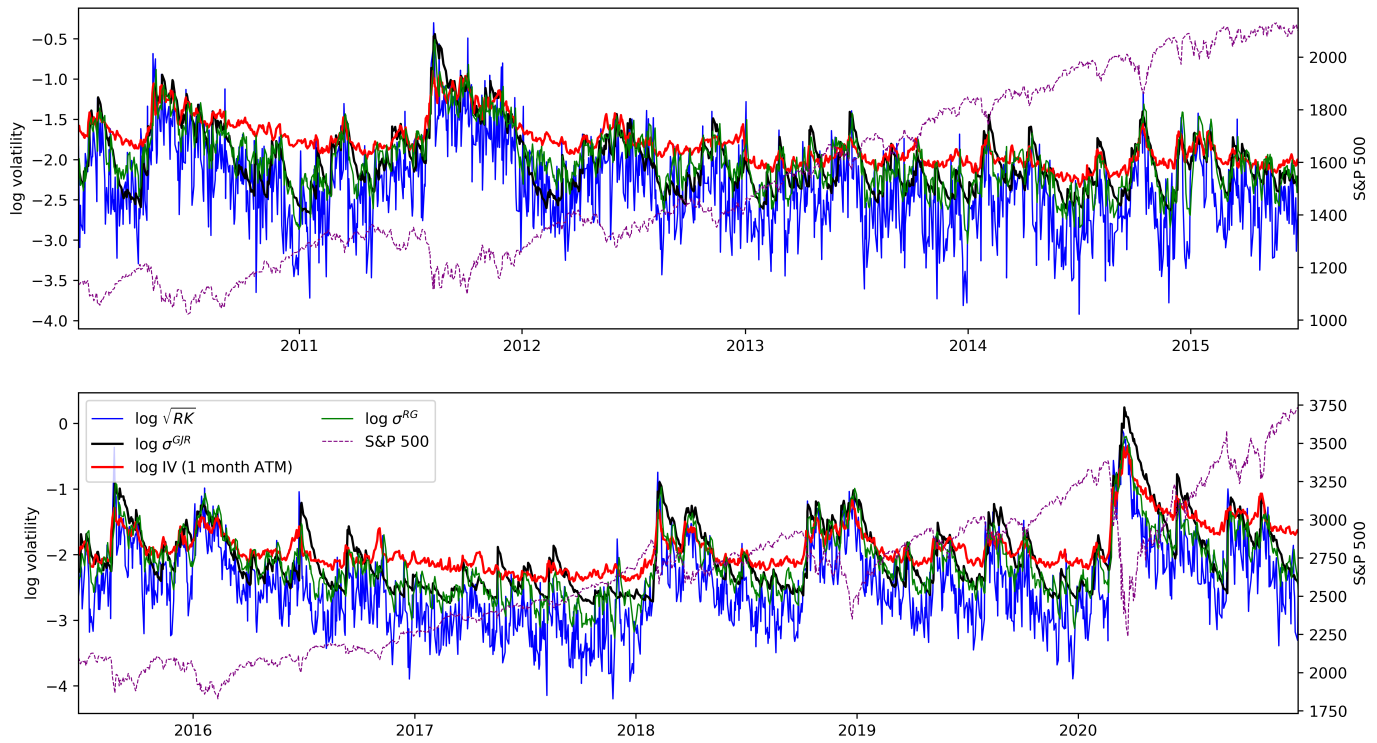
Notably, the stationary level of the risk-neutral variance process ($\sqrt{\theta^Q} \simeq 26\%$ on average) is significantly higher than what is implied by the historical measure. The average GARCH filtered volatility over the same period is just around 15%, confirming the presence of a negative variance risk premium over the period in consideration. The options market implies a significant excess of kurtosis and skewness of returns under the pricing measure, c.f. the negatively calibrated values for $\tilde{\rho} \simeq -0.8$ and the fairly high vol-of-vol, ε . I verify that the calibrated parameters correspond very well to the results in e.g. Kokholm and Stisen (2015). However, I find the vol-of-vol parameter ε , typically calibrating at around 1.3, to be quite high. One could criticize that this is a result of not imposing the Feller condition. However, when imposing said condition, I find that the lower vol-of-vol is simply compensated for by lowering the correlation $\tilde{\rho}$ essentially to -1 to fit the steep smile for short-term OTM options.

FIGURE 6: OBSERVED AND CALIBRATED VOLATILITY SURFACES (JULY 20TH 2020)



Note: Figure displays market-implied and calibrated implied volatilities on July 20th 2020 for the Practitioner's Black-Scholes and Heston models.

FIGURE 7: VOLATILITY DYNAMICS



Note: Figure displays 1M ATM implied volatilities, observed intra-day realized volatilities calculated from high-frequency data, GJR-GARCH and Realized GARCH filtered conditional daily volatilities and the current Heston volatility as calibrated to options data. All volatility series are annualized. The figure furthermore shows the value of the S&P 500 index over the period 2010-2020.

Figure 7 displays various approximations to the true SPX volatility dynamics over the considered hedging period 2010-2020, all of which compose vital inputs to the empirical hedging exercise. The time series in the figure include the one month ATM implied volatility interpolated using the regression technique described in Section 5.1, the square root of the daily realized kernel-based estimate of the quadratic variation of daily open-to-close returns and the filtered conditional volatilities of daily close-to-close returns from GJR-GARCH and Realized GARCH model estimated on a large sample covering the period 2005-2020. I apply a log transformation to all series before plotting them. Furthermore, the figure displays the daily level of the S&P 500 index. The estimated full-sample parameters for the GJR-GARCH and Realized GARCH models can be found in Tables A1 and A2 in the appendix.

From this figure, we observe again that the volatilities implied by the options market are almost consistently higher than those inferred from the statistical measure. This suggests that a negative variance risk premium prevailed during the sample period. The level of the realized intra-daily volatility is lower than both the options market-implied and filtered conditional daily volatilities from the GARCH model. This is expected since the RV covers only open-to-close returns while the GARCH volatilities correspond to close-to-close

returns. E.g. Hansen et al. (2012) find that the open period SPX volatility corresponds to around 75% of daily volatility over the period 2002-2008.

A casual visual inspection of the volatility series clearly shows that they are persistent and inversely related to index returns. This is confirmed by the autocorrelations, typically around 0.8 at the weekly lag, and the correlation between log increments in the filtered GJR-GARCH volatilities and the SPX index at around -0.73. These are well-known characteristics of financial time series and are known to generate excess kurtosis in the returns distribution. The negative relation between volatility and returns, also known as the leverage effect, implies a left skew in the return distribution. The return distribution of the underlying index is naturally of great importance when hedging. All of the hedging strategies that I use in this thesis accommodate, to some extend and each of them in their own way, the stylized facts observed here.

The stylized facts presented here have been well known for a long time. Nevertheless, it is important to keep in mind that the models used for hedging should always be based on the characteristics of the market dynamics - different models than the ones considered in this thesis could be more appropriate when hedging claims on underlying assets with different characteristics. Furthermore, it is important to keep in mind that all the empirical results presented in the next section rely critically on proper data work and estimation, calibration and simulation procedures.

8 Empirical Evaluation

In this section, the global hedging performance of the models presented in past sections is evaluated empirically on options written on the S&P500 index. The general setup for the empirical exercise is as follows. Denote by \mathcal{T}_S the first trading date of the performance evaluation period and \mathcal{T}_E the last trading date of the sample period. Akin to the approach adopted in the empirical exercise in Buehler et al. (2019), I then consider the following set of m , potentially, overlapping hedging periods $\{\mathcal{T}_j^s, \mathcal{T}_j^e\}_{1 \leq j \leq m}$ such that $\mathcal{T}_S = \mathcal{T}_1 < \mathcal{T}_2 < \dots < \mathcal{T}_m = \mathcal{T}_E$, $\mathcal{T}_j^e - \mathcal{T}_j^s = \tau > 0$ and $\mathcal{T}_j^s - \mathcal{T}_{j-1}^s = \Delta\tau > 0$ for all $j = 1, \dots, M$. This structure implies that the hedging periods are overlapping whenever $\Delta\tau < \tau$. On each of these time intervals, I then consider the problem of risk-optimal hedging some derivative χ , exactly as described in Section 2 and with the models presented in Sections 3 and 5. Specifically, for the j 'th hedge period, a hedge on a claim χ expiring at time \mathcal{T}_j^e is initiated at time \mathcal{T}_j^s . Thus, in the notation from previous sections, $t_0 := \mathcal{T}_j^s$ and $T := \mathcal{T}_j^e$ for every hedge period. Throughout the analysis, I focus on hedging at-the-money (call) options because they have the highest gamma and hence present the greatest challenge for discrete-time hedging strategies.

Contrary to Mikkilä and Kannaiainen (2021) and Giurca and Borovkova (2021), but in line with Buehler et al. (2019), I focus on the case *without* transaction costs. In a real trading environment, trading costs are present. This means that I essentially put the deep hedging model at a disadvantage compared to what one would experience in real-life trading situations since the deep hedging model can easily adapt the strategy to such costs. The classic hedging models, on the other hand, will have to be modified in various more or less ad-hoc ways.

When hedging vanilla calls and puts, I always assume that the initial price charged for the hedged derivative \bar{p} is the actual market price quoted for the option. As discussed in Section 2.2, this choice does not affect the optimal hedging strategy for deep hedging. However, this choice *does* matter for comparing the distribution of terminal hedge errors in terms of a non-convex risk measure such as the MSE and SemiMSE risk measures in 2.17. In the empirical part of Buehler et al. (2019), losses are not centered at market prices. The reason for using actual market prices here is that it yields a more accurate representation of the model's hedging performance as measured e.g. by squared losses. A zero interest rate, $r = 0$, is assumed for calculating discounted hedging losses throughout the empirical section, given that riskless yields were negligible over the period of consideration and since I focus on rather short-lived options.

A consequence of insisting on hedging options for which a quoted price is available is that it is not possible to fix the time to maturity τ and the moneyness to be exactly as desired in a given experiment. In particular,

the option's time to maturity and moneyness will vary for each hedge experiment, i.e. for each \mathcal{T}_j^s . Due to the rich options dataset, this is however deemed to be a minor drawback. In practice, I find the best-suited option as follows. Firstly, I select the options for which the time to maturity is the closest to the desired one. Secondly, I select the option whose moneyness is as close as possible to the desired one.

8.1 Replicating Vanilla Options Hedging Experiment

As a first exercise, I test the performance of deep hedging in an empirical trading setting as close as possible to the one assumed in the empirical section of [Buehler et al. \(2019\)](#). Although doing such a replication exercise does not contribute with new insights, it serves as an important validity check of the entire setup around the empirical evaluation exercise of the thesis. After all, quite a few lines of code go into implementing these types of models on real data.

First, I restrict the evaluation period to the one considered in [Buehler et al. \(2019\)](#), which is Apr. 2012 - Nov. 2017. Over this period, I consider hedging, with a *weekly* rebalancing frequency, a short position in an ATM call option, that is $\chi = (S_T - K)^+$, with around $\tau = 1$ month to expiry. Said option is repeatedly sold and hedged over the course of the evaluation period with $\Delta\tau = 10$ calendar days in-between the hedging experiments. This means that the hedging periods are always overlapping. The choice to work with overlapping periods can be seen as a way to extract as much information from the data as possible - recall that although the periods are overlapping, the strategies, or delta functions, are always evaluated at different points on a given calendar date. However, the fact that the periods are overlapping also introduces autocorrelation in the observed hedge errors. It is important to keep this caveat in mind when interpreting e.g. empirically estimated global risk measures.

At the beginning of each hedge period, a deep hedge agent is trained to minimize the CVaR_{0.75} risk measure on ²¹⁹ market scenarios simulated from a GJR-GARCH model with Student's t-distributed innovations calibrated to the past five years of return data.²⁶ The market scenario generator is always recalibrated before training the deep hedging model. As in [Buehler et al. \(2019\)](#), the neural network specification is $L = 2$ hidden layers and $d_1 = d_2 = 20$ units in each layer, which I also find to be sufficient in this setting based on unreported experiments. The information set includes the logarithm of the current stock price, that is $\mathcal{I}_t = (\log S_t)$.

Precisely as in [Buehler et al. \(2019\)](#), I compare the terminal hedge losses for each hedge period $[\mathcal{T}_j^s, \mathcal{T}_j^e]$ for the deep hedging strategy against the version of the PBS strategy where, on each trading date, the volatility plugged into the BS delta [5.2](#) is the filtered volatility from a GJR-GARCH model re-estimated on

²⁶In particular, I pick out the relevant weekly stock price observations from the path of simulated daily prices.

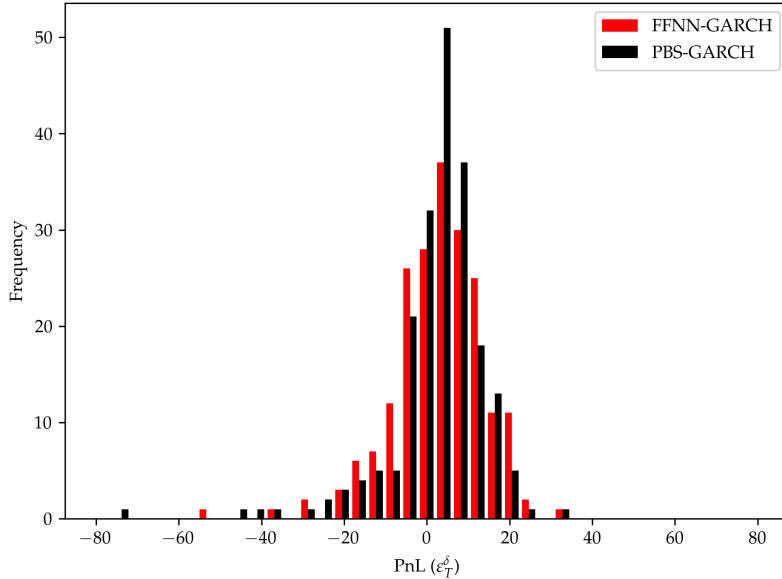
each trading date on a 5-year rolling window. The filtered volatilities used for hedging are *almost* the ones depicted in Figure 7, but not exactly due to the daily updating of the GJR-GARCH model parameters.

TABLE 3: EMPIRICAL LOSS DISTRIBUTION (SHORT ATM CALL, WEEKLY REBALANCING)

	RMSE	SemiRMSE	CVaR _{0.99}	CVaR _{0.95}	CVaR _{0.75}	CVaR _{0.5}	CVaR _{0.0}
PBS-GARCH	12.02	16.48	53.52	32.35	11.66	4.99	-2.37
FFNN-GARCH (Buehler et al. (2019))	-0.49	-3.92	-13.95	-7.07	-0.4	0.42	-0.31
	-	(-3.7)	-	-	-	-	(-1.1)

Note: The first row of the table displays risk measures for the PBS model when repeatedly hedging a 1-month short ATM call position over the period Apr 2012-Nov 2017 with weekly rebalancing. The second row displays the loss difference in 8.1 for the risk measure indicated in the columns where the benchmark model \mathcal{M}_2 is the PBS- model. The best model for each risk measure is indicated by a bold typography. The numbers in parentheses indicate the corresponding risk difference reported in Buehler et al. (2019).

FIGURE 8: DISTRIBUTION OF TERMINAL HEDGE ERRORS FOR 2012-2018 SUBSAMPLE



Note: Figure compares the distribution of terminal hedge errors (PnL) for the PBS model with GARCH filtered volatilities and the deep hedging strategy trained under estimated GJR-GARCH market dynamics. The hedge derivative is an ATM call option with 1 month to expiry. All losses are centered at the market-quoted option price and a weekly rebalancing frequency is assumed. No transaction costs.

Table 3 summarizes the empirical distribution of the realized terminal hedging losses for both strategies by evaluating the empirical counterparts to several of the risk measures introduced in 2.2. The first row of the table shows the absolute risk for the PBS-GARCH strategy. The second row shows the difference

$$\Delta^{\text{abs}} \rho(\mathcal{M}_1, \mathcal{M}_2) := \rho^{\mathcal{M}_1} - \rho^{\mathcal{M}_2} \quad (8.1)$$

where \mathcal{M}_1 is deep hedging and \mathcal{M}_2 is the PBS-GARCH strategy. implying that lower numbers indicate better performance. The RMSE and SemiRMSE risk measures are defined as the square-root of, respectively, the MSE and SemiMSE risk measures in 2.17. For comparison, I indicate the corresponding difference in risk reported in Buehler et al. (2019). As in their paper, I find that the deep hedging model improves on the PBS-GARCH hedging strategy in terms of both average and squared losses. The deep hedging model loses out only in terms of the median loss.

Figure 8 indicates the distribution of terminal profits and losses for both strategies and is directly comparable to Figure 13 in Buehler et al. (2019). As was the case in their paper, I find that the deep hedging model improves upon the PBS strategy primarily by reducing tail risk. However, the strategy is subject to a somewhat higher risk of facing medium-sized losses. One curiosity is that the improvement is rather small in terms of the CVaR_{0.75} risk, given that the deep hedging model is trained to minimize this risk measure. This finding, however, may easily be due to the small sample. In general, these results indicate that I find similar gains for switching to deep hedging similar to the original deep hedging paper.

In the next part, I extend the existing empirical results by examining the robustness of these conclusions towards 1) a different evaluation period, 2) including a more extensive line-up of benchmark hedging models, 3) different option maturities and rebalancing frequencies, and 4) using different types of market generating models \mathbb{G} for training the deep hedging model.

8.2 Deep Hedging ATM Call Options

In this section, I expand on the above empirical experiment with several amendments intended to provide new insights into the practical relevance of deep hedging. I maintain the assumption that the hedged asset is an at-the-money call option and use the same neural network structure with two hidden layers, each with 20 neurons as above. That choice is based on unreported simulated experiments, suggesting that this structure provides a sufficient flexible parametric approximation to the unknown policy functions.

I extend the sample period by four years to cover the entire period from Jan 2010 - Dec 2020 and thus include the period of the outbreak of the Covid crisis. It, however, turns out that an unfiltered, naïve, deep hedging strategy diverges during this period, in particular in the extreme market conditions experienced during the month of February 2020. When I report empirical risk measures, I always filter away the 3 terminal loss observations on hedges that were initiated during the month of February.

Second, one might rightly suspect that the above conclusions could change if we were to extend the set of benchmark models with a number of alternative models with roots in the standard continuous-time pricing

TABLE 4: EMPIRICAL RISK MEASURES FOR ATM CALL HEDGES 2010-2020

	RMSE	SemiRMSE	CVaR _{0.99}	CVaR _{0.95}	CVaR _{0.75}	CVaR _{0.5}	CVaR _{0.0}
<i>Freq. 2 / Mat. 14</i>							
PBS-IV	9.98	9.91	34.88	23.25	10.75	5.94	-0.75
FFNN-GARCH	0.13	-0.12	-3.85	-0.96	-0.27	-0.21	-0.44
FFNN-Heston	-0.55	-2.01	-8.61	-5.86	-1.16	-0.03	0.17
Heston	2.02	3.42	6.3	4.16	2.42	0.53	-0.98
Heston-RiskMin	-0.71	-1.06	-6.85	-4.11	-0.59	-0.04	0.27
PBS-GARCH	0.61	1.5	6.71	1.44	-0.12	-0.45	-0.6
<i>Freq. 5 / Mat. 35</i>							
PBS-IV	17.01	22.93	79.24	54.41	20.42	10.48	-0.14
FFNN-GARCH	3.05	-0.66	1.98	-4.34	-1.87	-1.3	-1.64
FFNN-Heston	-0.94	-3.94	-3.13	-6.13	0.22	1.82	1.43
Heston	6.98	12.39	34.89	16.6	7.16	1.43	-2.39
Heston-RiskMin	-1.61	-4.32	1.28	-8.75	-0.17	1.71	1.95
PBS-GARCH	3.53	7.3	32.75	12.56	1.18	-0.38	-1.13
<i>Freq. 10 / Mat. 60</i>							
PBS-IV	27.26	37.71	174.01	76.95	26.07	12.72	-2.2
FFNN-GARCH	6.17	13.0	36.42	4.69	-0.37	-1.8	-3.66
FFNN-Heston	-2.72	-9.2	-32.56	-12.66	1.8	4.28	2.8
Heston	8.26	14.8	17.26	17.91	8.63	0.6	-4.66
Heston-RiskMin	-3.17	-9.12	-35.3	-10.05	3.43	5.53	4.58
PBS-GARCH	6.16	17.36	57.76	12.13	2.12	-0.81	-2.17

Note: Table empirical risk measures over the period Jan 2010 - Dec 2020. All hedges are for a sold ATM call option and losses are centered at market option prices. The first row for each options maturity displays the absolute risk for the PBS-IV model. The remaining rows displays the difference in risk as measured by 8.1 where \mathcal{M}_2 is the PBS-IV strategy. For each risk measure, the best model is indicated with bold typography. Freq. x / Mat. y refers to a call option expiring in y calendar days and an x business day portfolio rebalancing frequency.

and hedging literature. In particular, given that the GARCH-filtered " \mathbb{P} "-volatilities are inherently backward-looking, it seems prudent to also include models building on volatility information from the options market, as previously argued. In the remainder of the thesis, I hence take the PBS model that hedges with a daily recalibrated implied volatility as described in 5.1 to be the benchmark model against which other hedging

strategies are compared. Furthermore, I include the two hedge strategies based on the Heston model defined in 5.10 and 5.11 that also use information embedded in the implied volatility smile. I make sure to recalibrate the parameters of the Heston model on each trading date according to the procedure described in Section 5.2 such that the strategy always reflects the newest volatility information. It is not completely obvious whether a frequent recalibration of the Heston model is optimal since it also introduces random day-to-day variation in the model parameters and hence also in hedges. This trade-off essentially exists for all models under consideration.

Just as is the case for Greeks-based hedging models, the deep hedging model intuitively also should be able to take advantage of the forward-looking information embedded in the options market. To examine whether that is the case, I compare deep hedging when the market simulator \hat{G} is the Heston model with variance dynamics inferred from the pricing measure to the case where \hat{G} is the GJR-GARCH model estimated under the historical measure. The former market simulator is used in the empirical work in [Mikkilä and Kannaiainen \(2021\)](#) and [Giurca and Borovkova \(2021\)](#) while the latter is used in the empirical section of [Buehler et al. \(2019\)](#). When simulating from the Heston model using 5.12, I employ a time discretization corresponding to 10 calendar hours. For now, I assume that the trader uses the information set $\mathcal{I}_t = (\log S_t)$ for all deep hedging models.

To quantify the significance of the rebalancing frequency, I allow for rebalancing every second day, once a week, and once every second week for options expiring in, respectively, 14, 35 and 65 days. That is, I let $\tau \in \{14, 35, 60\}$ calendar days.

Table 4 summarizes the results from this exercise by reporting key statistics for the empirical distribution of the realized terminal hedging losses. The figures for the PBS-IV strategy in the first row for a given maturity are the empirical counterparts to the risk measures introduced in 2.2, including the CVaR, MSE and SemiMSE risk measures. All other rows display the *difference* in risk compared to the PBS-IV strategy in the first row, precisely as in Table 3.

Contrary to the results presented in the previous section, this more thorough analysis shows that deep hedging is not an unconditionally better alternative to classic Greeks-based approaches. Especially, the addition of other types of Greeks-based models turns out to be empirically relevant. For instance, when hedging the same option as in the previous Section 8.1 over the extended sample period, the deep hedging model trained under GJR-GARCH \mathbb{P} -dynamics still yields an impressive improvement in terms of squared losses over the PBS-GARCH model with a reduction in SemiRMSE of around 26%. However, based on this evaluation metric, the PBS model that leverages implied volatility information from the options market performs almost as well as deep hedging. This highlights the importance of including other hedging models

that are known to work well in practice when evaluating the deep hedging model.

If the trader is concerned about minimizing tail risk, the locally risk-minimizing delta-vega Heston hedge in 5.11 is a better alternative than the GARCH-trained deep hedging model. The raw Heston delta strategy is associated with the lowest loss on average throughout the evaluation period and for all maturity/rebalancing frequency combinations. However, the low average loss comes at a substantial cost in the form of a very high tail risk. The observation that the raw Heston delta hedging strategy does not perform well is not surprising given that it ignores the correlation between the variance and the stock price.

Furthermore, contrary to what I would have expected, the gains from deep hedging do not increase monotonically as the rebalancing frequency declines. Quite notably, the FFNN-GARCH deep hedging model performs substantially *worse* in terms of minimizing extreme losses than the PBS-IV strategy when the hedge rebalancing frequency is bi-weekly (every second week). Again the importance of leveraging implied volatility information is apparent. In the setup of Buehler et al. (2019) where only the PBS-GARCH model was included as a benchmark, one would be falsely led to believe that deep hedging substantially outperformed classic Black-Scholes delta hedging for such infrequent rebalancing frequencies.

Compared to the GARCH-trained deep hedging strategy, I find that the deep hedging model, which is trained in a Heston model with variance dynamics inferred from the options market, reduces quite substantially the frequency of high losses. For long options maturities with infrequent rebalancing, this reduction in tail risk comes at the cost of a significant increase in average risk. However, when hedges are rebalanced frequently (every second day), the FFNN-Heston model reduces the average risk in the 5% worst cases by around 25% compared to the PBS-IV model and the deep hedging model trained with GARCH dynamics. The increase in average risk is economically small, around 22%. The empirically measured risk corresponding to the training objective, CVaR_{0.75}, is also the lowest for the FFNN-Heston model when hedges are rebalanced every second day.

An interesting observation is that the delta-vega Heston hedge (Heston-RiskMin) in 5.11 performs very similarly to the FFNN-Heston hedge, although the latter model has a lower average loss for all rebalancing frequencies. This finding can be interpreted in different ways, depending on the perspective of the observer. Either, this could be taken as indicating that a black-box neural network hedging model is actually able to almost recover a hedging strategy that is firmly rooted in financial theory and should work well in a continuous-time setting. Alternatively, this indicates that the theoretical continuous-time based strategy is not so bad at all and does a decent job at approximating the deep hedging model that, almost by construction, is optimal in the discretized Heston environment.

The average loss for most hedging strategies is negative, i.e. I find that one usually obtains a profit from

selling ATM call options and delta-hedging them. This finding is consistent with the idea of a negative variance risk premium, i.e. that implied volatilities are higher than realized ones, meaning that options sellers charge a volatility risk premium. As covered in e.g. Ellersgaard et al. (2017), delta-hedging an option essentially amounts to trading a variance swap. Since, in this experiment, we are selling optionality, it is not surprising that average profits are found to be positive.

In order to identify potential periods of over- or underperformance, Figure 9 compares the hedging performance of a given alternative strategy $\delta^{\mathcal{M}}$ to the PBS-IV benchmark strategy δ^{PBS} over time by displaying a 30-period moving average of their terminal loss differences. Specifically, the figure displays

$$\frac{1}{\min(j, 30)} \sum_{T \in \{\mathcal{T}_{j-\min(j, 30)+1}^e, \dots, \mathcal{T}_j^e\}} (\varepsilon_T^{\delta^{\mathcal{M}}} - \varepsilon_T^{PBS}), \quad j = 1, \dots, M, \quad (8.2)$$

which means that I use an expanding mean for the first 30 periods. For all options expiry/rebalancing frequency combinations, the GJR-GARCH trained deep hedging model (FFNN-GARCH) tends to perform particularly well during the period from 2012 and through 2018, which happens to coincide with the evaluation period in Buehler et al. (2019). Generally, this period is characterized by being quite tranquil with relatively low levels of volatility in the underlying index, as is clear from the volatility dynamics displayed in Figure 7. Based on the simulation result for the Black & Scholes model in Section 6.2, the observation that the efficiency of the deep hedging model declines during high volatility periods is not surprising.

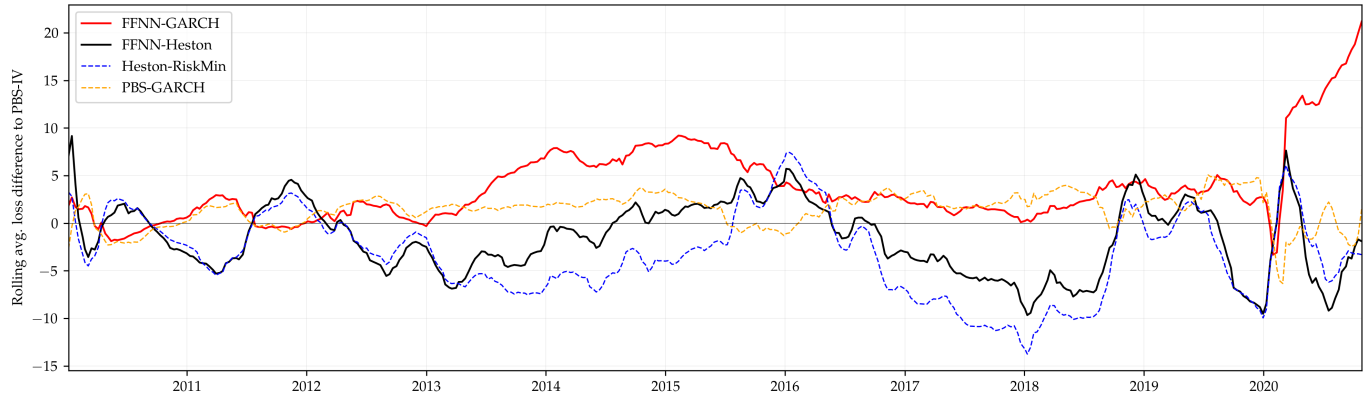
The performance of the deep hedging model trained under the physical GARCH dynamics deteriorates particularly sharply during the Covid crisis. Judging by the, unreported, hedging strategy employed by the FFNN-GARCH model during this particular period, that is likely because the neural network has not seen any simulated examples during model training of the rather extreme market scenario realizing during this period.

Upon observing the learned hedging strategies, it is apparent that the extreme market conditions cause the deep hedging policy to diverge, essentially. In practice, this is, however, unlikely to be as much of an issue as one might believe. Such divergence in the learned policy can potentially be solved in practice by artificially oversampling extreme scenarios. Furthermore, any serious practical implementation of such a deep hedging model would have an *insanity filter*, even the least useful of which would flag the hedge ratios close to 1 for far out-the-money options proposed by the deep hedging policy on some of these extreme occasions.

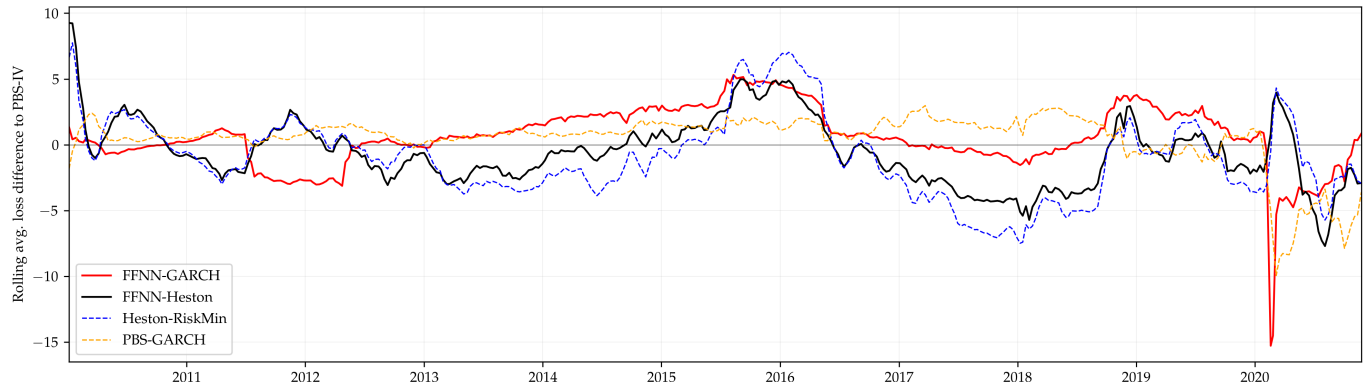
All in all, this analysis leaves a much more nuanced picture of empirical deep hedging performance, compared to the current literature. For instance, the analysis shows that deep hedging under options market-implied variance dynamics leaves a completely different risk profile compared to when the deep hedging model is

FIGURE 9: ROLLING AVG. DIFFERENCE IN HEDGE ERRORS (ATM CALL)

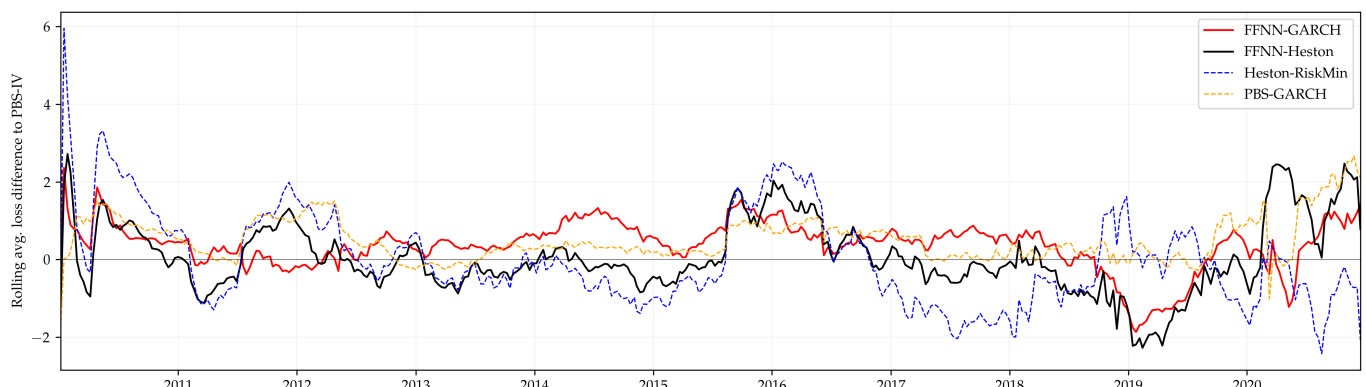
(A) Freq. 10 / Mat. 60



(B) Freq. 5 / Mat. 30



(C) Freq. 2 / Mat. 14



Note: Figure shows the moving average hedge differences defined in 8.2 for all hedging strategies. The derivative being hedged is a short ATM call option. Freq. x / Mat. y refers to a call option expiring in y calendar days and an x business day portfolio rebalancing frequency. No transaction costs are assumed. FFNN-GARCH is the deep hedging model trained under a GJR-GARCH simulated environment. FFNN-Heston is the deep hedging model trained under the simulated Heston environment.

trained with physical GARCH dynamics. Second, the analysis shows that deep hedging is also empirically relevant even when rebalancing is relatively frequent - every second day - and there are no transaction costs. In actual trading with positive trading costs, deep hedging will be able to outperform classic Greeks strategies even more if the latter are not adapted on an ad-hoc basis to take into account the additional frictions.

8.3 Deep Hedging Performance under \mathbb{P} -Estimated Dynamics

The empirical test of deep hedging applied to hedging of options written on a single time series naturally suffers from reflecting the performance on exactly that one path and is thus subject to statistical uncertainty. Said differently, the empirically realized distribution of hedge errors ε_T^δ just presented might very well differ from its population equivalent.

TABLE 5: SUMMARY OF SIMULATED HEDGE PNL DISTRIBUTION

	CVaR _{0.0}	RMSE	SemiRMSE	CVaR _{0.99}	CVaR _{0.95}	CVaR _{0.75}	CVaR _{0.5}
<i>Freq. 10 / Mat. 250</i>							
PBS (GARCH)	10.47	38.52	47.62	176.06	113.85	59.59	36.99
FFNN (SemiMSE)	-56.48%	-25.43%	-28.4%	-7.76%	-13.69%	-23.46%	-28.32%
<i>Freq. 5 / Mat. 125</i>							
PBS (GARCH)	16.61	33.94	39.59	151.36	99.66	55.87	37.73
FFNN (SemiMSE)	-15.87%	-17.49%	-21.61%	-7.72%	-8.21%	-10.73%	-12.85%
<i>Freq. 2 / Mat. 40</i>							
PBS (GARCH)	15.44	26.12	29.19	115.84	75.97	43.35	30.19
FFNN (SemiMSE)	-1.18%	-8.57%	-14.01%	-7.76%	-7.05%	-5.08%	-3.9%
<i>Freq. 1 / Mat. 25</i>							
PBS (GARCH)	12.28	21.15	23.86	94.24	61.67	35.13	24.37
FFNN (SemiMSE)	0.36%	-7.31%	-13.41%	-7.05%	-6.86%	-4.75%	-2.79%

Note: Table displays risk metrics for simulated hedge errors under a GJR-GARCH model estimated on data from 01/01/2012-03/01/2017. All hedges are for a sold ATM call option and losses are centered at market option prices, i.e. \bar{p} is the relevant option price quoted in the market on 03/01/2017 when the hedge is initiated. Freq. x / Mat. y refers to a call option expiring in y business days and an x business day portfolio rebalancing frequency. The first row for each options maturity displays absolute risk measures for the PBS model. The second row displays the normalized loss difference as measured by 6.1 where \mathcal{M}_1 is the deep hedging model. For each risk measure, the best model is indicated with bold typography.

This section tries to cope with this serious concern by assuming or, more accurately, imposing, that the market dynamics are in fact driven by a GJR-GARCH model with parameters estimated on the realized path

of stock prices over the period 01/01/2012 to 03/01/2017. I conduct precisely the same hedging experiment as above in the purely empirical section. Such a controlled experiment has the advantage of substantially reducing the statistical uncertainty carried by the empirical analysis since the performance may be evaluated on e.g. 2^{20} paths rather than 1. The obvious drawback is that the validity of such an analysis relies on the GJR-GARCH model representing the true market generating process well.

Again, I consider hedging a short ATM call option, but with different times to maturity and hedge rebalancing frequencies. The deep hedging model is the standard FFNN with two layers, 20 neurons per layer, and only the log stock price as information set. This time, I set the objective function to be the SemiMSE risk measure since the optimal strategy under that objective resembles more closely the PBS delta and thus yields a more meaningful comparison between the two. The batch size is $\tilde{B} = 2^{14}$ and the number of simulated samples $B = 2^{19}$. All simulated hedge experiments are initiated on 03/01/2017 - a representative date during the evaluation period.

When the option time to maturity is one calendar year and the rebalancing frequency once every second week (bi-weekly), this analysis presents an essentially exact replication of the experiment described in [Buehler et al. \(2019\)](#) p. 1289. In their Figure 12, the authors of this paper show an impressive improvement in hedging performance for deep hedging compared to a PBS strategy at the biweekly rebalancing frequency. I extend their analysis by carrying out the analysis for shorter horizon options and, arguably, more realistic hedge rebalance frequencies. I consider options expiring in 12, 6, 2, and 1 month with hedge frequencies, respectively, biweekly, weekly, every second trading day, and once a day. Furthermore, the analysis is based on charging the market-quoted option price \bar{p} rather than a fictitious price based on the filtered volatility at the start of the hedge period.

The results are presented in Table 5, which compares the simulated risk measures in terms of CVaR, MSE and SemiMSE risk for the deep hedging and PBS strategies. Histograms showing the full simulated PnL distributions are available in Figure A3 in the appendix. As in [Buehler et al. \(2019\)](#), I find that deep hedging improves dramatically on the PBS strategy at a biweekly rebalancing frequency. The estimated reduction in squared losses as measured by SemiMSE is 25%, and the average loss for deep hedging is 56% lower on average. Reassuringly, the PnL distribution in panel (A) of Figure A3 indeed resembles quite closely Figure 12 in [Buehler et al. \(2019\)](#). As expected, the PnL distribution for the PBS strategy is observed to become increasingly more desirable relative to deep hedging as the rebalancing frequency increases and higher order effects, not taken into account in the BS delta hedge, vanish. For daily rebalancing, deep hedging retains its advantage as measured by its ability to limit extreme losses. However, in expectation, the global hedging risk of deep hedging is no lower than the Practitioner's Black-Scholes strategy. These observations are in

line with the empirical results presented above.

8.4 Volatility Information and Hedging Performance

In the above analysis, no information about the state of the variance process was made *explicitly* available to the deep hedging model during the life of the hedged option. That is because the information, or feature, set was fixed as $\mathcal{I}_t = (\log S_t)$ for all t as in Buehler et al. (2019). However, in the Heston model and the family of GARCH models, the conditional distribution of returns depends on the current level of the variance, even after conditioning on the current value of the stock price. It would thus appear as if we are not exploiting the full potential of deep hedging, which allows for leveraging this type of information. Indeed, the information set of all other models is larger compared to deep hedging because, on each trading day when making the trading decision, they are fed with the newest volatility information, either from the options market or from the filtered GARCH variances. The deep hedging model must learn about the current level of volatility only through the level at which the simulations are initialized, i.e. the volatility information implicit in the simulated stock price paths. As mentioned several times in the past sections, one could even expect an improvement by moving from a deep hedging model with information set including GARCH-filtered variances, that is $\mathcal{I}_t = (\log S_t, h_{t+1}^{GJR})$, to one that includes a more accurate filtered variance based on realized measures, $\mathcal{I}_t = (\log S_t, h_{t+1}^{RG})$, as in the Realized GARCH model. The same reasoning goes for the PBS-GARCH model, which potentially also might benefit from exploiting the more accurate Realized GARCH-filtered conditional volatility.

TABLE 6: EMPIRICAL RISK DIFFERENCES WHEN INCLUDING VARIANCE INFORMATION

\mathcal{I}_t	RMSE	SemiRMSE	CVaR _{0.99}	CVaR _{0.95}	CVaR _{0.75}	CVaR _{0.5}	CVaR _{0.0}
$(\log S_t, h_{t+1}^{GJR})$	-13.51%	11.94%	0.28%	7.51%	2.70%	-5.22%	23.60%

Note: Table shows the normalized difference in risk measures as defined in 6.1 when extending the information set of the deep hedging model to include GJR-GARCH filtered volatilities. The market simulator is the GJR-GARCH model. The best model for each risk measure is indicated by a bold typography.

To address these issues, I assume an identical empirical trading setting as in the above section and consider the one-month option with an assumed weekly rebalancing.

Table 6 first quantifies the significance of enlarging the information set with the GJR-GARCH-filtered variance. The table shows that the addition of variance information leads to a 5% reduction in the average loss in the 50% worst cases in the sample period. However, the empirical tail risk also increases slightly. The

fact that the differences are so small may explain why Buehler et al. (2019) do not include this additional information in their empirical experiment. Overall, the results suggest that the deep hedging model does *not* benefit substantially from including updated variance information during the life of the hedged asset.

TABLE 7: EMPIRICAL RISK DIFFERENCES FOR REALIZED GARCH MARKET SIMULATOR

\hat{G}	RMSE	SemiRMSE	CVaR _{0.99}	CVaR _{0.95}	CVaR _{0.75}	CVaR _{0.5}	CVaR _{0.0}
Realized-GARCH	-1.7%	-4.9%	-4.7%	-4.4%	6.74%	9.26%	37.08%

Note: Table shows the normalized difference in risk measures as defined in 6.1 when switching from using daily updates GJR-GARCH-filtered volatilities (\mathcal{M}_2) to Realized-GARCH-filtered volatilities (\mathcal{M}_1). The best model for each risk measure is indicated by a bold typography.

Table 7 next compares the difference in risk when deep hedging under a simulated Realized-GARCH model instead of the GJR-GARCH model when the information set is $\mathcal{I}_t = (\log S_t)$ in both cases. Switching to the Realized GARCH model increases the average hedging loss from -1.78 to -1.12 , corresponding to a 37% increase in the average loss, but appears to also reduce slightly the frequency of extreme losses. The average loss in the 5% worst cases declines by almost 5% from around 50.1 to 47.8. As measured by the training objective, it does not pay off to use the more complicated Realized GARCH model for market simulations.

Figure 10 next seeks to identify whether consistent periods of over- or under-performance for the FFNN-

FIGURE 10: IMPACT OF ASSUMED MARKET ENVIRONMENT ON DEEP HEDGING PERFORMANCE



Note: Figure displays the 30-period moving average difference in deep hedging profit-and-loss when switching from the GJR-GARCH to the Realized GARCH market simulator.

RealizedGarch model compared to the FFNN-GARCH model is linked to volatility levels. The figure displays the 30-period moving average of terminal losses as defined in 8.2, but where the benchmark model is the FFNN-GARCH model rather than the PBS model and \mathcal{M} is the FFNN-RealizedGarch model. Alongside, the figure also displays a moving weekly average of the annualized volatility as measured by the realized kernel estimator. A reasonable prior hypothesis could be that over-performance of the FFNN-RealizedGARCH

model would be observed during periods of sudden increases in volatility due the Realized GARCH model's ability to respond more rapidly to volatility news. The results presented in the figure seem to provide some evidence that this is in fact the case, although the relationship is not completely unambiguous - the correlation between the two displayed series is 0.31.

A result of independent interest is that the Practitioner's Black-Scholes model is able to take advantage of the filtered volatilities from the Realized-GARCH model when switching from a standard GJR-GARCH model. Results for this model are available in Figure A3 in the appendix where the reduction in tail risk is seen to be of similar magnitude as for deep hedging.

8.5 The Empirical Significance of Training Risk Aversion

In recognition of the fact that the $\text{CVaR}_{0.75}$ risk measure previously used when training the deep hedging model is somewhat arbitrary. The previous Section 6.2 presented an analysis of deep hedging performance in a constant volatility environment with a controlled degree of model misspecification, showing that it can turn out costly to follow a deep hedging policy trained under a high risk-aversion level when volatility suddenly spikes. From a practical perspective, a relevant question is how the empirically realized distribution of deep hedging losses changes in response to an altered training objective. In any practical implementation, the deep hedging training objective is another hyperparameter that must be selected on a case-by-case basis and, in principle, can be optimized based on past empirical performance.²⁷ To address the impact of

TABLE 8: EMPIRICAL HEDGING RISK - THE SIGNIFICANCE OF THE TRAINING RISK AVERSION

	RMSE	SemiRMSE	$\text{CVaR}_{0.99}$	$\text{CVaR}_{0.95}$	$\text{CVaR}_{0.75}$	$\text{CVaR}_{0.5}$	$\text{CVaR}_{0.0}$
PBS-IV	17.01	22.93	79.24	54.41	20.42	10.48	-0.14
FFNN ($\alpha = 0.5$)	14.39	28.5	57.02	32.75	4.27	-2.53	-7.79
FFNN ($\alpha = 0.75$)	3.05	-0.66	1.98	-4.34	-1.87	-1.30	-1.64
FFNN ($\alpha = 0.95$)	-0.39	-4.18	-12.05	-8.92	0.21	1.23	-0.03

Note: Note: The first row of the table displays empirical risk measures for the PBS model when repeatedly hedging a one-month short ATM call position over the period Jan 2010-Dec 2020 with weekly rebalancing. All other rows display the absolute differences in risk as defined in 8.1 where \mathcal{M}_1 is a deep hedging model trained to minimize a given CVaR_α . The best model for each risk measure is indicated by bold typography.

employing different training risk aversions, I repeat the above experiment for the 1-month call option, but where three different risk objectives (CVaR_α for $\alpha \in \{0.5, 0.75, 0.95\}$) are employed during training of the

²⁷Although such data-snooping could turn out to be a poor choice.

deep hedging model. Table 8 displays the empirically realized difference in risk measures for these three different deep hedging models compared to the PBS-IV strategy. The corresponding relevant histograms are available in Figure A4 in the appendix. Based on this analysis, it is clear that the central mass of the deep hedging PnL distribution shifts to the left as training risk aversion increases while the frequency of extreme losses declines. This is what one would observe almost surely in a controlled setting. The observation that this relationship also exists in a real trading setting with model uncertainty is nevertheless a reassuring observation for practitioners.

9 Conclusion

This thesis studies practical applications of the Greeks-free hedging methods known as deep hedging, and in particular the performance of said hedging method in real-world and controlled trading environments with model uncertainty. As in Buehler et al. (2019), I find the method to work well in an empirical application to vanilla SPX options. However, the analysis provides several additional perspectives. In particular, I find that deep hedging does not *unconditionally* outperform classic Greeks-based approaches when hedging vanilla call options in a real trading environment. This stands in contrast to what one would observe in essentially any fixed incomplete model setting.

First, I show that deep hedging is significantly more vulnerable to an unexpectedly high volatility level in the constant volatility model. Second, I exhibit in a controlled Heston stochastic volatility environment the consequences of deep hedging under a variance process with parameters different from the ones governing the physical market dynamics. I find that if one goes ahead and trains the deep hedging strategy to minimize the 75% conditional value at risk, getting the level of the variance wrong has substantially smaller consequences than getting its volatility wrong if the trader's preferences are well described by the training objective. An important implication of this finding is that one does not significantly harm the efficiency of deep hedging by ignoring the fact that a negative variance risk premium typically exists. In other words, calibrating the Heston model to options data and subsequently training the deep hedging model on market scenarios generated under the inferred equivalent martingale (pricing) measure is no disaster when the trader's preferences are well described by the training objective.

In the empirical application of deep hedging to plain vanilla SPX call options, I find, in line with the controlled experiments, that the performance of deep hedging suffers when volatility suddenly spikes during the extreme market scenario of the Covid crisis. During this time, the neural network policy sometimes diverges due to not having seen such extreme figures during the model training phase. However, any serious practical implementation of the model would be more robust than the one considered in the analysis of this thesis. In any case, this finding at least highlights the demand for implementing, along with the deep hedging model, some type of sanity filter or to robustify the model by oversampling extreme scenarios during model training.

I find some evidence that using a Realized GARCH model for market simulations as opposed to the GJR-GARCH model performs better during sudden volatility spikes, attributable to its steeper news impact curve. Additionally, the empirical analysis shows that hedging with a model trained on simulated Heston stochastic volatility paths inferred from the pricing measure is a viable alternative to training the model under the

historical measure. This is in line with the findings from the controlled market environment. This is an important finding for practitioners, among which the Heston model is popular. Furthermore, it extends on the existing literature in [Giurca and Borovkova \(2021\)](#) and [Mikkilä and Kanniainen \(2021\)](#) who also test empirically the performance of deep hedging when the model is trained under a Heston model calibrated to the options market.

In the empirical test, I find, somewhat contrary to what one might expect, that the gains from switching from a Greeks-based hedging strategy to deep hedging are not always increasing in the degree of market incompleteness, as measured by the extent of time discretization between hedge rebalancing.

Finally, it is important to keep in mind that the analysis presented here has disregarded all types of trading costs and frictions, except the discretization of time - the reason being that it requires various ad-hoc adjustments to standard Greeks hedging methods to hedge efficiently under these conditions. On the other hand, accommodating such real-life frictions in the deep hedging strategy requires only a trivial adjustment of the profit-and-loss calculation during model training. Combined with the results presented throughout the thesis, this suggests that the efforts on practical implementations of the modern deep hedging strategy in larger financial institutions is going to continue.

While this thesis has provided some insights for the practical relevance of deep hedging for vanilla options hedging, there is still substantial work to be done. In particular, from the practical perspective also taken in this thesis, it might be interesting to explore other ways to incorporate high-frequency based trading information in the form of trading volumes or other realized measures. Deep hedging theoretically allows the trader to exploit a large information set when deciding on the strategy, but a question still to be answered is how one should incorporate information such as news. In practice, one must formulate a dynamic stochastic model for such alternative variables, at least with the approach taken in this thesis. An alternative to formulating a stochastic model for the market is to simply train the deep hedging model on historical data, thus making the strategy truly data-driven. This is the approach in [Mikkilä and Kanniainen \(2021\)](#). In such a setting, incorporating alternative information appears much more straightforward, thus really exploiting the flexibility of deep hedging. Research along those lines would be highly interesting and relevant in practice.

References

- Riaz Ahmad and Paul Wilmott. Which free lunch would you like today, sir?: Delta hedging, volatility arbitrage and optimal portfolios. *Wilmott*, pages 64–79, 2005.
- Yacine Aït-Sahalia and Robert Kimmel. Maximum likelihood estimation of stochastic volatility models. *Journal of financial economics*, 83(2):413–452, 2007.
- Gurdip Bakshi and Nikunj Kapadia. Delta-hedged gains and the negative market volatility risk premium. *The Review of Financial Studies*, 16(2):527–566, 2003.
- Ole E Barndorff-Nielsen, P Reinhard Hansen, Asger Lunde, and Neil Shephard. Realized kernels in practice: Trades and quotes, 2009.
- Aharon Ben-Tal and Marc Teboulle. An old-new concept of convex risk measures: The optimized certainty equivalent. *Mathematical Finance*, 17(3):449–476, 2007. ISSN 0960-1627.
- Tomas Bjork. Arbitrage theory in continuous time, 3rd ed. oxford university press. 2009.
- Fischer Black. The pricing of commodity contracts. *Journal of financial economics*, 3(1-2):167–179, 1976.
- Mark Broadie and Özgür Kaya. Exact simulation of stochastic volatility and other affine jump diffusion processes. *Operations research*, 54(2):217–231, 2006.
- Hans Buehler, Lukas Gonon, Josef Teichmann, and Ben Wood. Deep hedging. *Quantitative Finance*, 19(8):1271–1291, 2019.
- Hans Buehler, Phillip Murray, Mikko S Pakkanen, and Ben Wood. Deep hedging: Learning to remove the drift under trading frictions with minimal equivalent near-martingale measures. *arXiv preprint arXiv:2111.07844*, 2021.
- Alexandre Carboneau. Deep hedging of long-term financial derivatives. *Insurance: Mathematics and Economics*, 99:327–340, 2021.
- Alexandre Carboneau and Frédéric Godin. Equal risk pricing of derivatives with deep hedging. *Quantitative Finance*, 21(4):593–608, 2021a.
- Alexandre Carboneau and Frédéric Godin. Deep equal risk pricing of financial derivatives with non-translation invariant risk measures. *arXiv preprint arXiv:2107.11340*, 2021b.

- Fulvio Corsi. A simple approximate long-memory model of realized volatility. *Journal of Financial Econometrics*, 7(2):174–196, 2009.
- Kingma Da. A method for stochastic optimization. *arXiv preprint arXiv:1412.6980*, 2014.
- Freddy Delbaen and Walter Schachermayer. A general version of the fundamental theorem of asset pricing. *Mathematische annalen*, 300(1):463–520, 1994.
- Darrell Duffie, Jun Pan, and Kenneth Singleton. Transform analysis and asset pricing for affine jump-diffusions. *Econometrica*, 68(6):1343–1376, 2000.
- Bernard Dumas, Jeff Fleming, and Robert E Whaley. Implied volatility functions: Empirical tests. *The Journal of Finance*, 53(6):2059–2106, 1998.
- Simon Ellersgaard, Martin Jönsson, and Rolf Poulsen. The fundamental theorem of derivative trading-exposition, extensions and experiments. *Quantitative Finance*, 17(4):515–529, 2017.
- Robert F Engle. Autoregressive conditional heteroscedasticity with estimates of the variance of united kingdom inflation. *Econometrica: Journal of the econometric society*, pages 987–1007, 1982.
- William Feller. An introduction to probability theory and its applications. *Vols. I & II, Wiley I*, 968, 1971.
- Hans Föllmer, Martin Schweizer, et al. *Hedging of contingent claims under incomplete information*. Rheinische Friedrich-Wilhelms-Universität Bonn, 1990.
- Jim Gatheral. *The volatility surface: a practitioner’s guide*. John Wiley & Sons, 2011.
- Alexandru Giurca and Svetlana Borovkova. Delta hedging of derivatives using deep reinforcement learning. *Available at SSRN 3847272*, 2021.
- Lawrence R Glosten, Ravi Jagannathan, and David E Runkle. On the relation between the expected value and the volatility of the nominal excess return on stocks. *The journal of finance*, 48(5):1779–1801, 1993.
- Frédéric Godin. Minimizing cvar in global dynamic hedging with transaction costs. *Quantitative Finance*, 16(3):461–475, 2016.
- Peter Reinhard Hansen, Zhuo Huang, and Howard Howan Shek. Realized garch: a joint model for returns and realized measures of volatility. *Journal of Applied Econometrics*, 27(6):877–906, 2012.
- Steven L Heston. A closed-form solution for options with stochastic volatility with applications to bond and currency options. *The review of financial studies*, 6(2):327–343, 1993.

- Sepp Hochreiter and Jürgen Schmidhuber. Long short-term memory. *Neural computation*, 9(8):1735–1780, 1997.
- Blanka Horvath, Josef Teichmann, and Žan Žurič. Deep hedging under rough volatility. *Risks*, 9(7):138, 2021.
- John Hull and Alan White. Optimal delta hedging for options. *Journal of Banking & Finance*, 82:180–190, 2017.
- Aytaç Ilhan, Mattias Jonsson, and Ronnie Sircar. Optimal static-dynamic hedges for exotic options under convex risk measures. *Stochastic Processes and their Applications*, 119(10):3608–3632, 2009.
- Peter Jäckel. Let's be rational. *Wilmott*, 2015(75):40–53, 2015.
- Thomas Kokholm and Martin Stisen. Joint pricing of vix and spx options with stochastic volatility and jump models. *The Journal of Risk Finance*, 2015.
- Eva Lütkebohmert, Thorsten Schmidt, and Julian Sester. Robust deep hedging. *Quantitative Finance*, pages 1–16, 2021.
- Oskari Mikkilä and Juho Kanniainen. Empirical deep hedging. *Available at SSRN 3923529*, 2021.
- Charles R Nelson and Andrew F Siegel. Parsimonious modeling of yield curves. *Journal of business*, pages 473–489, 1987.
- Rolf Poulsen, Klaus Reiner Schenk-Hoppé, and Christian-Oliver Ewald. Risk minimization in stochastic volatility models: model risk and empirical performance. *Quantitative Finance*, 9(6):693–704, 2009.
- Stephan R Sain. The nature of statistical learning theory, 1996.
- Martin Schmelzle. Option pricing formulae using fourier transform: Theory and application. *Preprint, http://pfadintegral.com*, 2010.
- Martin Schweizer. Variance-optimal hedging in discrete time. *Mathematics of Operations Research*, 20(1): 1–32, 1995.
- Martin Schweizer. A guided tour through quadratic hedging approaches. Technical report, SFB 373 Discussion Paper, 1999.
- Neil Shephard, Asger Lunde, Ole E Barndorff-Nielsen, and Peter R Hansen. Designing realised kernels to measure the ex-post variation of equity prices in the presence of noise. 2008.

Johannes Siven and Rolf Poulsen. Risk-minimizing static hedges of exotic options.

Bernard Wong and CC Heyde. On changes of measure in stochastic volatility models. *International Journal of Stochastic Analysis*, 2006, 2006.

Liuren Wu and Peter Carr. Variance risk premia. In *AFA 2005 Philadelphia Meetings*, 2007.

Yun Yin and Peter G Moffatt. Correcting the bias in the practitioner black-scholes method. *Journal of Risk and Financial Management*, 12(4):157, 2019.

Appendices

List of Tables

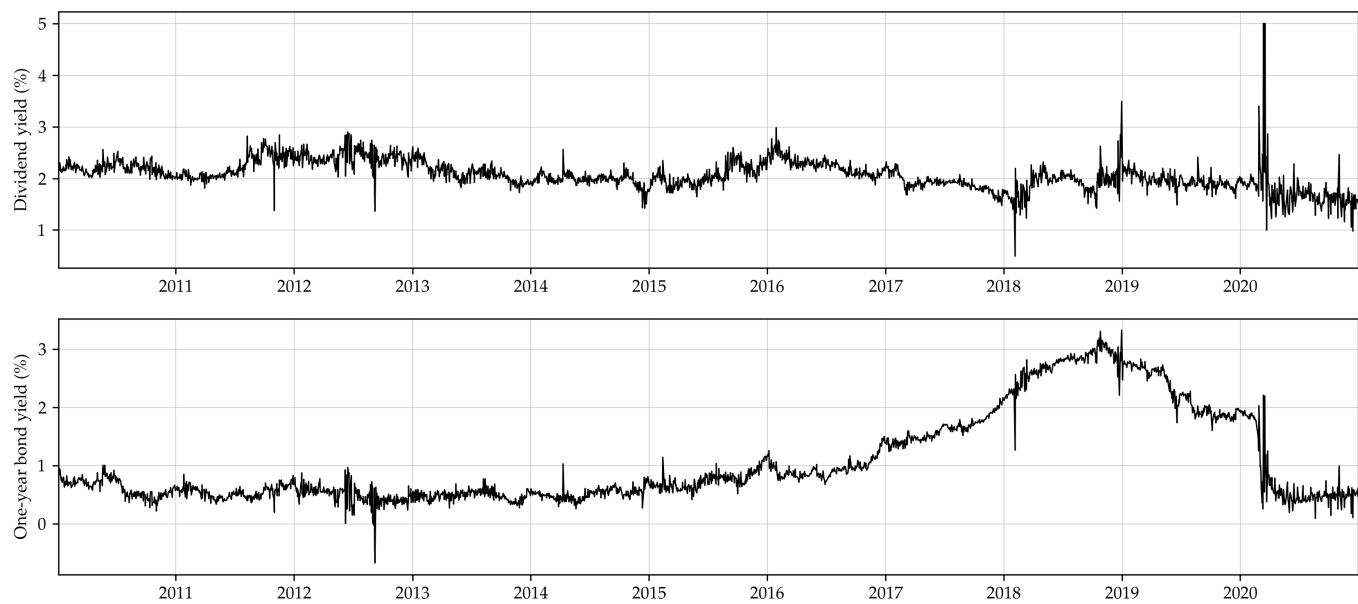
1	SUMMARY OF SIMULATED HEDGE PnL DISTRIBUTION	34
2	DISTRIBUTION OF CALIBRATED HESTON PARAMETERS AND VOLATILITIES	41
3	EMPIRICAL LOSS DISTRIBUTION (SHORT ATM CALL, WEEKLY REBALANCING	46
4	EMPIRICAL RISK MEASURES FOR ATM CALL HEDGES 2010-2020	48
5	SUMMARY OF SIMULATED HEDGE PnL DISTRIBUTION	53
6	EMPIRICAL RISK DIFFERENCES WHEN INCLUDING VARIANCE INFORMATION	55
7	EMPIRICAL RISK DIFFERENCES FOR REALIZED GARCH MARKET SIMULATOR	56
8	EMPIRICAL HEDGING RISK - THE SIGNIFICANCE OF THE TRAINING RISK AVERSION	57
A1	ESTIMATED REALIZED GARCH MODEL PARAMETERS	70
A2	ESTIMATED GJR-GARCH MODEL PARAMETERS	70
A3	EMPIRICAL RISK IMPACT OF SWITCHING TO REALIZED GARCH VOLATILITIES IN PBS MODEL	70

List of Figures

1	DIFFERENCE BETWEEN DEEP HEDGING AND BLACK-SCHOLES HEDGING STRATEGIES	32
2	ESTIMATED KERNEL DENSITY OF HEDGE PnL	33
3	BLACK-SCHOLES HEDGE AND DEEP HEDGE ALONG A SIMULATED MODEL PATH	34
4	THE RISK OF DEEP HEDGING WITH THE WRONG VOLATILITY	35
5	DEEP HEDGING MODEL RISK IN THE HESTON MODEL	37
6	OBSERVED AND CALIBRATED VOLATILITY SURFACES (JULY 20TH 2020)	41
7	VOLATILITY DYNAMICS	42
8	DISTRIBUTION OF TERMINAL HEDGE ERRORS FOR 2012-2018 SUBSAMPLE	46
9	ROLLING AVG. DIFFERENCE IN HEDGE ERRORS (ATM CALL)	52
10	IMPACT OF ASSUMED MARKET ENVIRONMENT ON DEEP HEDGING PERFORMANCE	56
A1	OPTION-IMPLIED DIVIDEND YIELD AND 1-YEAR INTEREST RATE	66
A2	HESTON PRICING ERRORS	67
A3	SIMULATED DISTRIBUTION OF HEDGE ERRORS UNDER ESTIMATED GJR-GARCH MODEL . .	68
A4	EMPIRICAL PnL DISTRIBUTIONS - THE SIGNIFICANCE OF TRAINING RISK AVERSION	69

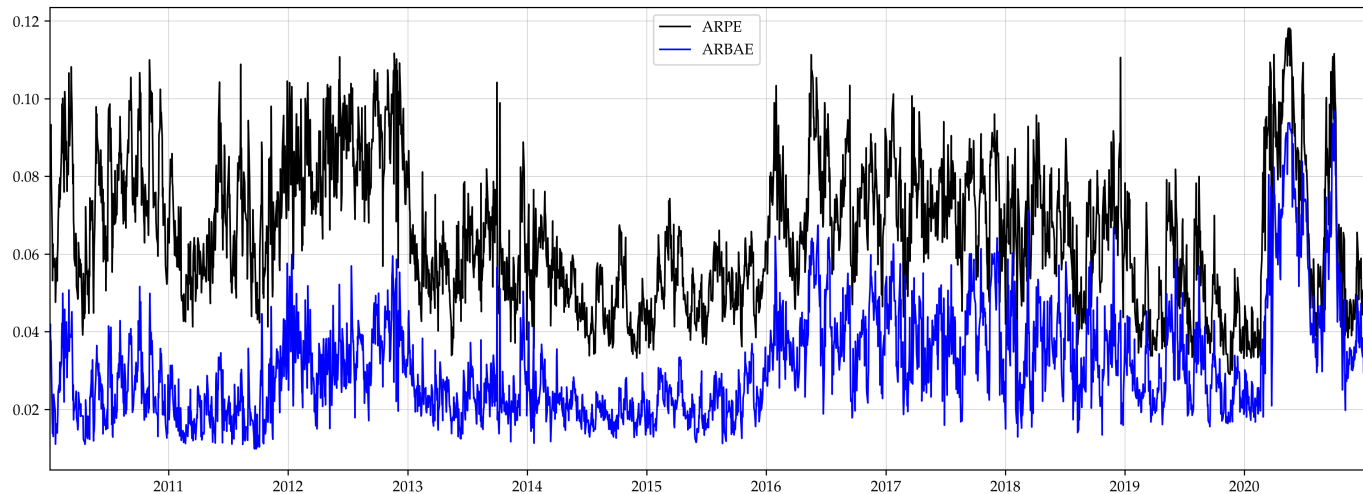
A Figures

FIGURE A1: OPTION-IMPLIED DIVIDEND YIELD AND 1-YEAR INTEREST RATE



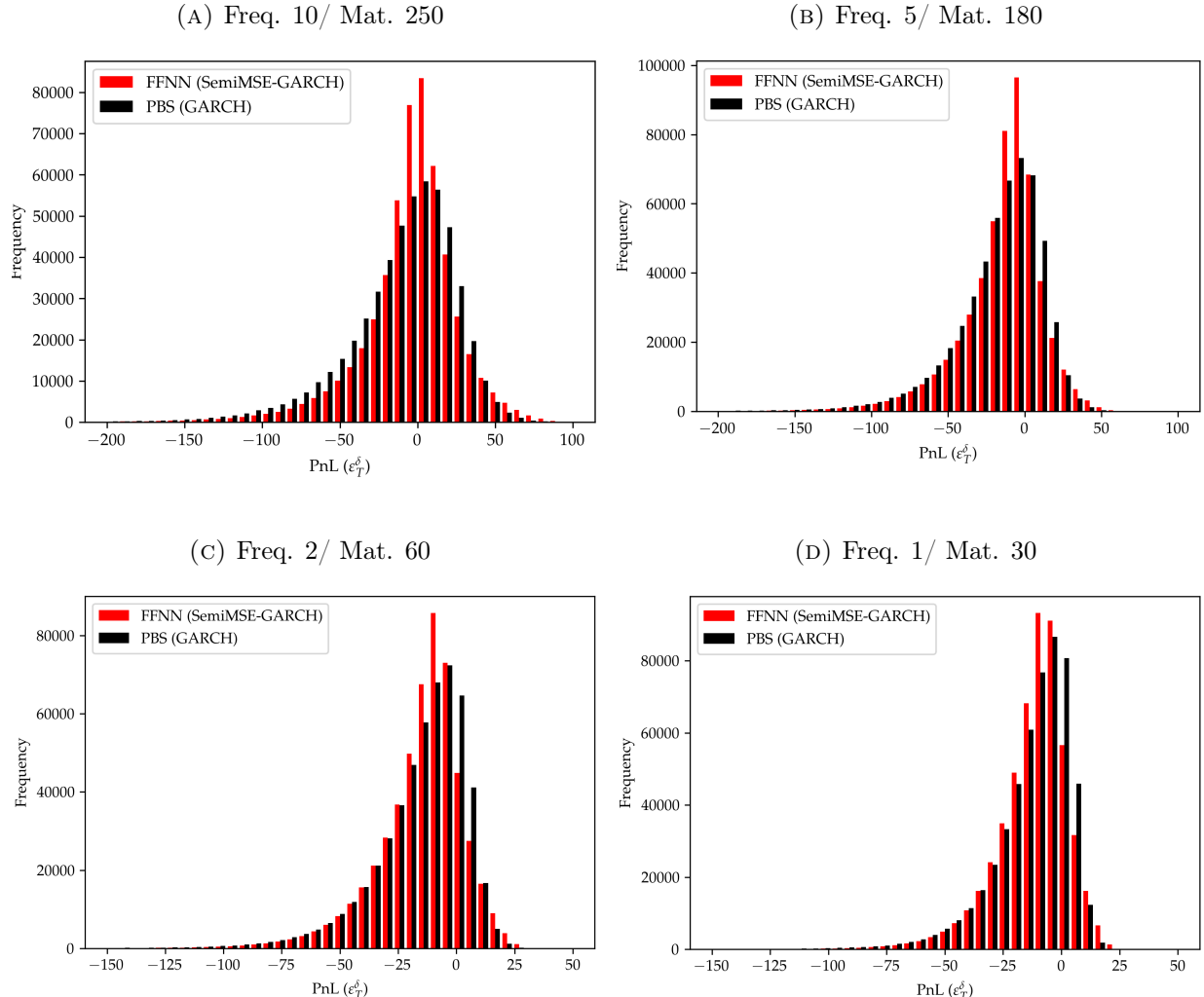
Note: Figure shows dividend yield implied by liquid call and put option quotes and the put-call parity. The procedure for calibrating the yield curve is described in Appendix (C).

FIGURE A2: HESTON PRICING ERRORS



Note: Figure shows the time series of daily Heston calibration errors. The ARPE and ARBAE are defined as in Kokholm and Stisen (2015), respectively, as the averages of $\frac{|c^{Lewis} - c^{Market}|}{c^{Market}}$ and $\frac{(c^{Lewis} - c^{Ask})^+ + (c^{Bid} - c^{Lewis})^+}{c^{Market}}$.

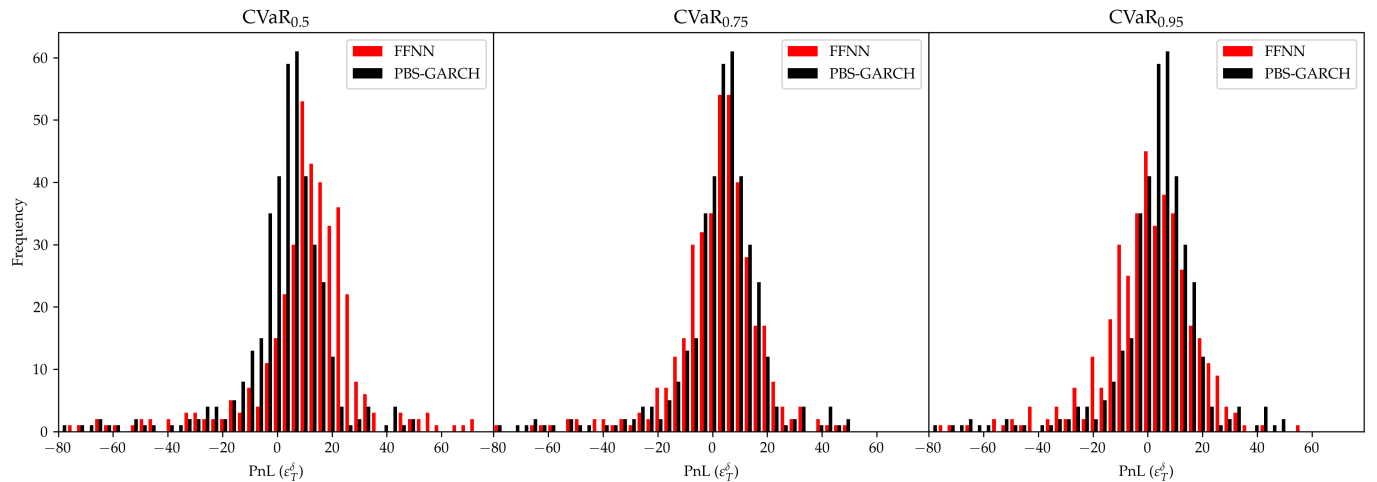
FIGURE A3: SIMULATED DISTRIBUTION OF HEDGE ERRORS UNDER ESTIMATED GJR-GARCH MODEL



Note: Figure shows histograms of simulated terminal hedge profits under the GJR-GARCH model defined in 4.2 and 4.3 estimated on data from 01/01/2012-03/01/2017. All hedges are for a sold ATM call option and losses are centered at market option prices, i.e. \bar{p} is the relevant option price quoted in the market on 03/01/2017 when the hedge is initiated. Freq. x / Mat. y refers to a call option expiring in y business days and an x business day portfolio rebalancing frequency. The volatility used in the PBS strategy is the one induced by the GJR-GARCH filter in 4.3.

The deep hedging model is a FFNN trained under the SemiMSE risk measure and with the same GJR-GARCH market generator used for evaluating the strategies.

FIGURE A4: EMPIRICAL PnL DISTRIBUTIONS - THE SIGNIFICANCE OF TRAINING RISK AVERSION



Note: Figure compares the distribution of terminal hedge errors for the PBS-GARCH model and the deep hedging strategy trained under estimated GJR-GARCH market dynamics. Each panel corresponds to a different risk aversion level α during model training. The hedge derivative is an ATM call option with 1 month to expiry. All losses are centered at the market-quoted option price and a weekly rebalancing frequency is assumed.

B Tables

TABLE A1: ESTIMATED REALIZED GARCH MODEL PARAMETERS

ω	α	β	ξ	ϕ	τ_1	τ_2	σ^2	μ
0.219	0.357	0.590	-0.671	0.976	-0.102	0.159	0.475	0.033

Note: Table displays estimated Realized Garch model parameters based on an estimation sample covering data from Jan 2005 to Dec 2020.

TABLE A2: ESTIMATED GJR-GARCH MODEL PARAMETERS

ω	α	γ	β	μ	ν
0.020	0.000	0.250	0.861	0.060	5.282

Note: Table displays estimated GJR-GARCH model parameters based on an estimation sample covering data from Jan 2005 to Dec 2020.

TABLE A3: EMPIRICAL RISK IMPACT OF SWITCHING TO REALIZED GARCH VOLATILITIES IN PBS MODEL

	RMSE	SemiRMSE	CVaR _{0.99}	CVaR _{0.95}	CVaR _{0.75}	CVaR _{0.5}	CVaR _{0.0}
PBS-RealizedGarch	-0.46%	-5.92%	-4.03%	-1.44%	-2.4%	-0.66%	2.58%

Note: Table shows the normalized difference in risk measures as defined in 6.1 for the Practitioner's Black-Scholes model when switching from using daily updated GJR-GARCH-filtered volatilities (\mathcal{M}_2) to Realized-GARCH-filtered volatilities (\mathcal{M}_1). The best model for each risk measure is indicated by a bold typography.

B Equivalent Measure Changes in the Heston Model

This appendix gives a brief account of equivalent changes of measure in the Heston model when the Girsanov kernel is assumed affine in the state vector. The exposition takes inspiration from Wong and Heyde (2006). Using the Cholesky factorization, the Heston model dynamics in 5.6 may be written as

$$\begin{aligned} dS_t &= \mu S_t dt + S_t \sqrt{v_t} \left(\tilde{\rho} dZ_t^1 + \sqrt{1 - \tilde{\rho}^2} dZ_t^2 \right) \\ dv_t &= \kappa^{\mathbb{P}} \left(\theta^{\mathbb{P}} + v_t \right) dt + \varepsilon \sqrt{v_t} dZ_t^2 \end{aligned} \quad (.1)$$

Given that the model is now written in terms of the *standard* bivariate Wiener process $\mathbf{Z}_t = (Z_t^1, Z_t^2)^{\top}$, we may now apply the Girsanov theorem in 2.2. Write the kernel of the stochastic exponential process as $\varphi_t = (\varphi_t^S, \varphi_t^v)^{\top}$ and define the new probability measure $\tilde{\mathbb{P}}$ via the Radon-Nikodym derivative

$$\frac{d\tilde{\mathbb{P}}}{d\mathbb{P}} \Big|_{\mathcal{F}_t} = \exp \left(\int_0^t \varphi_s d\mathbf{Z} - \frac{1}{2} \int_0^t \varphi_s^{\top} \varphi_s ds \right), \quad t \in [0, T]. \quad (.2)$$

By the Girsanov theorem, $Z_t^{2,\tilde{\mathbb{P}}} := Z_t^2 - \int_0^t \varphi_s^v ds$ is a univariate $\tilde{\mathbb{P}}$ Brownian motion, which means that we may write the CIR variance dynamics in .1 as

$$dv_t = \kappa^{\mathbb{P}} \left(\theta^{\mathbb{P}} - v_t \right) dt + \varepsilon \sqrt{v_t} \left(dZ_t^{2,\tilde{\mathbb{P}}} + \varphi_t^v dt \right) \quad (.3)$$

Under the assumption of an affine market price of variance risk, i.e. $\varphi_t^v = \frac{\lambda}{\varepsilon} \sqrt{v_t}$, we get

$$\begin{aligned} dv_t &= \kappa^{\mathbb{P}} \left(\theta^{\mathbb{P}} - v_t + \frac{\kappa^{\mathbb{P}} - \lambda}{\kappa^{\mathbb{P}}} v_t \right) dt + \varepsilon \sqrt{v_t} dZ_t^{2,\tilde{\mathbb{P}}} \\ &= \kappa^{\mathbb{P}} \left(\theta^{\mathbb{P}} - v_t \frac{\kappa^{\mathbb{P}} + \lambda}{\kappa^{\mathbb{P}}} \right) dt + \varepsilon \sqrt{v_t} dZ_t^{2,\tilde{\mathbb{P}}} \\ &= \left(\kappa^{\mathbb{P}} + \lambda \right) \left(\frac{\theta^{\mathbb{P}} \kappa^{\mathbb{P}}}{\kappa^{\mathbb{P}} + \lambda} - v_t \right) dt + \varepsilon \sqrt{v_t} dZ_t^{2,\tilde{\mathbb{P}}} \end{aligned}$$

Defining $\kappa^{\tilde{\mathbb{P}}} := \kappa^{\mathbb{P}} + \lambda$ and $\theta^{\tilde{\mathbb{P}}} := \frac{\theta^{\mathbb{P}} \kappa^{\mathbb{P}}}{\kappa^{\mathbb{P}} + \lambda}$ shows that the variance process is also a CIR process under the new measure $\tilde{\mathbb{P}}$, albeit with a different stationary level and speed of mean reversion. The fact that $\tilde{\mathbb{P}}$ was chosen as an arbitrary equivalent measure means that it also holds for the choice of φ_t^S that makes it a martingale measure, thus confirming the assertion in 5.7.

C Extracting Implied Dividend Yield and Bond Yields from Option Prices

This appendix describes in some more detail the procedure that I apply on each trading day to back out an implied dividend yield for the S&P500 index and a yield curve based on the available options data. The procedure that I use is almost equivalent to what I did in an old project titled "*Derivatives on variance: VIX option pricing*" in the course 5360: Financial Engineering. The exposition here is hence similar to the one in that project.

Assume to observe prices on N options on a given day, quoted for a given current level of the index S . By put-call parity, the relation between call and put prices must be

$$p_{\text{parity}}(K, \tau, c(K, \tau; q, r_\tau); q, r_\tau) = c(K, \tau; q, r_\tau) + K \exp(-r_\tau \tau) - S \exp(-q\tau) \quad (4)$$

where q is the dividend yield and r_τ is the yield of a riskless bond with time to maturity τ . When the observed times to expiry for the options are $\boldsymbol{\tau} = (\tau_1, \dots, \tau_k)$, the corresponding yield for these dates \mathbf{r}_τ^* and the dividend yield q^* may be calibrated by enforcing the parity to hold for the \bar{x} pairs of most liquid calls and puts for each option maturity, i.e.

$$q^*, \mathbf{r}_\tau^* = \arg \min_{q, \mathbf{r}} \sum_{i=1}^k \sum_{j=1}^{\bar{x}} (p_{\text{market}}(K_j, \tau_i; q, r_{\tau_i}) - p_{\text{parity}}(K_j, \tau_i, c(K_j, \tau_i; q, r_{\tau_i}); q, r_{\tau_i}))^2. \quad (5)$$

For a given maturity, I rank the liquidity of a put-call pair quoted for a given strike by the joint open interest for the pair relative to that of all other options pairs for that maturity. In my implementation, I set $\bar{x}=5$. This procedure gives a discrete number of calibrated points on the yield curve. I subsequently fit a [Nelson and Siegel \(1987\)](#) yield curve to the observed points to obtain a complete term structure curve, which is just a function mapping from a given time to maturity τ to its corresponding discount rate r_τ .

D Heston Characteristic Function and Greeks

This appendix states the formulation of the Heston characteristic function and shows how the relevant Greeks required for the hedge strategies may be computed by inverting this function.

Denote present time by t and let $t + \tau = T$ as in the main text. To be slightly more precise, the general pricing formula in 2.5 combined with the fact that the Heston model is Markovian with respect to the pair (S_t, v_t) implies that the relevant c.f. for options pricing and hedging is the following conditional expectation

$$\phi_\tau(u; \boldsymbol{\theta}^Q) := \mathbb{E}^Q \left[e^{iu(\log S_T - \log S_t - (r-q)\tau)} \mid S_t = s, v_t = \bar{v} \right] \quad (6)$$

where S_T is the solution to the SDE in 5.6 and the significance of the notation implying that the conditional expectation should be taken under an EMM is that the parameters $\boldsymbol{\theta}^Q = (\kappa^Q, \theta^Q, \tilde{\rho}, \varepsilon, \bar{v})$ are the ones corresponding to the EMM. Notice that the only way the initial variance \bar{v} , which is typically considered a calibration parameter, enters the pricing and hedging problem is through the initial conditioning in the conditional expectation.

I use the formulation of the c.f. in Schmelzle (2010), which reads

$$\begin{aligned} \phi_\tau(u; \boldsymbol{\theta}^Q) &= \exp(A(u) + \bar{v}B(u)) \\ A(u) &= \frac{\kappa^Q \theta^Q}{\varepsilon^2} \left[(\beta - d) - 2 \ln \frac{ge^{-d\tau} - 1}{g - 1} \right] \\ B(u) &= \frac{\beta - d}{\varepsilon^2} \frac{1 - e^{-d\tau}}{1 - ge^{-d\tau}} \\ d &= \sqrt{\beta^2 - 4\hat{\alpha}\gamma}, \quad g = \frac{\beta - d}{\beta + d} \\ \hat{\alpha} &= -0.5u(u + i), \quad \beta = \kappa^Q - iu\varepsilon\tilde{\rho}, \quad \gamma = 0.5\varepsilon^2 \end{aligned} \quad (7)$$

The delta and vega of the Heston call option price appearing in 5.10 and 5.11 are given by

$$\begin{aligned} \nabla_s c^{Lewis}(s, K, \tau; \boldsymbol{\theta}^Q) &= e^{-q\tau} \left(1 - \frac{Ke^{-r\tau}}{s\pi} \int_0^\infty \text{Re} \left[e^{(iu+0.5)k} \phi_\tau(u - 0.5i; \boldsymbol{\theta}^Q) (iu + 0.5) \right] \frac{du}{u^2 + 0.25} \right) \\ \nabla_v c^{Lewis}(s, K, \tau; \boldsymbol{\theta}^Q) &= -e^{-q\tau} \frac{Ke^{-r\tau}}{s\pi} \int_0^\infty \text{Re} \left[e^{(iu+0.5)k} \nabla_{\bar{v}} \phi_\tau(u - 0.5i; \boldsymbol{\theta}^Q) \right] \frac{du}{u^2 + 0.25} \end{aligned} \quad (8)$$

Where the derivative $\nabla_{\bar{v}} \phi_\tau(u - 0.5i; \boldsymbol{\theta}^Q) = \phi_\tau(u; \boldsymbol{\theta}^Q) B(u)$

E Delta Hedging and Options Pricing in the Black & Scholes Model

This appendix gives the formula for the famous Black & Scholes call option pricing formula and the associated delta. The pricing formula can be derived in several ways. One possible way is to employ the martingale pricing approach described in Section 2.1 and work out the conditional expectation in 2.5 for a constant interest rate r and dividend yield q . The integral appearing there can be solved in analytically by noting that the BS stock price process in 5.1 is Markovian, which means that one may condition on S_t in 2.5 rather than the filtration \mathcal{F}_t .

Alternatively, the original paper [Black \(1976\)](#) derives the arbitrage-free price process using Ito's Lemma and by requiring that a riskless, delta-hedged, portfolio earns the rate of return of the bank account, r . By use of such no-arbitrage arguments, the authors derived the famous BS partial differential equation (PDE) that must be solved by the arbitrage-free price process. The PDE can be solved by applying the Feynmann-Kac Theorem to get

$$p_t^{BS}(s, K, \tau; \sigma) = se^{-qT} \mathcal{N}(d) - Ke^{-r\tau} \mathcal{N}(d - \sigma\sqrt{\tau}), \quad d := \frac{\ln(\frac{s}{K}) + (r - q + \frac{1}{2}\sigma^2)\tau}{\sigma\sqrt{\tau}} \quad (.9)$$

If one took the latter, delta-hedging, approach to deriving the pricing formula one would already have at hand the corresponding delta. In any case, one can obtain the BS delta of a call option by noticing that the call price is order 1 homogeneous in (s, K) . Euler's theorem for homogeneous functions hence implies that

$$\nabla_s p_t^{BS}(s, K, \tau; \sigma) . = e^{-qT} \mathcal{N}'(d). \quad (.10)$$